7-25-2014

DESIGN AND SYNTHESIS OF CHELATING COMPOUNDS AND SOLID-SUPPORTED CHELATORS FOR METAL DEPLETED SOLUTIONS

Surendra Dawadi
University of Missouri-St. Louis, sd88f@mail.umsl.edu

DESIGN AND SYNTHESIS OF CHELATING COMPOUNDS AND SOLID-SUPPORTED CHELATORS FOR METAL DEPLETED SOLUTIONS

By

SURENDRA DAWADI

Master of Science (Chemistry), 2010

A DISSERTATION

Submitted to the Graduate School of the

UNIVERSITY OF MISSOURI - ST. LOUIS

In partial Fulfillment of the Requirements for the Degree of

DOCTOR OF PHILOSOPHY

in

CHEMISTRY

August, 2013

Dissertation Committee

Prof. Christopher D. Spilling, Ph.D. (Advisor)

Prof. Wesley R. Harris, Ph.D.

Prof. Alexei V. Demchenko, Ph.D.

Prof. James J. O'Brien, Ph.D.

ACKNOWLEDGEMENTS

Foremost, I would like to express my profound gratitude to my mentor Professor Christopher D. Spilling for his guidance, encouragement, enthusiastic support, and useful critiques during these past five years. He has always been motivating, encouraging, and enlightening. Dr. Spilling's humor and friendly sarcasm allowed me to laugh, lightening my perspective when I became too serious. He continually delivered not only a motivation towards research but also an excitement in teaching. His impression will always be a part of my professional life. Without his guidance and persistent help, this dissertation would not have been possible.

I sincerely thank Professor Wesley R. Harris for his help in this research project and also for being in my dissertation committee. I would like to thank him for teaching me analytical techniques required for the completion of the project and answering my numerous questions. I would like to express my sincere gratitude to other dissertation committee members Prof. Alexei Demchenko and Prof. James O'Brien for their time and effort. I would also like to thank Dr. Bruce Hamper, Prof. Valerian D'Souza, and all my teachers for contributing to my graduate school and research experience and their encouragement. I would like to thank Department of Chemistry and Biochemistry at the University of Missouri-St. Louis (UMSL) for providing me a platform to gain teaching and research experience.

It is my pleasure to thank my former and current labmates in the UMSL Spilling group: Dr. Raj Malla, Dr. Mahesh Paudyal, Dr. Sudeshna Roy, Benjamin Martin, Mercy Kiiru, and Jeremy Ridenour, who provided excellent support in the lab. Special thanks go to Jeremy and Ben for proofreading the whole thesis. I would like to thank Harris lab

member Nicolas Bardol for his help during my intermittent presence in the Harris lab. I would also like to thank all my friends at UMSL and in St. Louis. Without them I could not have done my PhD while enjoying every moment of it.

I would like to acknowledge Alkymos Inc., a startup company, and its principal investigator Robert A. Yokel (College of Pharmacy, University of Kentucky), and the National Institute of Health (NIH) for financial support. I would like to thank Dr. Spilling along with Dr. Harris and Dr. Yokel for bringing me into this extremely important project.

My highest gratitude goes to my father, Ganesh Prasad Dawadi; brother, Ananda Dawadi; and sisters, Kamala and Sabitra, for their love, support, and understanding during the long years of my education.

Finally, and most importantly, I would like to thank my wife Sarmila. Her support, encouragement, and steady love are undeniably the most important factors for this achievement. I would like to thank her for being able to take care of our five-year-old daughter Renesa and two-year-old son Rohan in my long absences. I would like to thank my daughter and son for making me laugh when I arrive home after a long day.

LIST OF ABBREVIATIONS

3,4-HP 3-hydroxy-4-pyridinones

Å .....Angstrom

AAS.....Atomic absorption spectroscopy

Ac.....Acetyl

AHA.....Acetohydroxamic acid

APDMES.....(3-aminopropyl)dimethylethoxysilane

BAL.....British anti-Lewisite

BH_3.....Borane

Bn.....Benzyl

Boc.....*tert*-butoxycarbonyl

$Ca(glu)_2$.....Calcium gluconate

Cbz.....Carboxybenzyl

CERCLA.....Comprehensive Environmental Response, Compensation, and Liability Act

$CHCl_3$.....Chloroform

CH_2Cl_2.....Dichloromethane

$Cu(acac)_2$.....Copper acetylacetonate

d.....Doublet

DCC.....*N*,*N*′-Dicyclohexylcarbodiimide

DCM .....Dichloromethane (or Methylene chloride)

dd.....Doublet of doublets

DFO.....Desferioxamine-B

DIPEA.....Diisopropylethylamine

DMF.....N,N-Dimethylformamide

DMAP.....N,N-Dimethylamino pyridine

DMPS.....2.3-dimercaptopropane sulfonate

DMSA.....2,3-dimercaptosuccinic acid

DMSO.....Dimethyl sulfoxide

DNA.....Deoxyribonucleic acid

dr.....Diastereomeric ratio

EDC .....1-ethyl-3-(3-dimethylaminopropyl)carbodiimide

EDTA.....Ethylenediamine tetraacetic acid

Et.....Ethyl

EtOAc.....Ethyl acetate

Et_2O.....Diethyl ether

EtOH..... Ethanol

Et_3N.....Triethylamine

FAB.....Fast atom bombardment

FDA.....Food and Drug Administration

h..... Hour(s)

HCl.....hydrogen chloride

HOBt.....Hydroxybenzotriazole

HPLC.....High performance liquid chromatography

HRMS.....High resolution mass spectrometry

HSAB.....Hard and soft acids and bases

HySS.....Hyperquad Simulation and Speciation

Hz..... Hertz

ICP-MS.....Inductively coupled plasma-Mass Spectroscopy

IR.....infrared

IV.....intravenous

i-PrOH.....Isopropanol

K_2CO_3.....Potassium carbonate

KOH.....Potassium hydroxide

LFER.....Linear free energy relationship

LVP's.....Large volume parenterals

m.....Multiplet

min.....Minute

Me.....Methyl

MeCN.....Acetonitrile

MeOH.....Methanol

MES.....2-(N-morpholino)ethanesulfonic acid

$NaBH_4$.....Sodium borohydride

$NaBH_3CN$.....Sodium cyanoborohydride

NaOH.....Sodium hydroxide

NH_2OTMS.....O-trimethylsilyl hydroxylamine

NMR.....Nuclear magnetic resonance

PCC.....Pyridinium chlorochromate

Ph.....Phenyl

PTSA/*p*-TsOH.....*p*-Toluenesulphonic acid

ppm .....Parts per million

Rf .....Retention factor

$Rh_2(OAc)_4$.....Rhodium acetate

RNA.....Ribonucleic acid

ROS.....reactive oxygen species

rt .....Room temperature

s .....Singlet

SVP's.....Small volume Parenterals

t.....Triplet

TBAF.....Tetrabutylammonium fluoride

TFA.....Trifluoroacetic acid

TsCl.....*p*-toluene sulfonyl chloride

TsOH.....*p*-toluene sulfonic acid

THA.....Trihydroxamic acid

THF.....Tetrahydrofuran

THP.....Tetrahydropyran

$TMSCHN_2$.....Trimethylsilyl diazomethane

TLC.....Thin layer chromatography

TMS.....Trimethylsilyl

TPN.....Total parenteral nutrition

TREN.....Tris(2-aminoethyl)amine

tris.....Tris(hydroxymethyl)aminomethane

TRPN.....Tris(3-aminopropyl)amine

UV-Vis….....Ultraviolet-visible

ABSTRACT

Metals are essential to life, yet they can be toxic (or even fatal) for biological systems when present in excessive amounts. The major source of metal overload in humans is diet; and in some cases, intravenous feeding. Thus the removal of toxic metal ions from contaminated clinical products such as total parenteral nutrition (TPN) solutions, and drinking and waste water systems is extremely important. The use of chelating resins, which are polymeric solids containing covalently immobilized chelating compounds, for the selective removal of metal ions from contaminated solutions has been conceptualized long ago. Herein, the design and synthesis of metal specific chelating compounds and chelating resins will be presented, along with the application of these materials to remove toxic metals from aqueous solutions.

Solution phase hydroxamate based chelating compounds have been synthesized for the selective binding of trivalent metals such as iron and aluminum in the presence of divalent metals such as calcium. Iron complexation behavior of these solution phase chelating compounds has been studied by UV-Vis spectrophotometric methods. These hydroxamate chelators have potential applications as chelating agents in the treatment of iron and aluminum overload. A set of the strongly binding chelators have been immobilized on solid support via various linkages. These solid supported chelators have been employed to selectively remove aluminum from contaminated TPN components such as a solution of calcium gluconate. Our resins are able to remove more than 90% of aluminum from commercial calcium gluconate solutions. This technology of employing hydroxamate functionalized resins for the removal of aluminum from calcium gluconate solution will be available in hospitals soon and will greatly benefit premature neonates

and critically ill patients who receive TPN solutions for life support. Additionally, citramide functionalized chelating resins have been prepared for the removal of trivalent metals from contaminated solutions at low pH, and dithiolate based chelating resins were prepared for the removal of high priority environmental metal toxins such as lead, cadmium, mercury, and arsenic. Overall, this dissertation embodies the design, synthesis, and metal binding studies of novel chelators and chelating resins and the applications of these resins for the selective removal of metal ions from contaminated solutions.

LIST OF CONTENTS

LIST OF FIGURES

LIST OF SCHEMES

LIST OF TABLES

CHAPTER 1: Introduction

1.1 Metals in biology

Although biology is generally associated with organic chemistry, inorganic elements are also essential to life processes. Metals are ubiquitous in our environment, and they play important biological functions in all forms of life.[1] Not surprisingly, metals are essential for humans. Metals play a critical role in protein and nucleic acid biochemistry. Proteins associated with metals are called metalloproteins where metals function as redox centers, transport oxygen, and utilize their ligand-binding abilities in acting as molecular sensors in signal transduction.[2] Some metalloproteins that catalyze biochemical reactions are called metalloenzymes. Though a variety of metals are necessary in biological systems, they are usually required only in trace amounts and can be toxic, if not fatal, when present in excess.[3] Many diseases are related to improper metal ion concentrations in the body. Some diseases are directly linked to a deficiency of certain metals and others are due to their overload. Some examples of diseases related to metal deficiency are anemia due to iron deficiency, bone and teeth diseases due to calcium deficiency, hyperexcitibility and muscle weakness due to magnesium deficiency, among many others. The recent rapid growth of bioinorganic chemistry has helped us to understand the role of metals in biological systems in more detail.

Living organisms utilize some metals in large amounts and other metals in ultra trace amounts. Main group metals such as sodium (Na), potassium (K), magnesium (Mg), and calcium (Ca) are present in large amounts. Transition metals such as iron (Fe), zinc (Zn), and copper (Cu) are present in trace amounts, and manganese (Mn), cobalt (Co), chromium (Cr), vanadium (V), nickel (Ni), cadmium (Cd), and a few others are present in ultra trace amounts. Transition metals are chiefly concerned with catalyzing reactions

either through complex formation with biological ligands or via redox reactions between their available oxidation states. Main group elements, on the other hand, function as charge carriers in biological systems.[4]

1.2 Metal overload and toxicity

Recent human activities have dramatically altered the distribution of metals in the environment. Due to the recent mining boom and industrialization, metal distribution in the environment has greatly increased. Not only the persons working directly in metal industry, but also the general public and consumers of metal products are exposed to higher levels of metals. Chronic exposure to higher levels of metals can lead to very serious toxicological consequences. These effects depend primarily on the type of exposure (ingestion, inhalation, or dermal absorption), the form of the metal (elemental, salt, vapor, or alloy), the dose, and the length of exposure.[3]

The present study focuses on the overload and toxicity of iron (Fe), aluminum (Al), and soft heavy metals such as lead (Pb), mercury (Hg), arsenic (As), and cadmium (Cd) and ways to remove such metals from biological systems and contaminated solutions. Sources and clinical manifestations of overload of these metals are presented below.

1.2.1 Iron toxicity

Iron is essential for all living organisms as it is involved in many biological functions such as oxygen transport, electron transport, and photosynthesis. Almost all serum iron is bound to the iron binding protein transferrin, resulting in a very low free

serum iron concentration of 10^{-24} M. As there is no known specific mechanism for iron removal in primate metabolism, iron overload is observed when it is introduced in excessive amounts into this closed metabolic loop. In other words, iron toxicity results when the concentration of non-heme iron in the blood stream exceeds the transferrin iron-binding capacity. High iron diet, acute iron ingestion, which can damage intestinal lining and result in increased iron uptake, chronic transfusion therapy for disorders such as thalassemia, hereditary hemochromatosis, etc. are some of the causes of iron overload.[5] Chronic overload leads to peroxidative tissue damage due to the ability of the ferrous ion to catalyze the formation of reactive oxygen species (ROS), such as the hydroxyl radical.[6] These ROS may react with several endogenous molecules (sugars, lipids, proteins and nucleic acids), with subsequent lipid peroxidation, sugar and protein oxidation, as well as DNA and RNA damage, thus leading to various pathological situations.[7] This can lead to organ failure, usually liver and heart, and eventually to death.

1.2.2 Aluminum toxicity

Although aluminum is the third most common element in the earth's crust, it is not essential for plants and animals. In humans, aluminum has no biological function. Unlike other trivalent metals, it has a single oxidation state (+3) and cannot undergo redox chemistry.[8] Aluminum becomes toxic when accumulated in organisms. Cumulative aluminum toxicity has been overlooked until recently. While aluminum has historically been regarded as biologically inert, recent studies suggest toxicity for vulnerable individuals such as premature neonates and patients with renal problems. Acute aluminum toxicity is almost always limited to patients with insufficient renal

functioning.[9] Aluminum toxicity was first recognized in the 1970s as the cause of osteodistrophy and dialysis dementia in patients with renal failure receiving dialysis treatment.[10] Although aluminum toxicity in a healthy human is limited by a combination of poor intestinal absorption and effective renal clearance, it still poses a great threat to the premature neonates and patients with impaired renal function.[11]

There are many sources of aluminum. The major source for most humans is diet. Underarm antiperspirants, vaccines, antacids, parenteral fluids and inhaled fumes and particles from occupational exposure can be significant sources for some people.[12] Parenteral nutrition solutions have been shown to be highly contaminated with aluminum and are the sources of aluminum overload in premature neonates and in patients receiving parenteral nutrition for life support. Aluminum contamination of parenteral fluids and its adverse effects will be described later in this chapter.

Aluminum toxicity has mostly been associated with bone disorders and neurological diseases. Aluminum overload causes a metabolic bone disease by binding phosphate and inducing phosphorus deficiency. Aluminum can also prevent calcium absorption which is vital for bone formation.[13] Due to the binding of aluminum with transferrin (although Al^{3+} cannot displace Fe^{3+} from transferrin), aluminum overload causes hypochromic microcytic anemia. Chronic aluminum toxicity is occasionally seen in chronic dialysis patients. This is termed as the dialysis encephalopathy syndrome. Neurodegenerative diseases like Alzheimer's disease[14] and Parkinson's dementia[15] have also been linked to aluminum overdose. Aluminum overdose does have the potential to produce some neurobehavioral and neuropathologic changes that are seen or are similar to those seen in Alzheimer's disease.[12]

1.2.3 Heavy metal poisoning

Heavy metals are commonly defined as those having a specific density of more than 5 g/cm^3 such as Pb, Hg, As, Cd, etc. They are present in ultra trace amounts in the body but even trace amounts cause serious problems. Heavy metals are toxic because their accumulation causes chronic degenerative changes to the nervous system, liver, and kidneys. In some cases, heavy metals also have carcinogenic effects. They exert their toxic effects by binding with one or more reactive groups such as -SH, -SS-, -NH_2 that are essential for normal physiological functions of biomolecules.[16] The mechanism of toxicity of some heavy metals still remains unknown, although enzymatic inhibition, impaired antioxidants metabolism, free radical formation, and oxidative stress may play a role.[17] Alissa and Fern[17] compiled a table which lists the organs affected by heavy metals and the toxic effects of four heavy metals, As, Pb, Cd, and Hg. Table 1.1 is adapted from Alissa and Fern.[17] Heavy metal poisoning and the efforts by our group to selectively remove heavy metals from environmental waters will be discussed in detail in Chapter 5.

Table 1.1 Toxic effects and organs affected by heavy metals[17]

Heavy metal	Most affected organs	Chronic health effects
Arsenic (As)	• Central nervous system • Lungs • Digestive tract • Circulatory system • Kidneys	• Cancers • Peripheral vascular disease • Skin lesions • Hearing loss • Reproductive toxicity • Hematologic disorders • Neurological diseases • Developmental abnormalities • neurobehavioral disorders
Lead (Pb)	• Central nervous system • Erythropoiesis • Kidneys • Liver	• Cancers • Kidney damage • Neurological diseases • Impaired intellectual ability and behavioral problems in children
Cadmium (Cd)	• Liver • Bone • Lungs	• Cancers • Kidney damage • Bronchiolitis, COPD, emphysema, fribosis • Impaired intellectual ability and behavioral problems in children • Skeletal damage
Mercury (Hg)	• Central nervous system • Liver • Kidneys • Lungs	• Lung damage • Kidney damage • Neurological diseases • Impaired intellectual ability and behavioral problems in children • Metallic mercury is an allergen, which may cause contact eczema • Mercury from amalgam fillings may give rise to oral lichen

1.3 Chelation therapy of metal overload

Chelation therapy has been the major treatment method for metal overload and toxicity. Chelation therapy employs a chelating agent which complexes with metals and allows a swift removal of excess metals from biological systems. The chelating agent displaces metal ions from biological ligands such as proteins and converts them into less toxic forms which can be easily excreted without further interaction with the body.

A chelating agent or a chelator is a multi-dentate ligand that binds to more than one coordination site of a metal ion. The number of coordination sites occupied by a ligand is referred to as denticity. Chelating compounds bind metal ions more tightly than monodentate ligands. The heterocyclic ring formed by the binding of at least two functional groups of a chelator with a metal ion is called a chelate. As an example, catechol **1.1** (Figure 1.1) is a bidentate chelator which forms a five membered chelate ring **1.2** when it binds with metals.

1.1 **1.2**

Figure 1.1 Catechol and its chelation with metals

1.3.1 Iron and aluminum chelating agents

Al^{3+} and Fe^{3+} have ionic radii of 54 pm and 65 pm, respectively. Due to their short ionic radius and their high charge, both metals are hard ions. Their interaction with ligands is a non-covalent interaction which involves ionic or electrostatic bonds.[10] Thus, they have similar binding properties and preferentially bind to hard, negatively charged

oxygen donor ligands such as carboxylates, catecholates, and hydroxamates. Al^{3+} is however less acidic than Fe^{3+}, and therefore, has less affinity towards most hard basic donors than Fe^{3+}.[18] The preferred coordination number for both metal ions is 6, producing octahedral complexes. All Fe chelators are also Al chelators, although the Fe complexes are more stable in most cases. There are no known metal specific chelators between these two metals. Iron overload and toxicity has been long known and the development of iron chelating agents has been extensively studied, thus, development of aluminum chelators is heavily influenced by the known iron chelators. The studies towards the development of iron and aluminum chelating agents are presented below.

The first iron chelating agent introduced to the market was Desferrioxamine (DFO) **1.3** (Figure 1.2) which has been in continuous use for more than 40 years. DFO is a trihydroxamate siderophore produced by *Streptomyces pilosus*.[19] Siderophores are low molecular weight, high affinity, iron chelating compounds secreted by microorganisms for iron uptake and transport. DFO forms a very strong 1:1 octahedral complex with iron and aluminum involving six oxygen atoms of three hydroxamate groups (see Chapter 2 for detail). The main shortcomings associated with DFO are its lack of oral bioavailability and high cost. Other problems such as low efficiency, poor patient compliance, and toxic side effects further complicate DFO treatment.[20] Thus there have been a number of studies related to the development of orally active chelators that are economically and therapeutically more useful.[21] Many DFO analogues and variants have been developed to address this issue, but most of them turn out to be even more impractical than DFO due to their increased molecular weight. Non-hydroxamate based

chelators also have been developed over the years in order to address the same problem.[22] Effort to develop better therapeutic agents for iron chelation therapy is still ongoing.

The most important element in such efforts is the need for the development of orally active iron chelators. Iron chelators currently in clinical practice, other than DFO, are deferiprone **1.4**, and deferasirox (Exjade) **1.5** (Figure 1.2). Deferiprone is a member of the class of compounds 3-hydroxy-4-pyridinones (3,4-HP). Other members of this class of compounds are also investigated as potential iron chelating agents.[7] The oral, three-times-daily agent deferiprone appeared to be a promising advance; however, its use has been limited owing to serious adverse events, such as neutropenia and agranulocytosis. Deferasirox is a novel, orally active agent that provides 24 hour chelation with a once-daily dose.[23] Other potential Fe chelators are deferrithiocin **1.6**, 1-Phenyl-1-hydroxymethylene bisphosphonic acid **1.7**, and kojic acid **1.8** (Figure 1.3), among many others.[24]

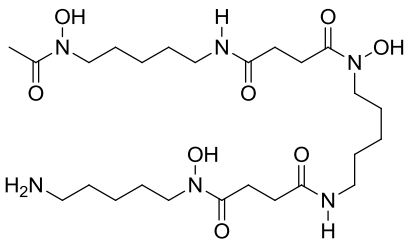

DFO **1.3**

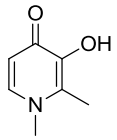

deferiprone **1.4**

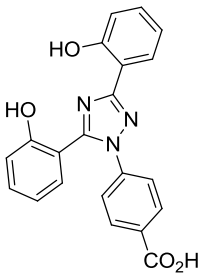

deferasirox **1.5**

Figure 1.2 Structures of iron chelating agents in clinical use[7]

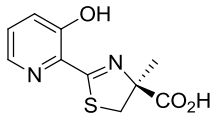

deferrithiocin **1.6**

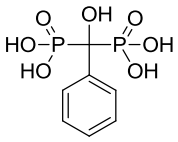

Bis-phosphonic acid **1.7**

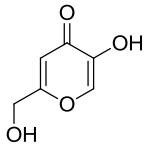

Kojic acid **1.8**

Figure 1.3 Structures of potential iron chelating agents

The first chelating agent introduced into clinical practice for aluminum related diseases was DFO **1.1**. DFO was initially investigated as an aluminum chelator in hemodialysis patients suffering from chronic aluminum intoxication. The choice of DFO was based on its previous use in removing Fe from the liver of dialysis patients. It was found that DFO can reduce aluminum induced mortality associated with the dialysis encephalopathy syndrome, can reduce bone aluminum, and can improve bone histomorphometry.[12] Studies in animals have shown that DFO can increase Al clearance, decrease tissue Al concentrations, and reduce measures of Al-induced toxicity in Al-loaded rats and rabbits. As DFO is not an ideal chelator, particularly for long-term treatment of Al accumulation, there has been a concerted effort to identify orally-effective alternatives. One such alternative is 3,4-hydroxypyridinone (3,4-HP), such as deferiprone **1.4** which has been used in aluminum related conditions. Deferiprone has aluminum chelation efficacy comparable to that of DFO, and more importantly, it is orally active. One shortcoming related to deferiprone, excluding its adverse side effects as mentioned earlier, is that it is a bidentate ligand. A three times higher molar dose is required for the formation of a 1:3 metal to ligand complex.[12] Thus, a search for an orally effective hexadentate aluminum chelator is also still ongoing.

1.3.2 Heavy metal chelating agents

Ethylenediaminetetraacetic acid (EDTA) **1.13** (Figure 1.4) and its various salts are some of the most widely used chelating agents. Unsurprisingly, EDTA has been used for the treatment of lead poisoning. EDTA is a hard and strong chelator and binds not only heavy metals but also hard metal ions unselectively. Thus, preferred ligands for soft metal ions such as Pb^{2+}, Hg^{2+}, Cd^{2+} and As^{3+} are thiolates. Thiols are soft ligands and preferentially coordinate to soft heavy metals. Dimercaprol **1.9** (Figure 1.4), which is also known as British anti-Lewisite (BAL), was discovered and used during World War II in reversing the effects of the chemical weapon, Lewisite (2-chloroethenyl–dichloroarsine).[25] Since then, it has been used clinically as a heavy metal chelating agent. Dimercaprol has serious side effects, which led researchers to develop less toxic analogs. 2,3-dimercaptopropane sulfonate (DMPS) **1.10** is a derivative of dimercaprol and has been used as chelating agent in mercury poisoning, although it is not very effective against lead.[25] D-penicillamine **1.11** is a thiol containing amino acid and another example of a chelating agent for heavy metal toxicity. Only the D isomer of penicillamine is a useful chelating agent, as L-penicillamine is quite toxic. *Meso*-2,3-dimercaptosuccinic acid (DMSA) **1.12** has gained more attention in recent years as a very potent heavy metal chelator.

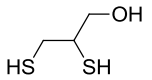

dimercaprol **1.9**

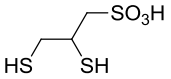

DMPS **1.10**

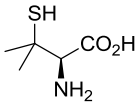

D-penicillamine **1.11**

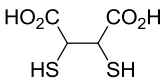

DMSA **1.12**

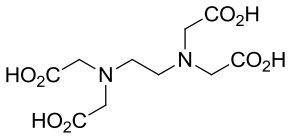

EDTA **1.13**

Figure 1.4 Structures of heavy metal chelating agents

1.4 Premature neonates and total parenteral nutrition (TPN) solutions

Nearly fifteen million babies are born prematurily each year around the world. This is about 10% of the total births. Most premature neonates do not tolerate oral feeding because their gastrointestinal system is not fully developed and require intravenous (IV) feeding. IV feeding is accomplished with a total parenteral nutrition (TPN) solution, which is prepared from a number of component solutions. These additive solutions are categorized into two groups, large-volume parenterals (LVP) and small-volume parenterals (SVP). LVP's are usually solutions of electrolytes, carbohydrates, proteins and emulsion of lipids, and usually packaged in volumes of 100 ml or more. SVP's are usually bottled in 100 ml or less and include solutions of mineral supplements such as calcium gluconate, potassium phosphate, magnesium sulphate, etc.

1.4.1 Aluminum contamination of TPN additives

Aluminum contamination of TPN solutions has been a well recognized problem for many years. Some SVP solutions, especially calcium gluconate and some phosphate

and acetate salts, are substantially contaminated with aluminum. Studies showed that three SVP solutions, calcium gluconate, potassium phosphate, and sodium acetate contribute greater than 90% of aluminum to the final TPN mixture. Calcium gluconate alone accounts for 81% of the aluminum.[26] This contamination is due to the strong binding of ubiquitous aluminum by the gluconate anion during manufacture. Calcium gluconate is manufactured by the oxidation of glucose to gluconic acid followed by treating with calcium carbonate. The exact source of aluminum contamination in calcium gluconate is not known. Aluminum, most probably, comes from raw materials.[27] It also leaches into the solution from glass containers during autoclaving and storage.[27]

1.4.2 Clinical manifestation of aluminum overload in premature neonates

While aluminum has historically been regarded as biologically inert, recent studies suggest toxicity for vulnerable individuals such as premature neonates. Aluminum accumulates in the body when the protective gastrointestinal system is bypassed and renal function is impaired, both of which apply to premature neonates. Premature neonates who receive TPN solution are especially prone to aluminum toxicity as their kidney function is immature, and the TPN solution bypasses the protective barrier of the gastrointestinal tract. Clinical manifestations of long term exposure to toxic levels of aluminum include anemia, impaired bone growth,[28] and delays in mental development[29] because most of the aluminum gets deposited in the bone, liver, and brain. Neonates who receive TPN solution are thus at high risk for impaired neurologic development and metabolic bone disease. It is reported that neonates receiving 3 weeks of parenteral therapy have 10 times higher aluminum concentration in bone marrow than those receiving limited parenteral

therapy.[30] A study by Bishop and coworkers showed that premature infants who received standard TPN had lower neurologic development scores than those who received a specially-made aluminum-depleted TPN solution.[31] Many studies confirm that neonates receiving parenteral therapy are at high risk of aluminum overload and toxicity. The US Food and Drug Administration (FDA) has recognized aluminum contamination in TPN solution and has established an upper limit on the permissible amount of aluminum.[27] However, industry has been unable to meet this standard because there is no technology available to effectively remove aluminum from the calcium gluconate.

1.4.3 Previous attempts to address the problem

At present, there are very few options to reduce the aluminum load in TPN solutions. Bishop and coworkers[31] suggested the use of calcium chloride instead of calcium gluconate in TPN solutions. Calcium chloride is inherently less contaminated with aluminum and in theory can replace calcium gluconate. However, as a chloride salt, calcium chloride can predispose children to a greater risk of developing metabolic acidosis due to the increased chloride load.[32] One study in Germany showed a significant reduction in the amount of aluminum in calcium gluconate by using plastic containers instead of glass containers to store calcium gluconate solution.[26] This solves the problem only if the source of aluminum is glass containers. The United States Food and Drug Administration (FDA) recognized the aluminum contamination of TPN additives, established the upper limit of aluminum in large-volume parenterals (25 µg/L), and requested manufacturers to label the maximum amount of aluminum in small-volume parenterals at the product's date of expiration.[27] This only documents estimated

aluminum concentration and neither gives exact aluminum concentration nor reduces the aluminum in SVPs. The FDA also established a safe level of aluminum exposure in a TPN therapy which is less than 5 µg/Kg/day. In one attempt to address the problem, Hayes and coworkers[33] tried to form an Al-DFO complex and irreversibly bind all aluminum present in TPN prior to its administration with DFO. This was accomplished by determining mean Al concentration in TPN solutions, followed by adding a sufficient amount of DFO to chelate any aluminum and iron present. No real solution of effectively removing aluminum from TPN components is available yet. Manufacturers continue to work on reducing aluminum content in their products, though it is impractical as yet to get to the desired safe level. It is currently impossible to get aluminum levels below 12-13 µg/Kg/day in a normal mix of TPN without removing essential components.[34] The FDA cautions that it is more important to receive the essential nutrients in TPN as prescribed by a physician than to omit any ingredient because of possible aluminum toxicity.

1.5 The technology of employing immobilized chelators

We recently developed a technology to remove aluminum from contaminated calcium gluconate solutions without affecting the essential calcium present in the solution. We designed and synthesized metal specific chelators and immobilized these chelators on a solid support resin.[35] These chelator functionalized resins, called chelating resins, are used to remove toxic metal ions from such contaminated solutions. Hydroxamate and citratamide based chelators are employed to extract trivalent metal ions

such as aluminum and iron, whereas dithiolate based chelators are used for removing soft metals such as lead from contaminated solutions.

There have been previous examples of chelating resin for similar applications. Detailed explanations and literature examples of related chelating resins are provided in chapters 3, 4, and 5.

A chelating resin is made up of three parts, a solid support, a linker, and a functional unit involved in the binding. The parts of a chelating resin are shown in Figure 1.5 as a representative example. A polystyrene resin is a solid support which is extremely cost effective and can be purchased with various bead sizes and other resin properties. A linker is a group that covalently attaches the functional unit to the solid support. In this work, various linkers such as urea, sulfonamide, and secondary amine will be employed. The functional unit is usually a multidentate ligand designed to selectively and strongly bind the targeted metal ion. The example in Figure 1.5 shows a hydroxamate chelator as a functional unit which is immobilized on a polystyrene resin solid support via a urea linker. As mentioned earlier, the design of the chelator group is solely dependent on the nature of the metal ion to be extracted from aqueous solution.

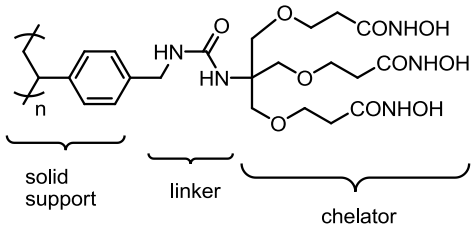

Figure 1.5 Parts of a chelating resin

Our hypothesis is that if a metal contaminated solution is passed through a cartridge filled with a chelating resin, the toxic metal for which the chelator was designed should be selectively removed, and the solution should pass through virtually unchanged in terms of the other essential metal ions. In this particular example, as the binding affinity of hydroxamates with trivalent metal ions such as aluminum is much higher than with divalent metal ions such as calcium, hydroxamate functionalized chelating resin should remove aluminum from calcium gluconate solutions.

Before immobilizing the chelators on solid support, analogous solution phase hydroxamate ligands were designed and synthesized. Aluminum and iron binding affinities of these ligands were determined using potentiometric and UV-Vis spectrophotometric titration methods. These solution phase hydroxamate ligands have potential application as chelating agents in iron and aluminum overload conditions. The design, synthesis, and trivalent metal binding studies of novel hydroxamate ligands will be discussed in chapter 2. Some of the hydroxamate ligands with highest binding affinity were immobilized on solid support such as macroporous polystyrene resin via various possible linkages. The effect of the linker on binding was studied. The synthesis and aluminum extraction from commercial calcium gluconate solution by our hydroxamate resins will be discussed in chapter 3. Some applications may require chelating resins be able to bind trivalent metals at low pH. As citrate binds trivalent metal ions more strongly than hydroxamates in highly acidic solutions, citramide functionalized resins were synthesized for such applications. The design, synthesis, and iron chelation of citramide functionalized resins will be discussed in chapter 4.

1.6 Application of chelating resin in environmental remediation of soft metals

The current technology of environmental remediation from highly toxic soft metals such as Hg, Pb, Cd, and As relies on methods such as reverse osmosis, chemical precipitation, ion exchange, and bioremediation. None of these methods are without some drawbacks. Thus, effective environmental remediation of heavy metals usually requires a combination of these methods. There have been few previous research efforts to design and synthesize soft metal specific chelating resins. We propose the immobilization of dithiolate ligands such as dimercapto succinic acid (DMSA) on polystyrene resin for the preparation of soft metal selective chelating resins. There are numerous applications for resins capable of removing hazardous metal ions from water, including treatment of runoff and waste water, and the purification of drinking water. An effective resin would allow one to produce large volumes of purified water while concentrating the metals into a small volume for recycling or disposal. These chelating resins can be easily transported to the site of metal removal. The design, synthesis, and lead chelation studies of dithiolate resins will be discussed in chapter 5.

References

[1] Lippard, S. J.; Berg, J. M. *Principles of Bioinorganic Chemistry*, University Science Books, **1994**, p 1.

[2] Guengerich, P. F. *The Journal of Biological Chemistry* **2012**, 287, 13508-13509.

[3] Hollenberg, P. F. *Chem. Res. Toxicol.* **2010,** *23*, 292-293.

[4] Suckling, K. E; Suckling, C. J. *Biological chemistry: the molecular approach to biological systems*, Cambridge University Press, **1980**, p 188.

[5] Bergeron, R. J.; Liu, C. Z.; McManis, J. S.; Xia, M. X. B.; Algee, S. E.; Wiegand J. *J. Med. Chem.* **1994**, 37, 1411-1417.

[6] Turcot, I.; Stintzi, A.; Xu, J.; Raymond, K. N. *J. Biol. Inorg. Chem.* **2000**, 5, 634-641.

[7] Santos, M. A.; Marques, S. M.; Chaves, S. *Coordination Chemistry Reviews* **2012**, 256, 240-259.

[8] (a) Bowen, H. J. M. *Environmental chemistry of the elements*, Academic Press: New York, **1979,** P 103. (b) Hawkins, N. M.; Coffey, S.; Lawson, M. S.; Delves, H. T. *J. Pediatr. Gastroenterol. Nutr*. **1994**, 19, 377.

[9] Phelps, K. R.; Naylor, K.; Brien, T. P.; Wilbur, H.; Haqqie, S. S. *Am. J. Med. Sci.* **1999**, 318, 181.

[10] Crisponi, G.; Nurchi, V. M.; Bertolasi, V.; Remelli, M.; Faa G. *Coordination Chemistry Reviews* **2012**, 256, 89-104.

[11] Wróbel, K.; González, E. B.; Wróbel, K. A. *Analyst* **1995**, 120, 809.

[12] Yokel, R. A. *Coordination Chemistry Reviews* **2002**, 228, 97-113.

[13] Gura, K. M.; Puder, M. *Current Opinion in Clinical Nutrition and Metabolic Care* **2006**, 9, 239-246.

[14] Good, P. F.; Perl, D. P.; Bierer, L. M.; Schmeidler J. *Ann. Neurol*. **1992**, 31, 286.

[15] Perl, D. P.; Gajfusek, D. C.; Garruto, R. M.; Yanagihara, R. T.; Gibbs, C. J. *Science* **1982**, 217, 1053.

[16] Margel, S. *J. Med. chem.* **1981**, 24, 1263-1266.

[17] Alissa, E. M.; Ferns, G. A. *J. Toxicol.* **2011**, volume 2011, Article ID 870125.

[18] Srisung, S. Ph. D. Dissertation, University of Missouri-St. Louis, **2007**.

[19] Bickel, H.; Fechtig, B.; Hall, G. E.; Keller-Schierlein, W.; Prelog, V. *Helv. Chim. Acta* **1960**, 43, 2129.

[20] (a) Kirking, M. H. *Clin. Pharm.* **1991**, *10*, 775-783. (b) Hershko, C.; Konijn, A. M.; Link, G. *Br. J. Haematol.* **1998**, 101, 399-406.

[21] (a) Bergeron, R. J.; Wiegand, J.; Bharti, N.; McManis, J. S. *J. Med. Chem.* **2012**, 55, 7090−7103 (b) Bergeron, R. J.; Wiegand, J.; McManis, J. S.; Bharti, N. *J. Med. Chem.* **2006**, 49, 7032−7043.

[22] (a) Abergel, R. J; Raymond, K. N. *Inorg. Chem.* **2006**, 45, 3622-3631. (b) Hay, B. P.; Dixon, D. A.; Vargas, R.; Garza, J.; Raymond, K. N. *Inorg. Chem.* **2001,** 40, 3922-3935. (c) Hou, Z; Stack, T. D. P.; Sunderland, C. J.; Raymond, K. N. *Inorganic Chemica Acta* **1997**, 263, 341-355.

[23] Cappellini, M. D.; Pattoneri, P. *Annu. Rev. Med.* **2009**, 60, 25-38.

[24] Crisponi, G.; Dean, A.; Marco, V. D.; Lachowicz, J. I.; Nurchi, V. M.; Remelli, M.; Tapparo, A. *Anal. Bioanal. Chem.* **2013**, 405, 585-601.

[25] Flora, S. J. S.; Pachauri, V. *Int. J. Environ. Res. Public Health* **2010**, 7, 2745-2788.

[26] (a) Mouser, J. F.; Wu, A. H.; Herson, V. C. *Am. J. Health Syst. Pharm.* **1998**, 55, 1071-1072. (b) Smith, B. S.; Kothari, H.; Hayes, B. D.; Tataronis, G.; Hudlin, M.; Doole, J.; Hartman, C. *Am. J. Health Syst. Pharm.* **2007**, 64, 730-739.

[27] Food and Drug Administration *Federal Register* **1998**, 63, 176.

[28] (a) Klein, G. L. *Am J Clin Nutrv* **1995**, 61, 449-456. (b) Fewtrell, M. S.; Bishop, N. J.; Edmonds, C. J.; Isaacs, E. B.; Lucas, A. *Pediatrics* **2009**, 124, 1372-1379.

[29] Mirtallo, J. M. *J. Parenter. Enteral. Nutr.* **2010**, 34, 346.

[30] Kerr, D. N. S.; Ward, M. K.; Arze, R. S.; Ramos, J. M.; Grekas, D.; Parkinson, I. S.; Ellis, H. A.; Owen, J. P.; Simpson, W.; Dewar, J.; Martin, A. M.; McHugh, M. F. *Kidney International Supplement* **1986**, 18, S-58.

[31] Bishop, N. J.; Morley, R.; Day, J. P.; Lucas, A. *The New England Journal of Medicine* **1997**, 22, 1557-1561.

[32] Gura K. M. *Nutrition* **2010**, 26, 585.

[33] Hayes, P.; Martin, T. P.; Pybus, J.; Hunt, J.; Broadbent, R. S. *Journal of Parenteral Science and Technology* **1992**, 46, 169-175.

[34] http://www.oley.org/lifeline/aluminum.html

[35] Yokel, R. A.; Harris, W. R.; Spilling, C. D.; Kuhn, R. J.; Dawadi, S. *U.S. Pat. Appl. Publ.* **2012**, US 2012/0061325 A1.

CHAPTER 2: Design, synthesis, and trivalent metal chelation properties of novel hydroxamate ligands

2.1 Specific objectives

The objectives of this project were:

1) Design and synthesize novel hydroxamic acid based chelating compounds such as tripodal trihydroxamate and dipodal tetrahydroxamate ligands. These hydroxamate ligands are designed to have strong affinity towards trivalent metal ions such as Fe^{3+} and Al^{3+} in aqueous solution. Such solution phase chelators have potential application as chelating agents in chelation therapy for the treatment of trivalent metal overload.

2) Study the coordination behavior of these chelators with trivalent metals such as iron and aluminum will be studied.

2.2 Background

A chelator or a chelating compound is a polydentate ligand that binds with metal ions to form a stable chelate ring in which a ligand binds to more than one coordination sites of the metal ion. The chelating compounds have long been used to bind metal ions in the fields of environmental remediation, mining industry, and relatively recently in medicine for the treatment of metal poisoning. They also have been used in chemical analysis. Ethylenediaminetetraacetic acid (EDTA) has been used extensively in complexation titration for the quantitative analysis of metal ions. In recent years, a treatment method employing chelating agents to remove toxic metals from biological systems, referred to as chelation therapy, has been developed. The major problem associated with chelation techniques is the lack of absolute metal specific chelator groups. The highest level of selectivity is achieved if the chelators are designed on the basis of the hard and soft acids and bases (HSAB) principle. Hard ligands prefer to bind hard metal ions and soft polarizable ligand groups prefer to bind soft metals. Trivalent

metal ions such as iron and aluminum are hard metal ions, and they prefer to bind with hard ligands such as hydroxamates and catecholates. Not surprisingly, hydroxamates and catecholates are also the most common binding groups present in natural siderophores.

Siderophores are low molecular weight high affinity iron chelating compounds secreted by microorganisms for iron uptake and transport. Microorganisms synthesize and utilize siderophores to sequester iron, which is present in the environment as ferric oxide or hydroxide, the predominant and very less soluble state of iron. Over the years, several siderophores have been isolated from various microorganisms and characterized. Most of these natural siderophores can be classified into two classes, hydroxamate and catecholate binding group containing compounds. Desferioxamine-B **2.1** (DFO)[1] and enterobactin **2.2** (Figure 2.1) are respective examples of these two classes of siderophores. These compounds form very stable complexes with iron. The stability constant, log β, for hydroxamate and catecholate siderophore-Fe^{3+} complexes are close to 30 and 49, respectively, indicating very strong binding.[2] These numbers also suggest that the catecholate chelators typically bind iron far more tightly than hydroxamates. The major functional difference between hydroxamate and catecholate siderophores is related to environmental iron concentration. The hydroxamates are generated by the microorganism in a high-iron environment, while the catecholate system is activated when iron concentrations are low.[3] Once the nutritious iron is taken into the cell, microorganisms release it from these tight binding siderophores either by the degradation of ligands or by the reduction of iron from ferric(III) to ferrous(II). The ferrous ion has much lower affinity towards siderophore ligands.

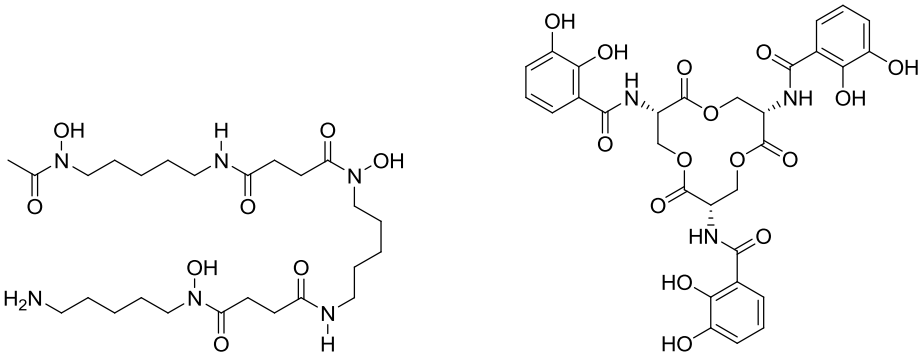

DFO **2.1** Enterobactin **2.2**

Figure 2.1 Two classes of siderophores, hydroxamates (DFO) and catecholates (enterobactin)

Siderophores can also be classified into three topological families, linear **2.3**, tripodal **2.4**, and macrocyclic **2.5** (Figure 2.2).[4] As seen from their structures, DFO and enterobactin are linear and tripodal siderophors, respectively. An example of a natural macrocyclic siderophore is nocardamine **2.6** (Figure 2.3).[5] It has a 33 membered macrocyclic ring containing three hydroxamate binding groups. It also has three amide groups for intramolecular hydrogen bonding, which are responsible for bringing hydroxamate groups in right orientation for strong binding.

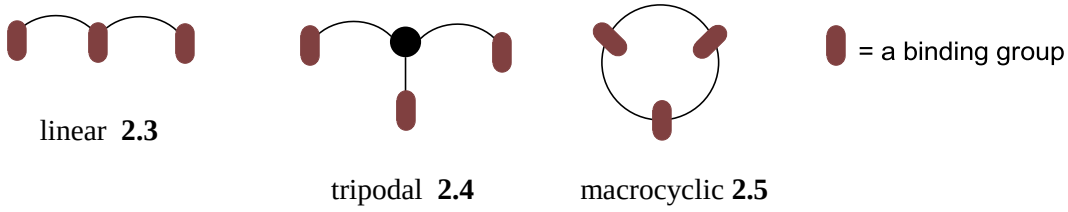

linear **2.3** tripodal **2.4** macrocyclic **2.5**

Figure 2.2 Three topological families of siderophores

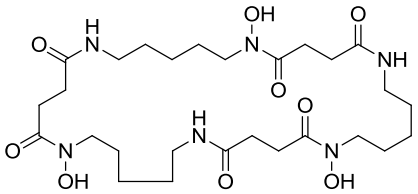

2.6

Figure 2.3 Macrocyclic siderophore nocardamine

Siderophores are almost always trihydroxamate or tricatecholate compounds. The reason for this is both hydroxamate and chatecholate are bidentate ligands and the six coordination sites of trivalent metals are fulfilled by three of these chelating groups. Hydroxamates and catecholates are both very basic, negative oxygen donors, and have high affinity towards highly acidic, hard metal ions such as Fe^{3+} and Al^{3+}. Single deprotonation of a hydroxamic acid **2.7** turns it into a hydroxamate group, a bidentate ligand (Figure 2.4). A hydroxamate group contains two donor oxygen atoms, one binds covalently through its negative charge, the other coordinate covalently through its lone pair of electrons to form a five membered chelate ring as shown in structure **2.8** (Figure 2.4).

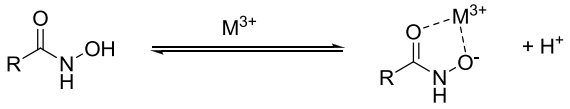

2.7 **2.8**

Figure 2.4 Trivalent metal coordination of a simple hydroxamic acid

Several research efforts have been undertaken to synthesize natural and unnatural siderophores since the 1980's, primarily to develop a better chelating agent in the chelation therapy of iron overload. Like natural siderophores, artificial siderophores were also designed mostly to have hydroxamate and sometimes catecholate binding sites. Early efforts in the design, synthesis, and metal chelation properties of natural and synthetic hydroxamate siderophores were reported by Bergeron,[3,6] Raymond,[7] Martell,[8,21] Miller,[9,19] Neilands,[10] Shanzer,[11] and Marshall.[12] Raymond particularly was more interested in catecholate siderophores.

There are several examples of the design and synthesis of natural and artificial DFO-like linear trihydroxamates reported in the literature. These linear trihydroxamates are usually unsymmetrical and require many synthetic steps for their preparation. This is one of the reasons for DFO being highly expensive which is why it is produced commercially by large-scale fermentation of a strain of *Streptomyces pilosus*.[13] There are also several examples of tripodal trihydroxamate ligands reported in the literature.[15-22]

Rationally designed tripodal chelators consist of three parts: a spacer group, a connecting group, and a binding group as seen in cartoon **2.9** (Figure 2.5).[14] The spacer group, sometimes referred to as an anchor, distributes three alkyl chains each bearing a binding unit around the central bridgehead atom called the pivotal atom. The nature and size of the spacer group are responsible for optimal binding. The connecting group determines the nature of the chain and is obtained by the coupling of the spacer group with the binding unit. The binding unit is usually a bidentate ligand such as a hydroxamate. The spacer unit is sometimes designed to possess a site for further functionalization or for immobilization of the chelator on a solid support.

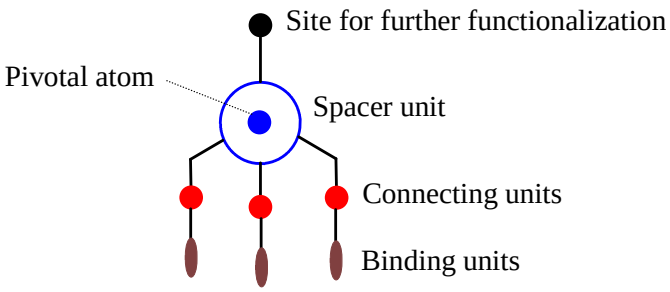

2.9

Figure 2.5 Parts of a tripodal chelator

Ferrichrome **2.10** (Figure 2.6) is an example of natural tripodal trihydroxamate siderophore. It has an 18 member macrocylic ring as spacer group which bears three side chains, each having a terminal hydroxamate group. The stability constant log β for the ferricrome iron complex is 29.1.[15]

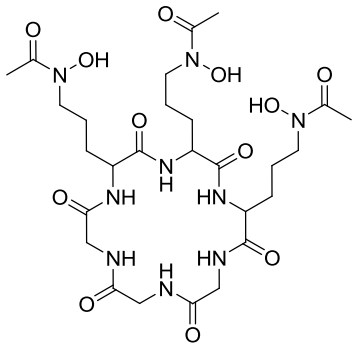

2.10

Figure 2.6 Natural tripodal siderophore ferrichrome

There are several examples of synthetic tripodal trihydroxamate chelators designed to bind trivalent metal ions. Most of these synthetic trihydroxamates were

designed as ferrichrome analogs where various tripodal spacers (anchors) are employed instead of the macrocyclic ring. Most of these artificial trihydroxamate ligands were designed to maintain the strong iron chelating affinity of natural siderophores. Almost all examples of these artificial tripodal trihydroxamates are symmetrical; i.e. they have exactly the same side chains each bearing a hydroxamate binding unit. The presence of symmetry makes synthesis of these chelators much easier than that of unsymmetrical linear siderophores such as DFO. Some of the literature examples of artificial tripodal trihydoxamate chelators will be discussed below.

Masuda and coworkers reported the synthesis of tris(2-aminoethyl)amine (TREN, **2.11**) anchored trihydroxamate ligands **2.12** and **2.13** (Figure 2.7) and their Fe^{3+} complexes.[15] The crystal structure of the tris(hydroxamato)Fe^{3+} complex of ligand **2.12** suggested that multi-intramolecular hydrogen bonding networks formed between amide N-H and coordinating N-hydroxy oxygen of hydroxamate group contribute to tight binding and stable complex formation when n=1.[15,16] The complex was less stable for ligand **2.13** due to the lack of such intramolecular hydrogen bonding which requires the formation of a seven membered ring. The stability constant log β for ligand **2.12** iron complex was reported to be 28.7 which is comparable to that of natural siderophore ferrichrome **2.10**, (29.1).

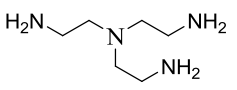

TREN **2.11**

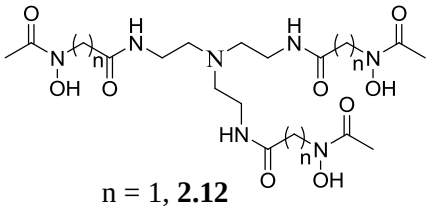

n = 1, **2.12**
n = 2, **2.13**

Figure 2.7 TREN and Masuda's TREN based trihydroxamate ligands

Masuda's group also reported the synthesis of tris(3-aminopropyl)amine (TRPN, **2.14**) anchored tripodal trihydroxamate ligand **2.15** (Figure 2.8) and its Fe^{3+} complex.[17] Previous studies by Raymond and coworkers suggested that the TREN **2.11** has too small a backbone for optimal binding, at least in the tricatecholate system of artificial enterobactin analogs.[18] TRPN has one more methylene unit in all of its three alkyl chains than in TREN. They concluded that the TRPN based trihydroxamate **2.15** indeed forms more stable iron complexes than the TREN based trihydroxamate **2.12**. The iron binding constant log β for ligand **2.15** was reported to be 30.6 which is almost 2 log units higher than that of ligand **2.12** (log β = 28.7).

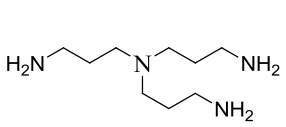

TRPN **2.14**

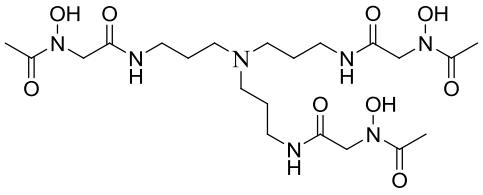

2.15

Figure 2.8 TRPN and Masuda's TRPN based trihydroxamate ligand

Masuda's group recently reported the synthesis of tripodal trihydroxamate **2.16** where the pivotal atom is a quaternary carbon rather than a tertiary nitrogen (Figure 2.9).[2] They prepared iron complex of ligand **2.16** and the stability constant log β was determined to be 31.0 which is very close to that of DFO (log β = 30.6) and higher than their previous ligands, indicating that **2.16** is strongly bound to Fe^{3+}.

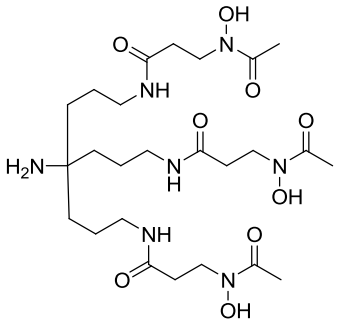

2.16

Figure 2.9 Masuda's recent trihydroxamate ligand

Miller and coworkers reported the design and synthesis of trihydroxamate ligands **2.17**, **2.18**, and **2.19** (Figure 2.10) anchored through amide bonds to tripodal spacers benzenetricarboxylic acid, nitrilotriacetic acid, and tricarballylic acid respectively.[19] These trihydroxamate ligands behaved as well as the natural siderophore ferrichrome for providing iron nutrition in *Escherichia coli* RW193, suggesting they are strong iron chelators.

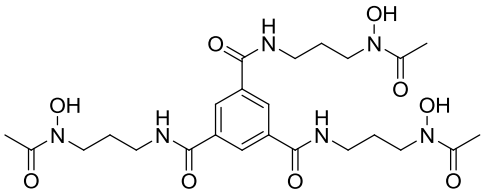

2.17

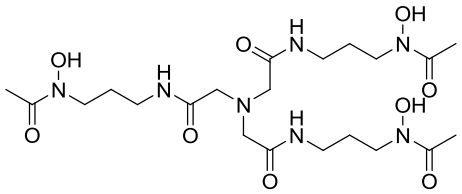

2.18

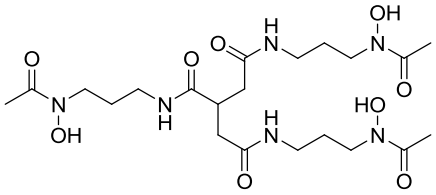

2.19

Figure 2.10 Miller's tripodal trihydroxamate ligands

Spacer groups containing N pivotal atom offers a severe limitation since its protonation results in the formation of quaternary ammonium salts which alter the optimum electronic and geometric properties of the overall molecules and their metal complexes.[14] Shanzer and coworkers reported the design and synthesis of tripodal trihydroxamates as ferrichrome analogs built on 1,1,1-tris(hydroxymethyl)propane anchor **2.20** (Figure 2.11) where the pivotal atom is a quaternary carbon.[20] They studied the iron chelation of these hydroxamate ligands and found that the number of atoms between pivotal atom and amide carbonyls plays an important role. Trihydroxamate **2.21** which has four such atoms has much better iron binding affinity than its shorter homologue having only three such atoms.

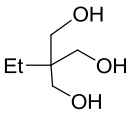

2.20

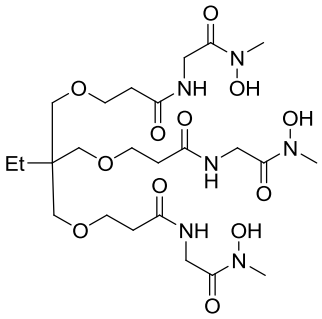

2.21

Figure 2.11 1,1,1-tris(hydroxymethyl)propane and Shanzers's trihydroxamate ligand

Martell and coworkers reported the design and synthesis of tripodal trihydroxamate ligands based on 1,1,1-tris(hydroxymethyl)ethane anchor **2.22** (Figure 2.12), and studied the binding properties of these ligands with Fe^{3+} and Ga^{3+}.[21] Ligand **2.23** which has four atoms between bridgehead carbon and first atom of hydroxamate, and ligand **2.24** which has five such atoms, were designed to be homologous. They were

designed to study the effect of chain length on binding affinities. Each side chain of these ligands possesses ether connecting group rather than amide groups despite the fact that amide is the most commonly used connector group between the bridgehead atom and the binding site. Compound **2.23** has terminal methylhydroxyamino hydroxamate groups whereas compound **2.24** has N-acetyl hydroxamates. Ligand **2.23** was found to have higher Fe^{3+} binding constants than **2.24**, although surprisingly, Ga^{3+} binding constants are in reverse order.

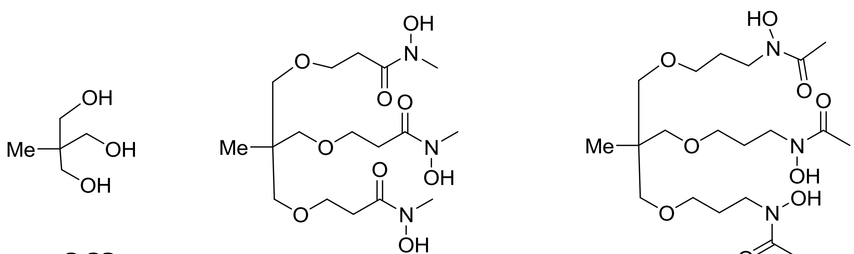

2.22 **2.23** **2.24**

Figure 2.12 1,1,1-tris(hydroxymethyl)ethane and Martell's trihydroxamate ligands

Dias and coworkers reported the design and synthesis of trihydroxamate **2.26** anchored on the tripodal support tris(hydroxymethyl)aminomethane (tris) **2.25** (Figure 2.8). Ligand **2.26** was designed to contain a terminal primary amine group on the bridgehead quarternary carbon. They also attached a fluorescent group on the free amine to prepare fluorescent labeled trihydroxamate chelator.[22] The fluorescent labeled siderophore was used to study iron uptake and transport in microorganisms. This trihydroxamate showed comparable iron uptake activities as natural siderophore ferrichrome in some microorganisms.

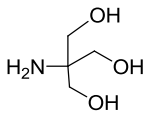

tris **2.25**

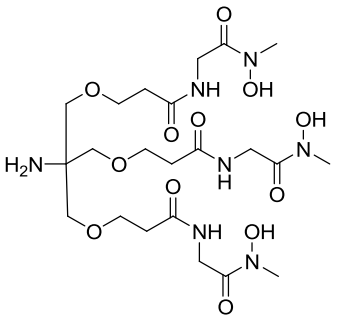

2.26

Figure 2.13 1,1,1-tris(hydroxymethyl)aminomethane (tris) and Dias' trihydroxamate ligand

These examples showed the availability of various tripodal anchors on which the trihydroxamates can be attached. The anchor backbone size plays an important role on the stability of metal ligand complex. In the present work, the use of hydroxyalkylaminomethanes as a tripodal anchor for the construction of tripodal trihydroxamates is described. Hydroxyalkylaminomethanes such as tris **2.25** contain a free primary amine group on bridgehead carbon. The presence of the free amine allows us to attach these compounds on a solid support for the preparation of chelating resins, which will be described separately in Chapter 3. Thus, combining the features of two previously mentioned trihydroxamates **2.23** and **2.26**, Spilling and coworkers designed trihydroxamate ligand 222-THA **2.27** (Figure 2.14). Two other tripodal trihydroxamate ligands **2.28** and **2.29** with slightly modified spacer and connecting groups were also designed and synthesized. In the present work, we report the design and synthesis of these three tripodal trihydroxamate ligands **2.27-2.29**. Two symmetrical dipodal tetrahydroxamates, which somewhat mimic the linear structure of high affinity siderophore DFO, were also designed and synthesized, and will be described later in this

chapter. All of these hydroxamate chelators are designed to have easy, high yielding, and cost effective synthetic routes. Iron and aluminum coordination behavior of these chelators was studied and will also be described later in this chapter.

2.3 Design and synthesis of novel tripodal trihydroxamate ligands

2.3.1 Design of trihydroxamate ligands

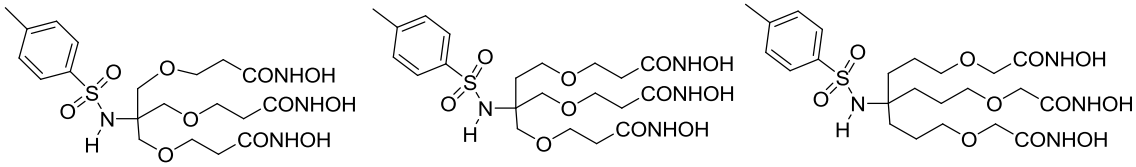

222-THA **2.27** 223-THA **2.28** 333-THA **2.29**

Figure 2.14 Trihydroxamate ligands 222-THA, 223-THA, and 333-THA

The original ligand designed was 222-trihydroxamic acid (222-THA) **2.27** (Figure 2.14).[23] Tris(hydroxymethyl)aminomethane (tris) **2.25** (Figure 2.13), which contains a quaternary carbon as a bridgehead atom, was used as the tripodal base. The number 2 in its name refers to the number of methylene groups between the original tris hydroxyl oxygen and hydroxamate carbon. It is a C_3 symmetrical tripodal ligand with N-terminal hydroxamic acids at the end of each arm. Each arm contains an ether connecting group instead of commonly used amide groups. The free amine present on the bridgehead carbon was protected with a tosyl group for the preparation of solution phase ligands. The free amine can also be used to attach these ligands to various solid supports for the synthesis of chelating resins. The tosyl group was specifically chosen as the amine protecting group because it not only resembles the sulfonamide, a possible linker that will

be employed to make chelating resins, but also the polystyrene resin backbone (see chapter 3).

Unsymmetrical 223 trihydroxamic acid (223-THA) **2.28** was designed to have one arm longer than other two arms (one methylene unit added at the position between tertiary carbon and ether oxygen). It was assumed that the two shorter arms would first form the bis-complex **2.30** with the metal and the third longer arm binds afterwards to form the tris-complex **2.31** (Figure 2.15). This process was expected to be easier than in 222-THA, where all the arms are equal. It was anticipated that the strain on the bridgehead carbon is somewhat relieved when one of the arms is slightly longer.

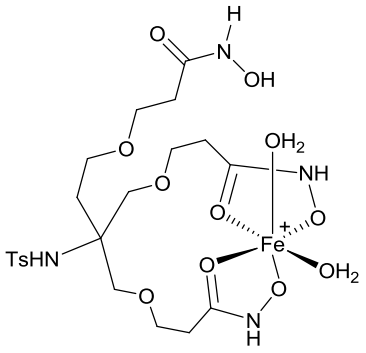

Bis-complex **2.30**

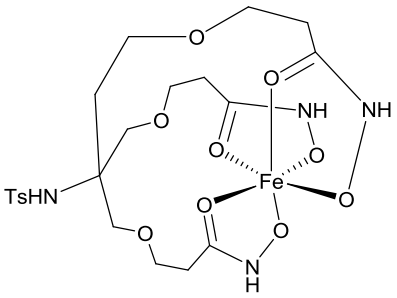

Tris-complex **2.31**

Figure 2.15 Bis- and tris-complexes of 223-THA with iron

The third trihydroxamate ligand designed was symmetrical 333-trihydroxamic acid **2.29** (333-THA), which has one more methylene group in each arm than in 222-THA. One methylene group is removed from the position between ether oxygen and hydroxamate, but two are added between the tertiary carbon and the ether oxygen. It was designed to have all three connecting groups longer than in the previous two ligands.

Commercial availability of the aminitriol **2.43** as a tripodal anchor was also a major factor for the selection of this ligand.

2.3.2 Synthesis of 222-THA

The trihydroxamate 222-THA **2.27** was previously synthesized by Spilling and coworkers[24] (Scheme 2.1). The tris **2.25** was reacted with acrylonitrile in the presence of catalytic amount of KOH to obtain the tris-nitrile **2.32**.[25] The low yield of 33% is presumably due to the low solubility of the triol in dioxane. The use of other solvents such as acetonitrile was recently shown to improve the yield. Reaction of **2.32** in refluxing methanolic HCl gave the tris-methyl ester **2.33**, which was then reacted with tosyl chloride (TsCl) and Et_3N in CH_2Cl_2 to obtain the sulfonamide tris-ester **2.34**. The ester was converted to the hydroxamic acid **2.27** by reacting with O-trimethylsilyl hydroxylamine (NH_2OTMS) in MeOH. The ligand **2.27** was solid and purified by recrystallization, and its structure was further verified by X-ray crystallography (Figure 2.16).

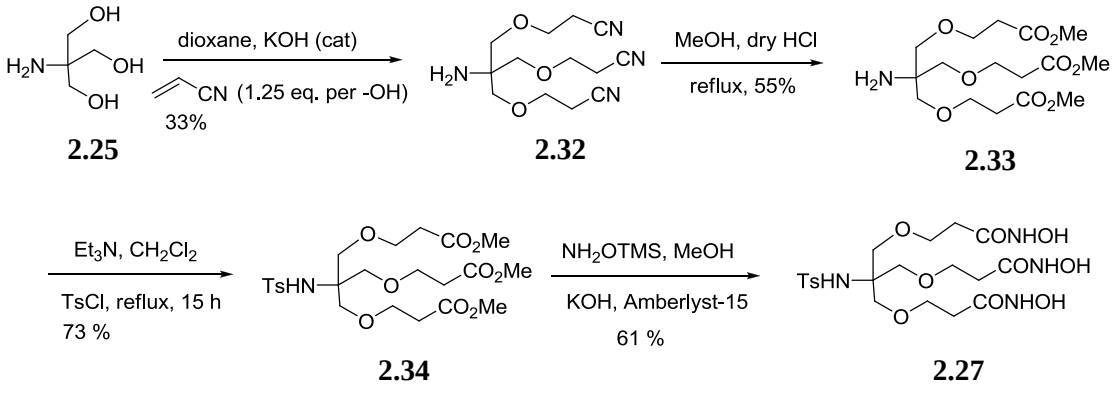

Scheme 2.1 Synthesis of 222-THA

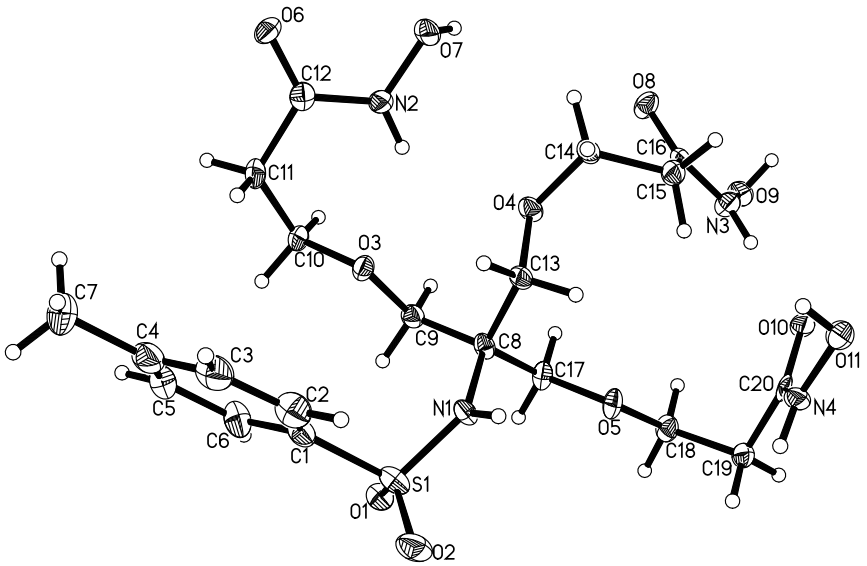

Figure 2.16 Crystal structure of 222-THA

A more efficient and higher yielding synthetic route from **2.25** to **2.33** has been developed (Scheme 2.2).[26] The reaction conditions were optimized and the synthesis was scaled up. The tris **2.25** was treated with *tert*-butyl acrylate in the presence of 5M NaOH in DMSO to give the compound tris-*tert*-butyl ester **2.35** in 75% yield.[27] Tert-butyl esters were converted to methyl esters by treating with concentrated sulfuric acid in dry MeOH to produce the compound **2.33** in 76% yield. The overall yield of 57% from **2.25** to **2.33** (Scheme 2.2) by this route is much better than that of 18% by previous route (Scheme 2.1). Compound **2.33** was prepared in more than a 20 g scale following this optimized synthetic route.

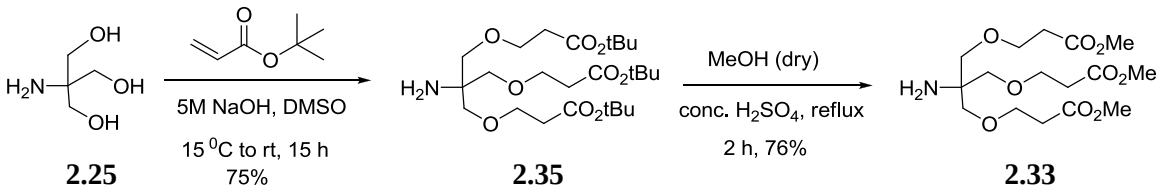

Scheme 2.2 A more efficient synthetic route to compound 2.33

2.3.3 Synthesis of 223-THA

Synthesis of the unsymmetrical tripodal ligand 223-THA **2.28** began from acrolein (Scheme 2.3). 3-Nitropropanol **2.36** was prepared from acrolein following the published procedure.[28] Michael addition of sodium nitrite to acrolein in the presence of acetic acid led to the formation of 3-nitropropanal, which was then reduced using sodium borohydride to give 3-nitro propanol **2.36** in 90% overall yield for the two steps. Base catalyzed addition of **2.36** with two equivalents of formaldehyde gave nitrotriol **2.37** in 84% yield. The nitro group of **2.37** was reduced to an amine by hydrogenation using specially generated T-1 Raney nickel as a catalyst[29] (see experimental section for the process of generating T-1 Raney Nickel) and hydrogen at 45 psi[30] to obtain aminotriol **2.38** in almost quantitative yield. T-1 Raney Nickel is extremely pyrophoric in nature because hydrogen gas generated during the reaction of aluminum and base is trapped on the highly porous nickel surface. Other hydrogenation conditions such as 10% palladium on charcoal with H_2, transfer hydrogenation employing ammonium formate and 10% palladium on charcoal, or employing ammonium formate and activated zinc were all unsuccessful for this reduction. Compound **2.38** was treated with acrylonitrile in the presence of a catalytic amount of KOH pellets in dioxane to obtain the tris nitrile **2.39**. The moderate yield of 49% was again attributed to the low solubility of the triol in

dioxane. Reaction of **2.39** in refluxing methanolic HCl gave the tris-methyl ester **2.40** in 74% yield, which was then reacted with tosyl chloride and Et_3N in CH_2Cl_2 to obtain the sulfonamide tris-ester **2.41** in 75% yield. Compound **2.41** was converted to the hydroxamate ligand **2.28** in 88% yield by the reacting with O-trimethylsilyl hydroxylamine and KOH in methanol followed by protonation with strong acidic resin (amberlyst-15). The crude product was a sticky solid, and ^{1}H-NMR suggested that it was contaminated with about 5% of carboxylic acid, presumably formed by the hydrolysis of hydroxamic acid groups. The product was purified by passing the compound through a short column of quaternary amine coated silica ISOLUTE PE-AX **2.42** (Figure 2.17). The quaternary amine had acetate as the counter anion. The carboxylic acid being more acidic than hydroxamic acid, has a longer retention time on such a column. It should be noted that hydroxamic acids cannot be purified by normal phase silica gel chromatography due to reaction with silica resulting in decomposition.

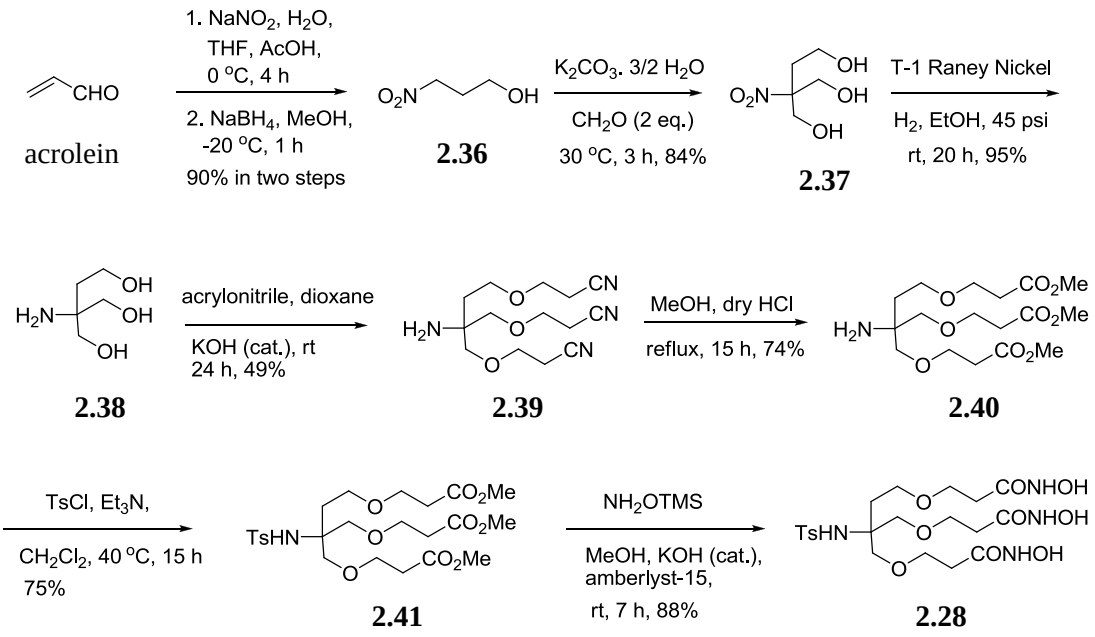

Scheme 2.3 Synthesis of 223-THA

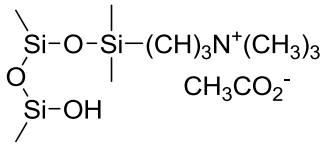

2.42

Figure 2.17 Quaternary amine coated silica ISOLUTE PE-AX from Biotage

2.3.4 Synthesis of 333-THA

Synthesis of the symmetrical tripodal ligand 333-THA started with commercially available 4-amino-4-(3-hydroxypropyl)heptane-1,7-diol **2.43** (Scheme 2.4). Selective Boc- protection of the amino group of **2.43** in the presence of three hydroxyl groups produced compound **2.44** in 68% yield. Rhodium acetate catalyzed alkylation of hydroxyl groups with ethyl diazoacetate gave triester **2.45** in 73% yield. Elimination of nitrogen gas from ethyl diazoacetate leads to the formation of a rhodium carbenoid species that inserts into the oxygen hydrogen bond of the alcohol. Mono- and di-alkylated compounds were also isolated, which were combined and treated with more alkylating reagents to obtain the trialkylated product **2.45**. Other catalysts such as $Cu(acac)_2$ were also used for this reaction, but the yield was lower (30%) even though the reaction was performed at 40 °C. Boc- deprotection with TFA produced the free amine **2.46** in 73% yield. Reprotection of the amine with the tosyl group proceeded smoothly to give the sulfonamide triester **2.47** in 91% yield. Reaction of tri-ester with O-trimethylsilyl hydroxylamine produced the 333-THA ligand **2.29** in 80% yield. This last reaction was performed in the absence of a catalytic amount of KOH unlike previous examples of conversion of esters to hydroxamates. The only difference is that **2.47** is an ethyl ester but previous examples were methyl esters.

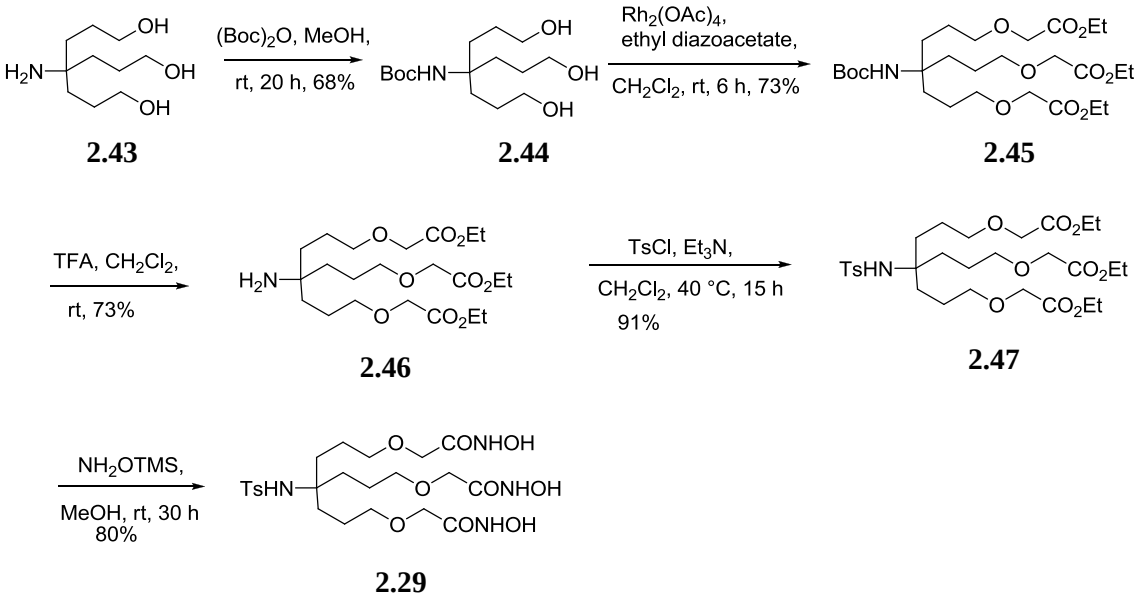

2.43 **2.44** **2.45**

2.46 **2.47**

2.29

Scheme 2.4 Synthesis of 333-THA

The trihydroxamate ligand **2.29** is a colorless solid and was purified by recrystalization from ethanol/isopropanol mixture (1:1), and its structure was further confirmed by X-ray crystallography (Figure 2.18).

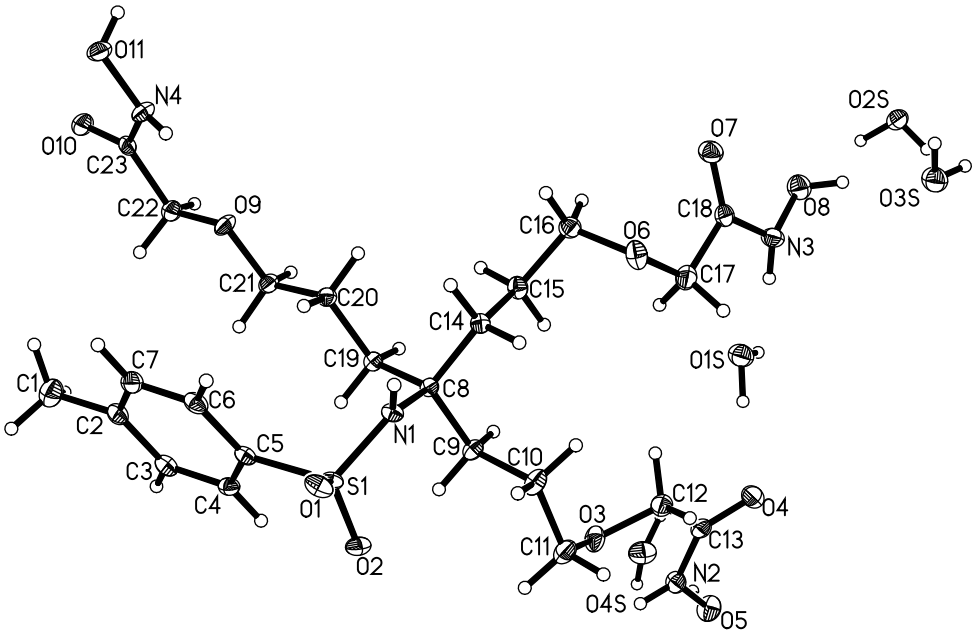

Figure 2.18 Crystal structure of 333-THA

2.4 Design and synthesis of novel tetrahydroxamate ligands

2.4.1 Design of tetrahydroxamate ligands

Two symmetrical dipodal tetrahydroxamate ligands tetrahydroxamate-A **2.49** and tetrahydroxamate-B **2.50** were designed (Figure 2.19). Both contain two inner and two outer hydroxamate groups. In both tetrahydroxamates, the two inner hydroxamates are separated by 9 atoms. In tetrahydroxamate-A, outer and inner hydroxamates are separated by 9 carbons, but in tetrahydroxamate-B they are separated by 8 carbon atoms. Previous research with a number of terminal dihydroxamic acids showed that optimal binding is achieved when two hydroxamates are separated by 8-10 atoms.[31] The two tetrahydroxamate ligands were designed to mimic the structure of high affinity linear

siderophore DFO which has 9 atoms between two hydroxamate groups. The availability and cost of starting materials with required chain lengths also played an important role in the design of these tetrahydroxamate chelators. These two tetrahydroxamates slightly differ structurally. In Tetrahydroxamate-A **2.49**, outer hydroxamic acids are internal (N-acyl), but in tetrahydroxamate-B **2.50** they are N-terminal.

Both tetrahydroxamates are designed to contain a dipodal anchor aminodiol **2.48** (Figure 2.19). The primary free amine present on the central carbon once again is protected with a tosyl group. As mentioned earlier, it can also be used to attach the ligands on a solid support for the preparation of chelating resins.

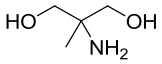

Aminodiol **2.48**

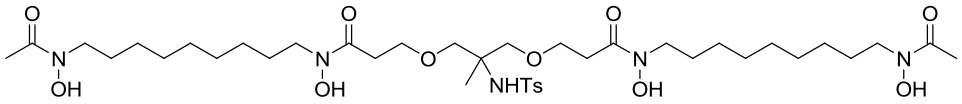

Tetrahydroxamate-A **2.49**

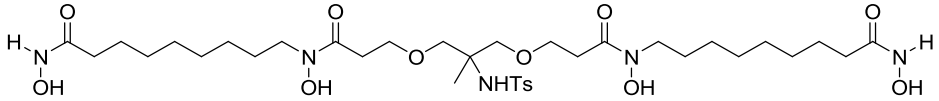

Tetrahydroxamate-B **2.50**

Figure 2.19 Aminodiol as dipodal base and two tetrahydroxamate ligands

2.4.2 Synthesis of tetrahydroxamate-A

The convergent synthesis of tetrahydroxamate-A **2.49** involved the synthesis of two coupling partners, benzyl protected hydroxylamine **2.57** (scheme 2.6) and di-carboxylic acid **2.61** (Scheme 2.7).

In the first attempted synthesis of bis-hydroxylamine **2.56,** which can be converted to the coupling partner **2.57**, 1,9-nonanediol was converted to dimesylate[32] **2.51** by reacting with methanesulfonyl chloride in the presence of triethylamine (Scheme 2.5). Attempted nucleophilic subtitution of mesyl groups with O-benzyl hydroxylamine was unsuccessful, and we were unable to obtain the benzyl protected dihydroxylamine **2.56**. In an another attempt, Finkelstein reaction successfully converted dimesylate **2.51** into 1,9-diiodononane **2.52** and 1,9-dibromononane **2.53**. Both diiodo and dibromo nonane failed to react with O-benzyl hydroxylamine to yield the required compound **2.56**.

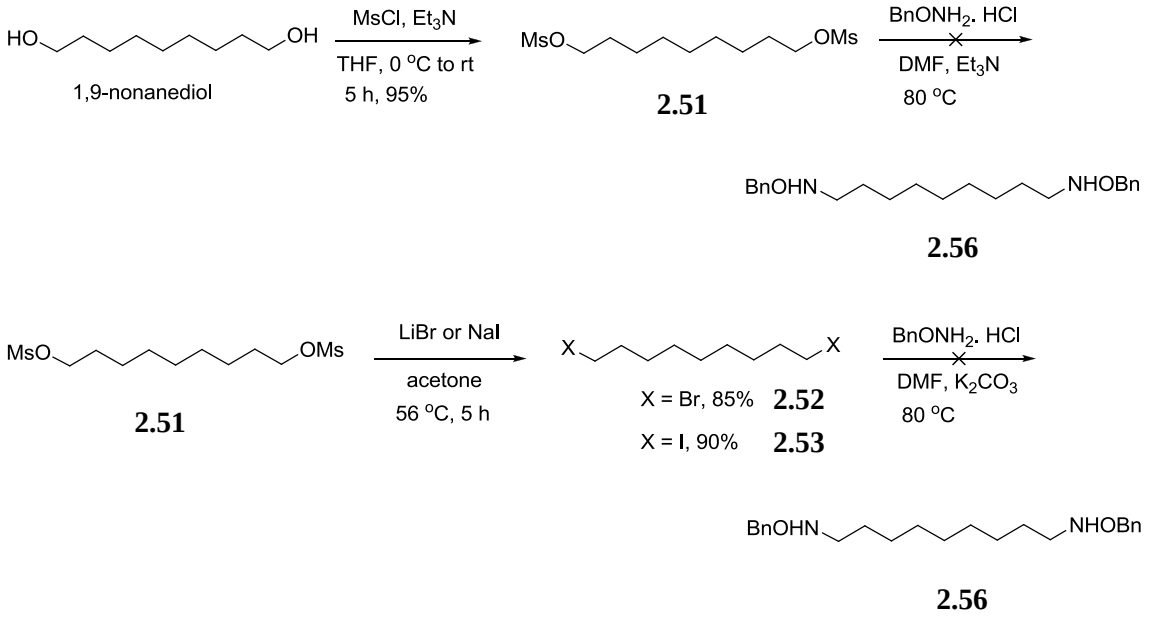

Scheme 2.5 Attempted synthesis of O-benzylhydroxylamine

In another route (Scheme 2.6), synthesis of hydroxylamine **2.57** began with the PCC oxidation of 1,9-nonanediol to form nonanedial **2.54**, which was reacted with O-benzylhydroxylamine hydrochloride and pyridine in refluxing ethanol to produce the dioxime **2.55** in 61% yield.[33] Sodium cyanoborohydride reduction of the dioxime

afforded the benzyl protected bis-hydroxylamine **2.56** in 76% yield.[34] Mono-acetylation[35] of one of the hydroxylamine nitrogens using one equivalent of acetic anhydride led to the formation of compound **2.57** in 48% yield. The di-acetylated byproduct was also isolated along with unreacted hydroxylamine **2.56**.

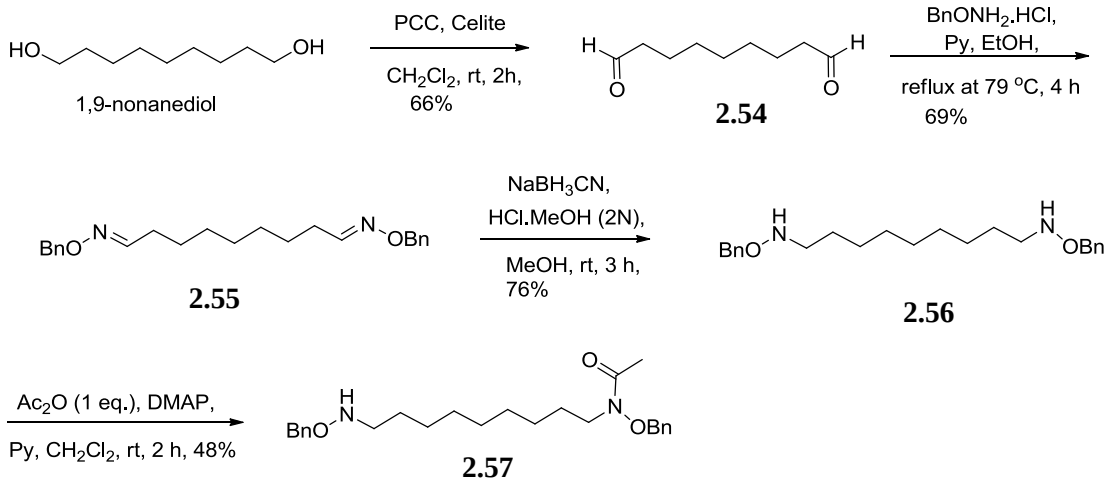

Scheme 2.6 Synthesis of O-benzylhydroxylamine

The di-carboxylic acid **2.61** (Scheme 2.7) was prepared by the alkaline hydrolysis of ester **2.60**, followed by the protonation of the carboxylate salt with a mineral acid. The ester **2.60** was prepared following the previously published procedure of Spilling et al.[24] The aminodiol was reacted with acrylonitrile in the presence of a catalytic amount of KOH to obtain the bis-nitrile **2.58**.[36] Reaction of **2.58** in refluxing methanolic HCl gave the bis-methyl ester **2.59**, which was then reacted with tosyl chloride and Et_3N in CH_2Cl_2 to obtain the sulfonamide bis-ester **2.60**.

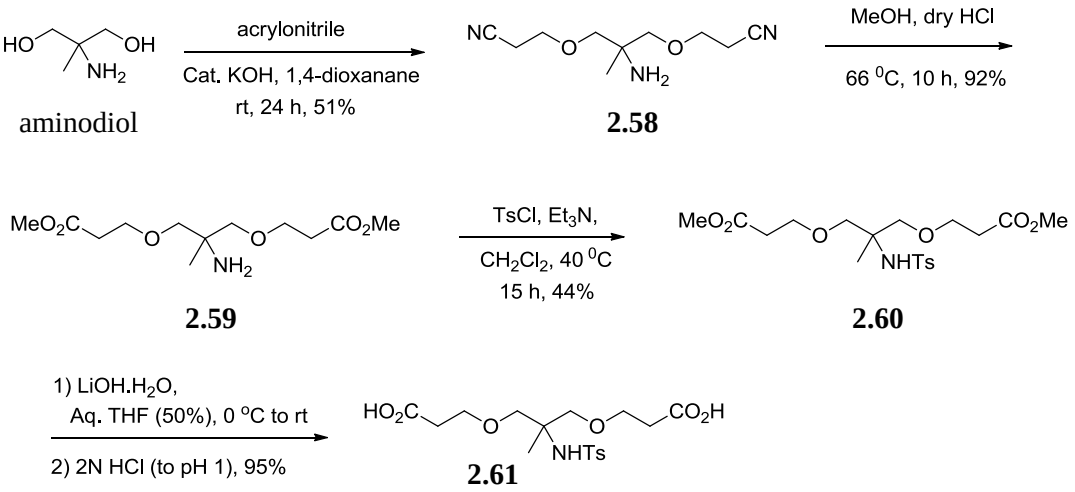

Scheme 2.7 Synthesis of dicarboxylic acid 2.61

The two partners **2.57** and **2.61** were coupled using DCC (Scheme 2.8) to obtain the benzyl protected tetrahydroxamate **2.62** in 65% yield. The final deprotection of benzyl groups by hydrogenation with H_2 over 10% Pd on C afforded the tetrahydroxamate-A **2.49** in 91% yield.

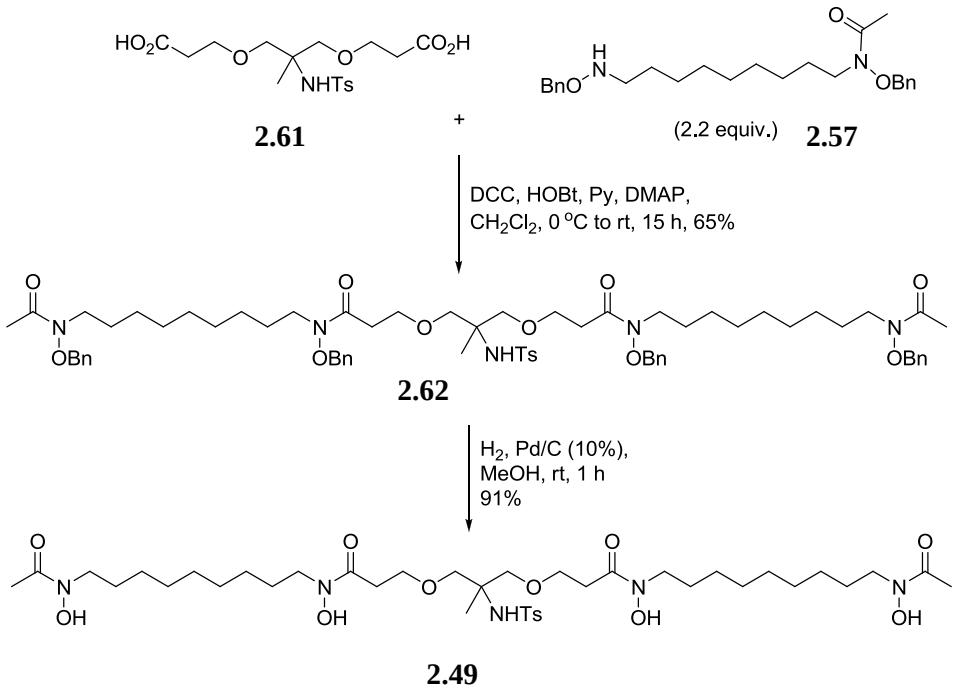

Scheme 2.8 Coupling of O-benzylhydroxylamine and dicarboxylic acid, and final synthesis of tetrahydroxamate-A

2.4.3 Synthesis of tetrahydroxamate-A with free amine

Tetrahydroxamate-A **2.49** was found to be poorly soluble in water, and it was impossible to measure metal binding affinities of this ligand in aqueous solution. Thus, we decided to synthesize the ligand **2.63** (Figure 2.20) which has the same tetrahydroxamate-A structure except for the presence of unprotected primary amine group. The amine is protected with a tosyl group in tetrahydroxamate-A. The hypothesis is that the presence of free amine will improve solubility of both the ligand and its trivalent metal complex in water.

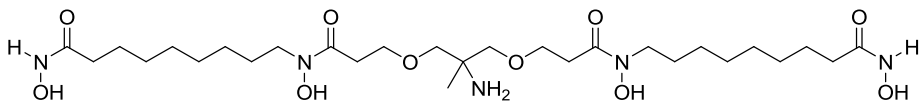

2.63

Figure 2.20 Tetrahydroxamate-A (free amine)

Attempted deprotection of tosyl group from the ligand **2.49** using sodium amalgam and dibasic sodium phosphate in MeOH was unsuccessful giving only decomposition products.[37] Most tosyl deprotection methods reported in the literature employ harsh reaction conditions. In such reaction conditions compound **2.49** may not survive. Thus, we decided to protect the amine with a protecting group that can be easily removed at the last step of the synthesis. Cbz- seemed to be a good choice because it can be deprotected along with benzyl groups by simple hydrogenolysis at the final step of synthesis.

Compound **2.59** was treated with benzyl chloroformate under a Schotten and Baumann condition (Scheme 2.9, condition II) to obtain ester **2.63** in 65% yield. Condition I which used organic base gave much lower yield. The ester **2.63** was then subjected to alkaline hydrolysis followed by protonation with mineral acid to give the di-carboxylic acid **2.64** in quantitative yield.

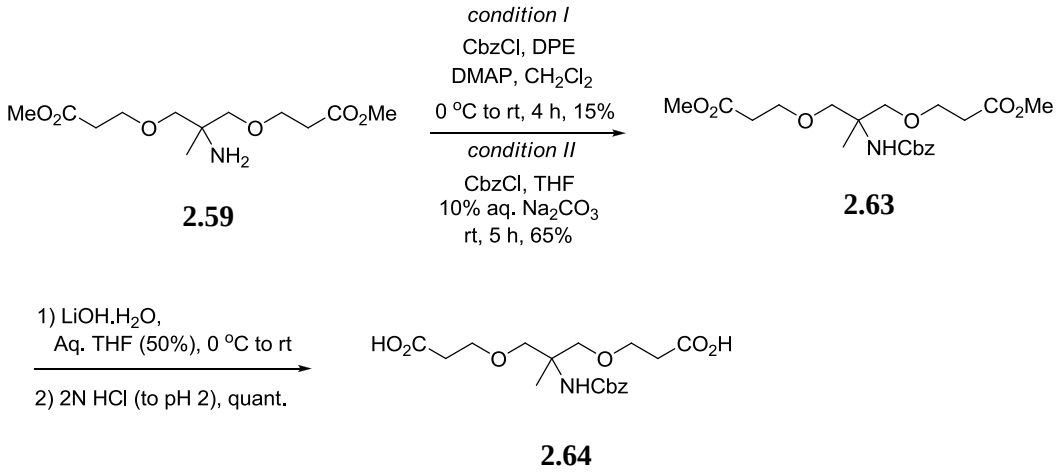

2.59 **2.63** **2.64**

Scheme 2.9 Synthesis of dicarboxylic acid 2.64

The di-carboxylic acid **2.64** was then coupled with hydroxylamine **2.57** using DCC to obtain the compound **2.65** in 56% yield, which was then globally deprotected by hydrogenolysis with H_2 over Pd/C to give the ligand **2.63**.

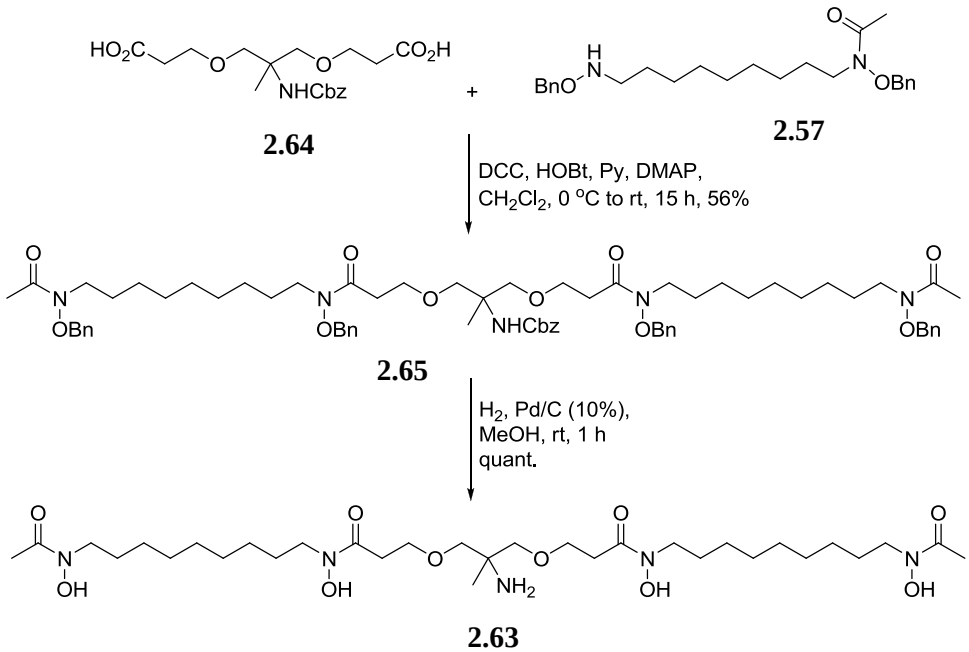

2.64 **2.57** **2.65** **2.63**

Scheme 2.10 Coupling of O-benzylhydroxylamine and dicarboxylic acid, and final deprotection

2.4.4 Synthesis of tetrahydroxamate-B

Tetrahydroxamate-B **2.50** was synthesized by coupling di-carboxylic acid **2.61** used in the synthesis of tetrahydroxamate-A with hydroxylamine **2.69**.

Synthesis of hydroxylamine **2.69** started with monomethyl azelate (Scheme 2.11). The aldehyde **2.67** was formed by oxidation of monomethyl azelate following a published procedure.[38] The carboxylic acid group of monomethyl azelate was selectively reduced to an alcohol in the presence of an ester group using borane in THF to give the alcohol **2.66**. The alcohol group of compound **2.66** was oxidized back to aldehyde **2.67,** which was then reacted with O-benzylhydroxylamine hydrochloride and pyridine in refluxing ethanol to produce the oxime **2.68** in 89% yield. Sodium cyanoborohydride reduction of the oxime afforded benzyl protected hydroxylamine **2.69** quantitatively.

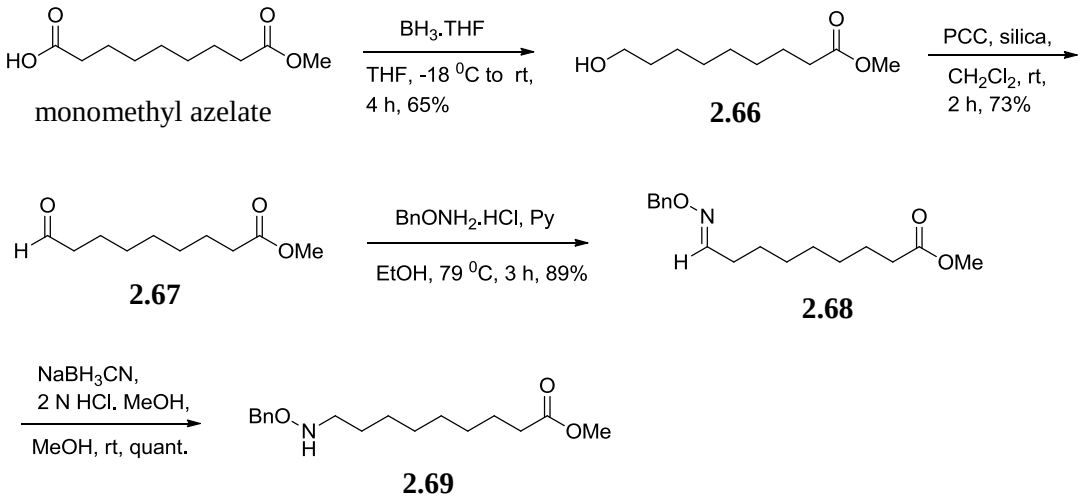

Scheme 2.11 Synthesis of O-benzylhydroxylamine

Hydroxylamine **2.69** was then coupled with di-carboxylic acid **2.61** using DCC (Scheme 2.12) to produce benzyl protected hydroxamic acid dimethyl ester **2.70** in 60%

yield, which was purified by chromatography. The ester groups of **2.70** were then converted to the hydroxamic acids by reaction with O-trimethylsilyl hydroxylamine to obtain the compound **2.71** in quantitative yield. The benzyl protected hydroxamic acid groups of **2.71** were deprotected by hydrogenolysis to obtain the tetrahydoxamate-B **2.50**. Unlike tetrahydroxamate-A, tetrahydroxamate-B is reasonably soluble in water, presumably due to the presence of terminal hydroxamic acid groups.

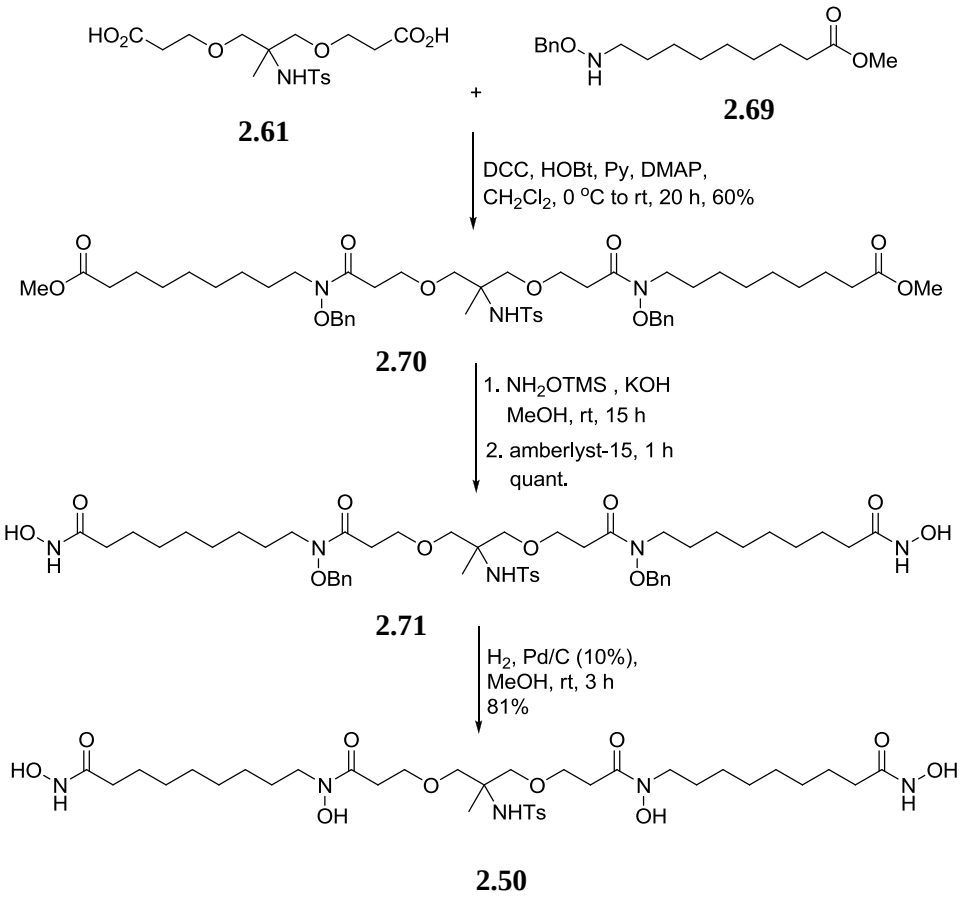

Scheme 2.12 Coupling of O-benzylhydroxylamine and dicarboxylic acid and final synthesis of tetrahydroxamate-B

2.5 Iron and aluminum binding properties of hydroxamate ligands

As DFO, the most commonly used chelating agent in chelation therapy, is associated with a number of drawbacks which includes severe side effects, development of new chelating agents is utterly important. Thus, iron and aluminum binding affinities of novel chelators should be studied to determine their possible use as chelating agents in chelation therapy.

The stability constants of hydroxamate ligands with the trivalent metal ions Al^{3+} and Fe^{3+} have been determined by potentiometric and UV-Vis spectrophotometric titrations, respectively. Iron forms colored complexes with hydroxamates, thus iron hydroxamate complexation can be studied by UV-Vis spectrophotometric methods. Previous studies[39] confirmed that there is a strong correlation between the stability constants for these two metal ions, which is illustrated by the linear free energy relationship (LFER) between log β (Al^{3+}) and log β (Fe^{3+}) (Figure 2.21). The stability constant of one metal can be estimated if the constant is known for another metal. The studies in the Harris lab and many other studies[40] suggested that iron complexes are almost always stronger than corresponding aluminum complexes.

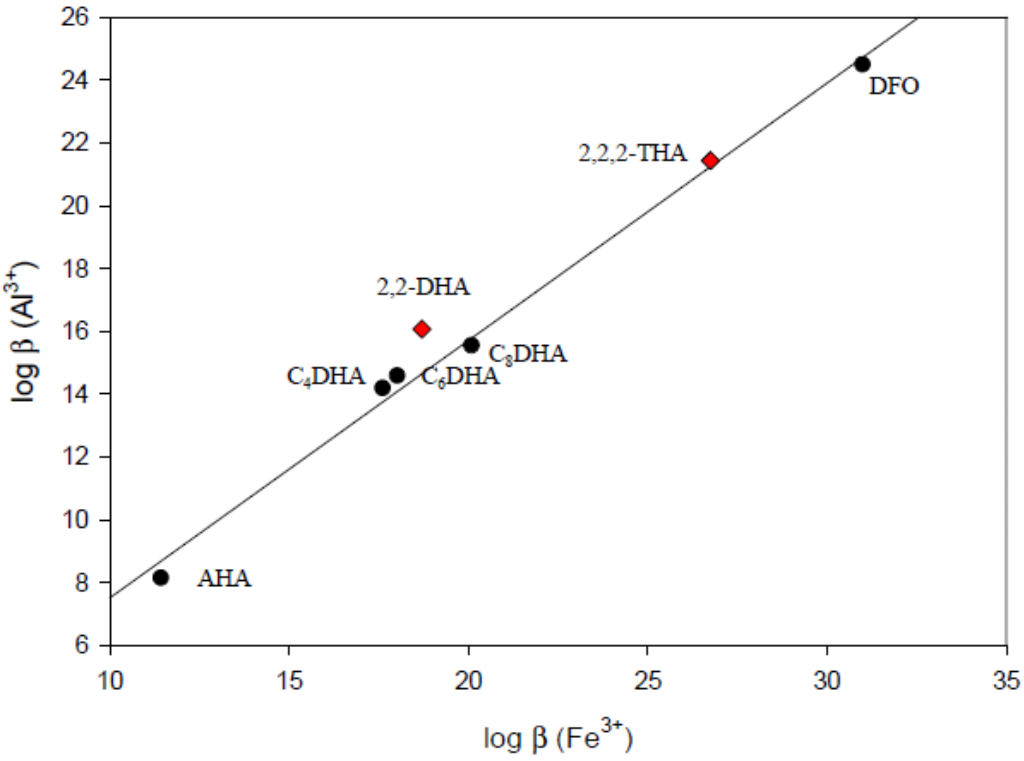

Figure 2.21 Linear free energy relationships for the complexation of Al^{3+} and Fe^{3+} by hydroxamic acids[39]

There are some advantages of spectrophotometric methods over potentiometric methods. The equilibrium system can be studied by spectrophotometric method at low pH, where very little complexation has occurred. The more important advantage of the spectrophotometric method is the fact that λ_{max} provides information on the number of hydroxamate groups coordinated to the metal at a given pH.

2.5.1 Iron binding properties by UV-Vis spectrophotomeric titration

The UV-Vis spectrophotometric spectral measurement was used to study the complexation behavior of ferric ion with hydroxamate ligands. The origin of the

absorption spectra is due to the ligand-to-metal charge-transfer band for the hydroxamate groups coordinated to Fe^{3+}. The λ_{max} for the charge transfer band provides exact information of the number of hydroxamate groups bound to Fe^{3+} at a given pH. Previous studies reported that mono, bis, and tris(hydroxamate) complexes of Fe^{3+} have λ_{max} values of 490, 460 and 430 nm respectively.[39] Usually, only two of these complexes, bis(hydroxamate)Fe^{3+} (111 complex) and tris(hydroxamate)Fe^{3+} complex (110 complex) were detected in the working pH range of 0.3 to 7.0. In the 111 complex, two hydroxamate groups of trihydroxamate ligand are coordinated to the Fe^{3+}, while the third group remains protonated and uncoordinated to Fe^{3+}. At lower pH, the 111 complex is formed as shown in the equation 2.1. The stability constant for the formation of the 111 complex log β_{111} is defined in equation 2.2.

$$M^{3+} + L^{3-} + H^{+} \rightleftharpoons MHL^{+} \qquad \textbf{Equation 2.1}$$

$$\beta_{111} = \frac{[MHL^{+}]}{[M^{3+}][L^{3-}][H^{+}]} \qquad \textbf{Equation 2.2}$$

At higher pH, the 110 complex is formed as shown in equation 2.3 and the stability constant for the formation of the 110 complex log β_{110} is defined in equation 2.4.

$$M^{3+} + L^{3-} \rightleftharpoons ML \qquad \textbf{Equation 2.3}$$

$$\beta_{110} = \frac{[ML]}{[M^{3+}][L^{3-}]} \qquad \textbf{Equation 2.4}$$

a) Complexation of Fe^{3+} by 222-THA 2.27

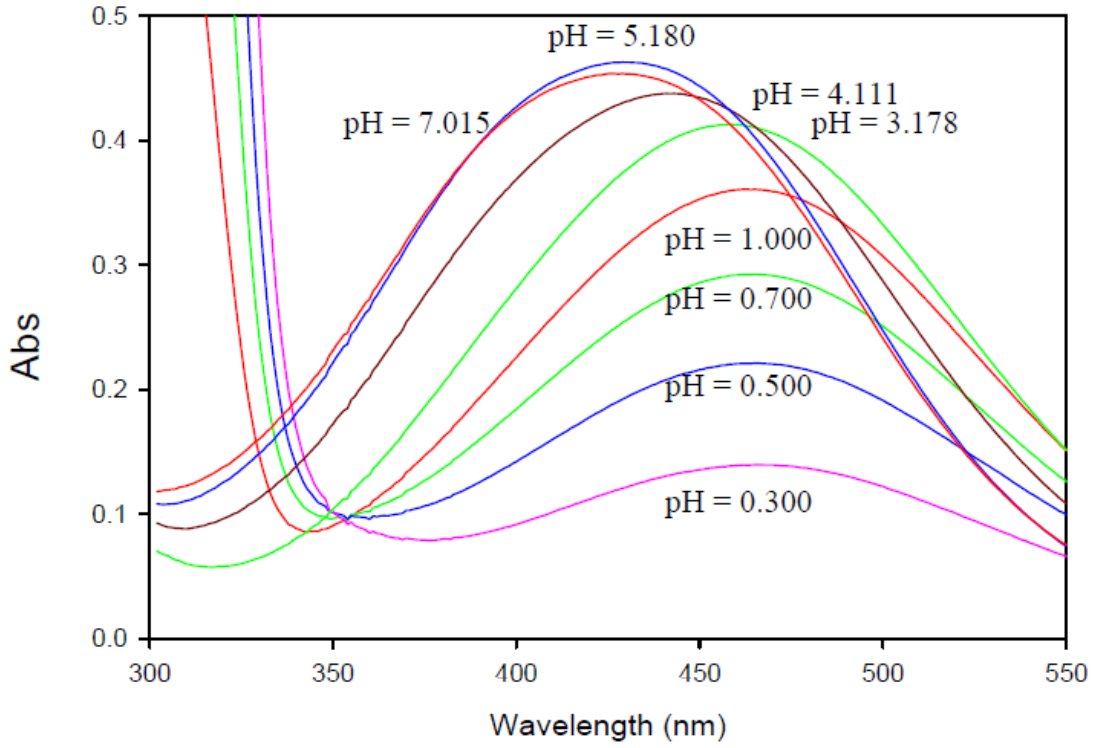

Figure 2.22 pH titration spectra of a 1:2 ratio of Fe^{3+} with 222-THA[39]

The complexation of Fe^{3+} with 222-THA was previously studied.[39] pH titration spectra of solutions of 1:2 concentration ratios of Fe^{3+} and 223-THA were recorded over the pH range 0.3 to 7.0 (Figure 2.22). At pH 3.2, bis(hydroxamato)Fe^{3+} complex **2.72** (Figure 2.23) was fully formed with λ_{max} = 460 nm and ϵ = 2,024 $M^{-1}cm^{-1}$. At higher pH, the tris(hydroxamato)Fe^{3+} complex **2.73** started to form which precipitated significantly above pH 5.2. The program Hypspec was used to calculate the followings: λ_{max} = 430 nm and ϵ = 2,515 $M^{-1}cm^{-1}$. The spectral data were fitted into a data analysis program SPECFIT, and stability constants were calculated. The log β_{111} and log β_{110} were determined to be 30.83 and 26.72 respectively.

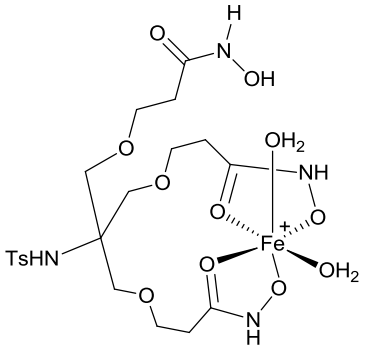

Bis(hydroxamate)Fe^{3+} complex **2.72**

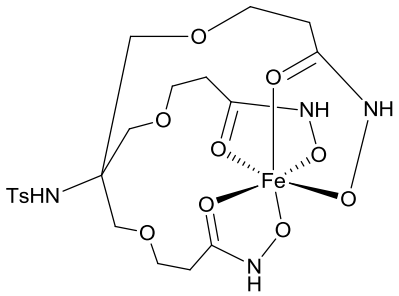

Tris(hydroxamate)Fe^{3+} complex **2.73**

Figure 2.23 Bis- and tris-complexes of 222-THA with iron

b) Complexation of Fe^{3+} by 223-THA 2.28

UV-Vis spectra of solutions of Fe^{3+} and 223-THA were recorded over the pH range 0.3 to 6.7. A detailed set of spectra collected between pH 0.3 and 1.5 is shown in Figure 2.24. A metal to ligand ratio of 1:1.5 was used. At lower pH, the λ_{max} is at 463 nm. This absorbance band increases with increasing pH and maximizes at pH 2.3. At pH 2.3, the bis(hydroxamato)Fe^{3+} complex (111 complex) is completely formed, with a molar extinction coefficient of ϵ = 2,005 M^{-1} cm^{-1}. The presence of an isosbestic point at 369 nm indicates that there is a simple equilibrium between free iron and the 111 complex. The absorption spectra in the Figure 2.24 were used to calculate the stability constant of the 111 complex by fitting the data in program Hypspec. The log β_{111} was calculated to be 30.20.

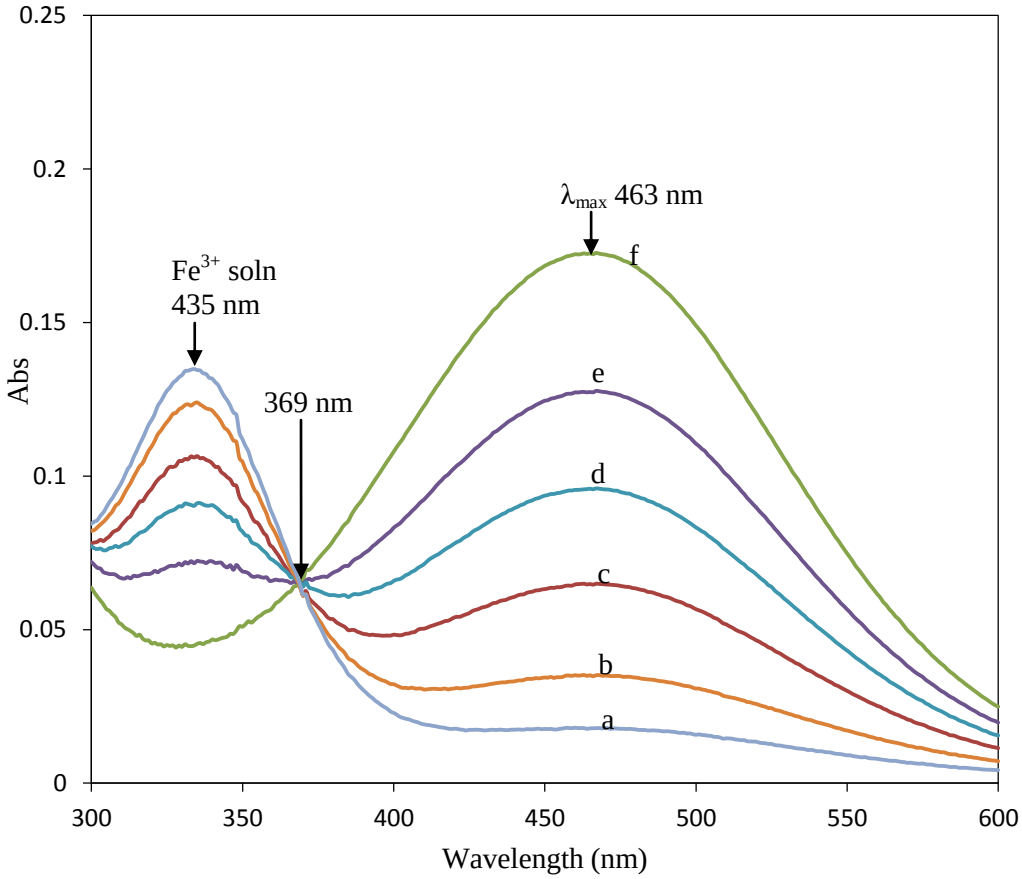

Figure 2.24 UV-Vis spectral changes of Fe^{3+}223-THA at low pH conditions: (a) 0.3, (b) 0.5, (c) 0.7, (d) 0.9, (e) 1.1, (f) 1.5. Conditions: [Fe^{3+}] = 100 µM, [223-THA] = 150 µM, ionic strength = 0.1 M KCl

Another detailed set of spectra were collected at pH values between 2.3 and 6.7 and shown in Figure 2.25. A metal to ligand ratio of 1:2 was used in this spectrophotometric titration. When the pH of a solution of Fe^{3+} and 223-THA is increased from 2.3 to 6.7 the absorbance band shifts to 430 nm. These changes are consistent with the formation of a tris(hydroxamate) complex (110 complex) which has a λ_{max} at around 430 nm. The formation of precipitate above pH 4.1 also suggested that the 110 complex is not very soluble in water. The presence of an isosbestic point at 457 nm

indicates that there is a simple equilibrium between the 111 and 110 complexes before the precipitation starts. There is no change in the absorption when the pH was increased from 5.1 to 6.7 which indicated that the 110 complex was fully formed at pH 5.1. Once again, the spectral data for this transition between pH 2.4 to 4.2 were fitted in the program Hypspec and the stability constant for 110 complex was determined. The log β_{110} was calculated to be 25.89.

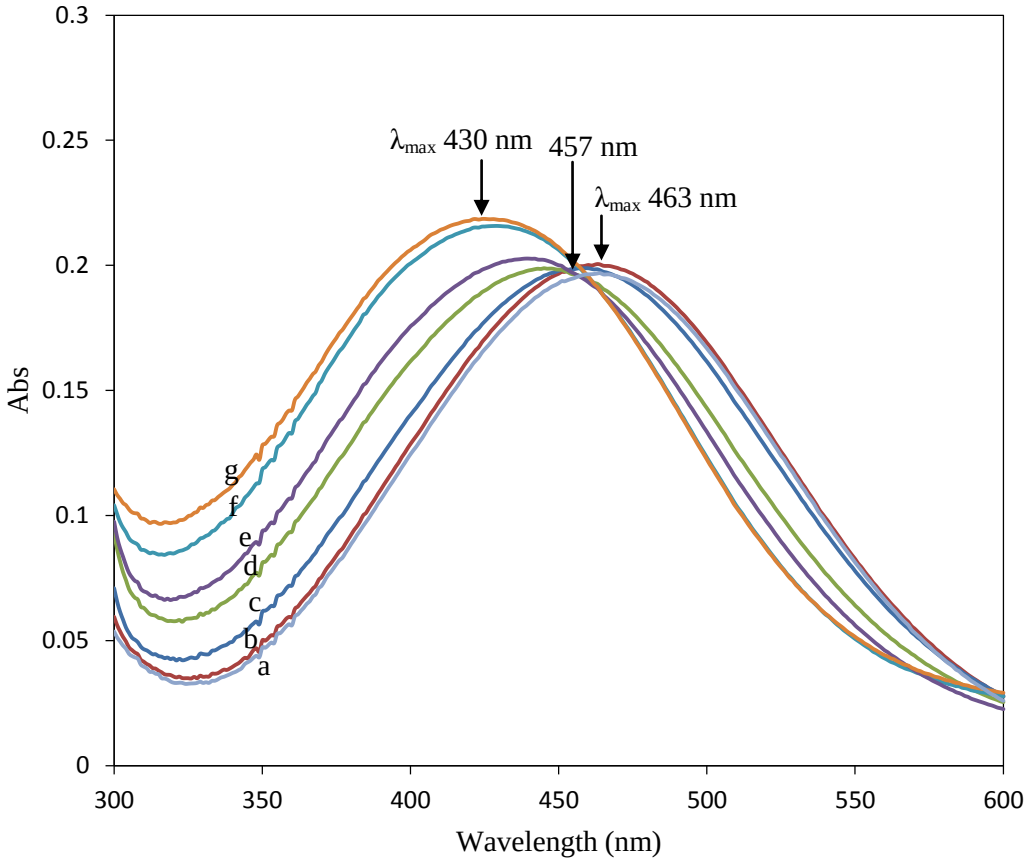

Figure 2.25 UV-vis spectral changes of Fe^{3+}223-THA at various pH conditions: (a) 1.9 (b) 2.4, (c) 3.3, (d) 3.9, (e) 4.2, (f) 5.1, (g) 6.7. Conditions: [Fe^{3+}] = 100 µM, [223-THA] = 200 µM, ionic strength = 0.1 M KCl

c) Complexation of Fe^{3+} by 333-THA 2.29

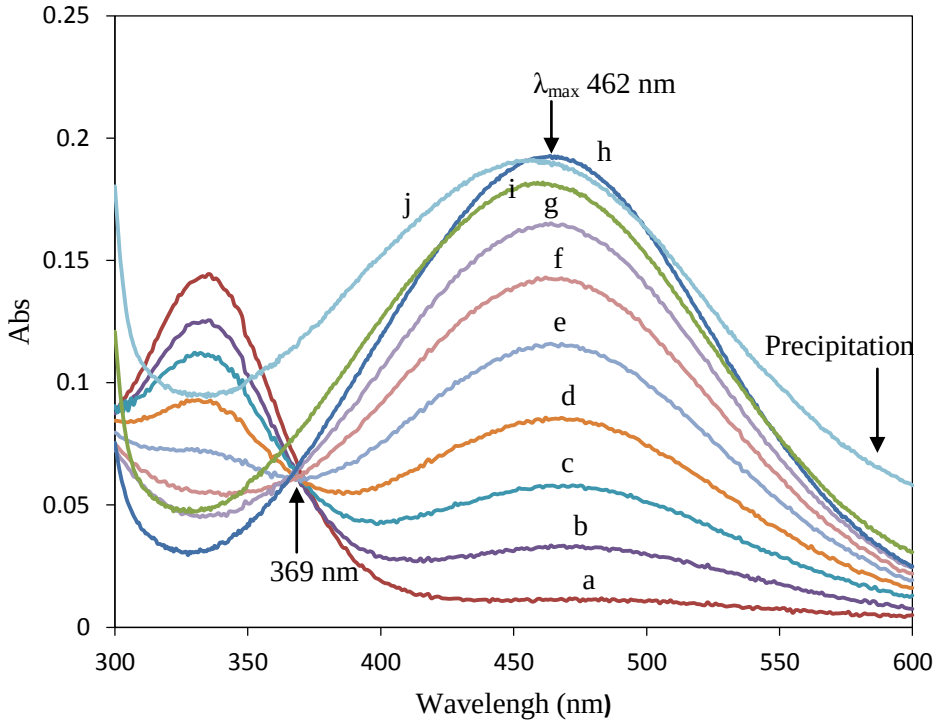

Figure 2.26 UV-Vis spectral changes of Fe^{3+}333-THA at various pH conditions: (a) 0.8, (b) 1.2, (c) 1.4, (d) 1.6, (e) 1.8, (f) 2.0, (g) 2.2, (h) 2.4, (i) 3.1, (j) 3.3. Conditions: [Fe^{3+}] = 100 µM, [333-THA] = 200 µM, ionic strength = 0.1 M KCl

UV-Vis spectra for solutions of Fe^{3+} and 333-THA were recorded over the pH range 0.3 to 4.0. A metal to ligand ratio of 1:2 was used in the spectrophotometric titration. A detailed set of spectra collected between pH 0.8 and 3.3 is shown in Figure 2.26. At lower pH, the λ_{max} is at 462 nm. This absorbance band increases with increasing pH and maximizes at pH 2.4. At pH 2.4, the bis(hydroxamato)Fe^{3+} complex (111 complex) is completely formed, with a molar extinction coefficient of ϵ = 1,930 M^{-1} cm^{-1}. The absorption spectra in the figure up to pH 2.0 were used to calculate the stability

constant of 111 complex by fitting the data in Hypspec. The log β_{111} was calculated to be 27.71.

When the pH of a solution of Fe^{3+} and 333-THA is increased from 2.4 to 4.0, the absorbance band shifts toward lower wavelength, but the absorbance also decreases. The absence of an isosbestic point indicates that 111 and 110 complexes are not the only species present. Additionally, considerable precipitation occurred in the titration mixture above pH 3.0. The precipitate was filtered, washed with water, dried, and the IR spectrum was obtained. The IR spectrum clearly showed that the precipitate was indeed a metal ligand complex, by comparing this IR with the IR of a $Fe(OH)_3$ precipitate. This result suggests that the tris(hydroxamato)Fe^{3+} complex of 333-THA is highly insoluble in water and crashes out as soon as it is formed. Thus, we are unable to calculate the stability constant for the 110 complex.

d) Complexation of Fe^{3+} by tetrahydroxamate-A (free amine) 2.63

UV-Visible spectra of solutions of Fe^{3+} and tetrahydroxamate-A free amine were recorded over the pH range 0.3 to 2.3 (Figure 2.27). A metal to ligand ratio of 1:1.5 was used in the spectrophotometric titration. At lower pH, the λ_{max} is at 464 nm. This absorbance band increases with increasing pH and maximizes at pH 1.1. At pH 1.1, the bis(hydroxamate) complex (111 complex) is completely formed, with a molar extinction coefficient of ε = 2,200 M^{-1} cm^{-1}. When the pH of a solution of Fe^{3+} and ligand **2.63** is increased from 1.1 to 2.3, the absorbance band shifts to 431 nm and the molar absorptivity increases to 2,525 $M^{-1}cm^{-1}$. These changes are consistent with the formation of a tris(hydroxamate) complex (110 complex). The presence of an isosbestic point at 469

nm indicates that there is a simple equilibrium between the 111 and 110 complexes. There is no change in the absorption when the pH was increased from 2.3 to 2.5 which indicated that the 110 complex was fully formed at pH 2.3. The log β_{111} and log β_{110} were calculated to be 31.44 and 27.38.

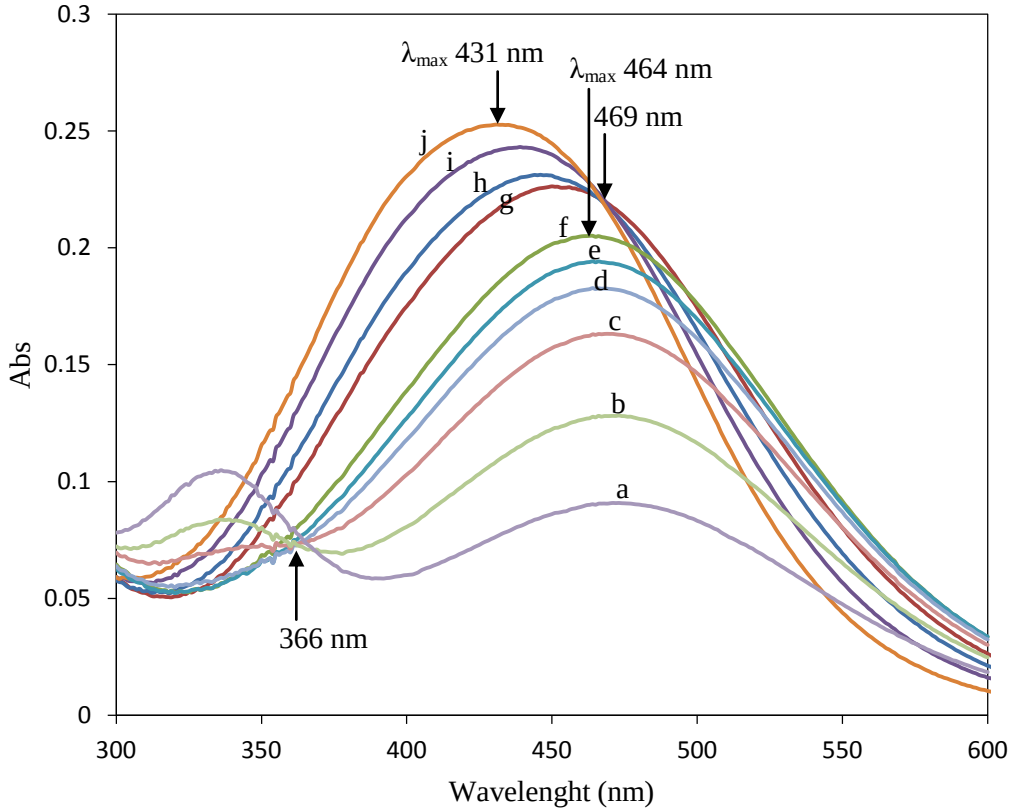

Figure 2.27 UV-Vis spectral changes of Fe^{3+}Tetrahydroxamate-A (free amine) at various pH conditions: (a) 0.3, (b) 0.5, (c) 0.7, (d) 0.9, (e) 1.0, (f) 1.1, (g) 1.4, (h) 1.6, (i) 1.9, (j) 2.3. Conditions: [Fe^{3+}] = 100 µM, [Tetrahydroxamate-A (free amine)] = 150 µM, ionic strength = 0.1 M KCl

e) Complexation of Fe^{3+} by tetrahydroxamate-B 2.50

UV-Vis spectra of solutions of Fe^{3+} and tetrahydroxamate-B were recorded over the pH range 0.3 to 2.0 which is shown in Figure 2.28. A metal to ligand ratio of 1:1.2 was used in this titration. At the pH range of 0.3 to 1.5, the λ_{max} is at 463 nm. This absorbance band increases with increasing pH and maximizes at pH 1.5. At that pH, the bis(hydroxamate) complex (111 complex) is completely formed, with a molar extinction coefficient of ϵ = 1,938 M^{-1} cm^{-1}. The log β_{111} was calculated to be 32.70. When the pH of a solution of Fe^{3+} and tetrahydroxamate-B is increased from 1.5, the precipitation occurs. Thus, we are unable to calculate the stability constant for 110 complex.

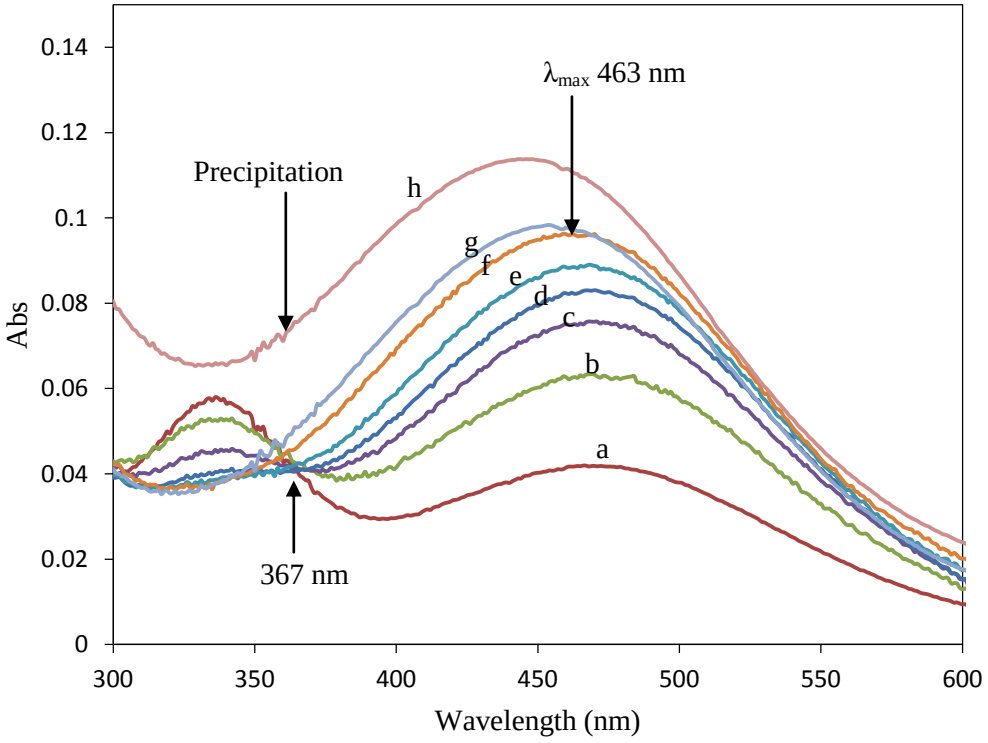

Figure 2.28 UV-Vis spectral changes of Fe^{3+}tetrahydroxamate-B at various pH values: (a) 0.3, (b) 0.6, (c) 0.8, (d) 1.0, (e) 1.2, (f) 1.5 (g) 1.7, (h) 2.0. Conditions: [Fe^{3+}] = 50 µM, [Tetrahydroxamate-B] = 60 µM, ionic strength = 0.1 M KCl

2.5.2 Aluminum binding properties by potentiometric titration method

Ligand protonation constants and aluminum binding constants of three trihydroxamic acids 222-THA **2.27**, 223-THA **2.28**, and 333-THA **2.29** are determined by a potentiometric titration method. These studies also suggested that the trihydroxamate ligands form an bis(hydroxamate)Al^{3+} complex (111 complex) at low pH, almost in the same pH range of formation for the bis(hydroxamate)Fe^{3+} complex. At higher pH, tris(hydroxamate)Al^{3+} complex (110 complex) starts to form. Precipitation of 110 complexes is an issue here too. Data from the potentiometric titration were used to calculate aluminum binding constants of trihydroxamates and are listed in the Table 2.1. Potentiometric titration studies of tetrahydroxamate ligands were not performed.

2.6 Summary

After thorough structural investigation of literature examples of natural and artificial siderophores, five high affinity trivalent metal chelators are designed and synthesized. Three of them were tripodal trihydroxamates, 222-THA **2.27**, 223-THA **2.28**, and 333-THA **2.29**; and other two were dipodal tetrahydroxamates, tetrahydroxamate-A 2.49, and tetrahydroxamate-B **2.50**. The structure of tetrahydroxamate-A **2.49** was slightly modified to compound **2.63** containing a terminal primary amine group for better aqueous solubility.

Fe^{3+} and Al^{3+} binding affinities of these trihydroxamate and tetrahydroxamate ligands were determined by UV-vis spectrophotometric and potentiometric titration methods and are listed in table 2.1. Binding affinities of natural siderophore DFO are also included for the comparison.

Table 2.1 Fe^{3+} and Al^{3+} binding constants of various hydroxamate ligands

		222-THA **2.27**	223-THA **2.28**	333-THA **2.29**	Tetrahydroxamate-A (free amine) **2.63**	Tetrahydroxamate-B **2.50**	DFO **2.1**
Fe^{3+}	**log β_{111}**	30.83	30.20	27.71	31.44	32.17	31.54
	log β_{110}	26.72	25.89	N/A	27.38	28.11	30.60
Al^{3+}	**log β_{111}**	25.86	25.49	23.35	-	-	25.32
	log β_{110}	20.74	20.45	18.44	-	-	24.14

The binding constant values in Table 2.1 suggested that the tetrahydroxamate ligands are almost as strong as DFO and much stronger than trihydroxamate ligands on binding ferric ion. Two tripodal trihydroxamates, 222-THA **2.27** and 223-THA **2.28** which differ by one methylene unit chain length in one of the arms, have almost equal affinities towards Al^{3+} and Fe^{3+} ions. The third trihydroxamate ligand 333-THA **2.29** was definitely weaker on binding Al^{3+} ion than other two trihydroxamates. The log β_{110} number for Fe^{3+}333-THA complex was not available due to the precipitation of 110 complex during the UV-Vis titration experiment.

The binding of divalent metal ions Cu^{2+}, Ni^{2+}, Zn^{2+}, Mn^{2+}, and Mn^{2+} by one of the trihydroxamate ligands, 222-THA **2.27**, has also been evaluated by potentiometric titration.[39, 41] The binding constants of 222-THA with these divalent metal ions along with Al^{3+} and Fe^{3+} are listed in Table 2.2.[41] The results indicate that 222-THA is very

selective for Al^{3+} and Fe^{3+} over divalent metal ions especially Ca^{2+}. This is a very important property for the proposed application of these chelators described in Chapter 3. However, the ligand has appreciable binding with Cu^{2+}.

Table 2.2 Binding constants of the metal complexes of 222-THA 2.27

	Fe^{3+}	Al^{3+}	Cu^{2+}	Ni^{2+}	Zn^{2+}	Mn^{2+}	Ca^{2+}
log β_{111}	30.83	25.86	23.61	19.10	19.13	17.06	13.34
log β_{110}	26.72	20.74	-	10.73	10.13	8.95	3.71

2.7 Experimental section

di-tert-butyl-3,3'-((2-amino-2-((3-(tert-butoxy)-3-oxopropoxy)methyl)propane-1,3-diyl)bis(oxy))dipropanoate (2.35). To a suspension of tris **2.25** (12.1 g, 100 mmol) in DMSO (20 ml) at 15 ^{0}C was added 5 M NaOH (2 ml) and the mixture was stirred under Argon for 15 minutes. *tert*- Butyl acrylate (50 ml, 340 mmol) was added drop wise over a period of 1 h at the same temperature. When the addition was complete, the reaction mixture was allowed to warm to room temperature. The mixture turned into a clear solution after about 1 h at room temperature. The reaction mixture was left stirring for an additional 15 h. To this mixture was added a phosphate buffer (150 ml, 0.1 M, made by dissolving 5 g H_3PO_4 and 6.5 g NaH_2PO_4 in 500 ml water, pH ~2), stirred for 5 minutes and extracted with EtOAc (2 × 150 ml). The combined EtOAc layers were evaporated to get colorless oil (41.3 g, 82%). The product was found to be impure and also contain a

little DMSO (^{1}H NMR, HPLC). The product was dissolved in EtOAc (150 ml) and the buffer (150 ml) was added, shaken and layers were separated. The aqueous layer was extracted with EtOAc (150 ml). After the extraction, the aqueous layer was found to be acidic with pH ~5. The combined EtOAc layers were evaporated under reduced pressure to obtain thick colorless oil (37.7 g, 75%). The product was analyzed by HPLC and ^{1}H NMR, and found to be purer and mostly in the form of free amine. The product was again dissolved in EtOAc (150 ml) and the buffer (500 ml) was added, shaken and layers were separated. The aqueous layer was extracted with EtOAC (2 × 300 ml). After the second extraction, pH of the aqueous layer (universal indicator) was found to be about 2. The combined EtOAc layers were evaporated under reduced pressure to obtain thick sticky colorless oil (37.5 g, 75%) in the form of protonated amine which was used in the next step without further purification. The product was previously characterized.[27]

Dimethyl-3,3'-((2-amino-2-((3-methoxy-3-oxopropoxy)methyl)propane-1,3-diyl)bis(oxy))dipropanoate (2.33). To a solution of tris *t*- butyl ester (36 g, 71.2 mmol) in MeOH (200 ml) was added conc. H_2SO_4 (9.6 ml, 179.8 mmol, 2.5 eq.) and refluxed at 63 ^{0}C for 2h. The mixture of the ester in MeOH was cloudy, but turned to a clear solution immediately after the addition of H_2SO_4. Reaction was monitored by HPLC and found to be completed in 2 h. The mixture was allowed to cool down to room temperature and 10% Na_2CO_3 (700 ml) was added cautiously with stirring as there was evolution of CO_2 gas. After the complete addition of Na_2CO_3, the mixture was basic with a pH of ~10 (universal indicator). It was extracted with EtOAc (3 × 300 ml) and combined EtOAc layers were evaporated under reduced pressure to obtain oil as the product which was

contaminated with white solid particles (Na_2CO_3). This mixture was filtered, washed with EtOAc and the filtrate was evaporated to obtain light yellow colored oil as the methyl ester (20.5 g, 76%). The product was previously characterized.[24]

2-(hydroxymethyl)-2-nitrobutane-1,4-diol (2.37). To a solution of 3-nitropropanol **2.36** (6.70 g, 63.7 mmol) in H_2O (7 mL) were added 37 weight % formaldehyde solution in H_2O (10 mL, 128 mmol) and solid $K_2CO_3.3/2H_2O$ (21.0 g, 127 mmol) and the mixture was stirred at room temperature for 1 h (reaction was exothermic) and then at 30 ^{0}C for 1 h. The reaction was monitored by TLC (10% MeOH in $CHCl_3$). 20% aqueous HCl solution was added drop wise with stirring until the effervescence of CO_2 ceased. The resulting mixture was washed with CH_2Cl_2 (2×30 mL) to remove some impurities and the aqueous layer was evaporated under reduced pressure. The residue was triturated with hot EtOH (3×50 mL) and the EtOH was filtered and evaporated under reduced pressure to yield the product as thick oil (8.85 g, 84%). IR (neat) 3378, 2949, 2888 cm^{-1}; ^{1}H NMR (D_2O) δ (ppm) 4.05 (ABq, Δδ = 22.2 Hz, *J* = 12.4 Hz, 4H) 3.73 (t, *J* = 6.6 Hz, 2H), 2.26 (t, *J* = 6.6 Hz, 2H); ^{13}C NMR (D_2O) δ (ppm) 93.9, 62.1, 57.0, 33.3.

Preparation of T-1 Raney Nickel. In a 250 ml two neck flask, 150 ml of 10% aqueous NaOH (15 g in 150 ml solution) solution was heated to 90 ^{0}C. Nickel/aluminum alloy (10 g) was added cautiously (reaction is vigorous) in small portions (<1 g at a time) over a period of 15 min while stirring the mixture. The temperature was kept between 85 to 90 ^{0}C during the addition. Heating was then removed and the mixture was stirred for additional 50 min at room temperature. The mixture was decanted and the residue was

washed with water (5×50 mL) and EtOH (5×15 mL) while always keeping it under the solvent because the catalyst is extremely pyrophoric when dry. The catalyst was stored in a flask under EtOH in a refrigerator.

2-amino-2-(hydroxymethyl)butane-1,4-diol (2.38). Freshly prepared T-1 Raney nickel (3.6 g) was transferred to a Parr hydrogenation flask as slurry in absolute EtOH (45 mL). 2-(Hydroxymethyl)-2-nitrobutane-1,4-diol **2.37** (4.80 g, 29.1 mmol) was dissolved in absolute EtOH (45 mL) and transferred to the hydrogenation flask. The resulting mixture was shaken on a Parr hydrogenator under 45 psi of H_2 at room temperature for 20 h. The flask was removed from the hydrogenator and flushed with argon for 20 min. The catalyst (pyrophoric when dry) was then filtered through a short pad of celite, which was never allowed to dry. The celite was washed with EtOH (3 × 30 mL). The EtOH was evaporated to give the product as a viscous brown gel (traces of EtOH were always present) (3.7 g, 95%) which was used in the next step without further purification. IR (neat) 2931, 2875 cm^{-1}; ^{1}H NMR (D_2O) δ (ppm) 3.72 (t, *J* = 7.2 Hz, 2H), 3.47 (s, 4H), 1.65 (t, *J* = 7.2 Hz, 2H); ^{13}C NMR (D_2O) δ (ppm) 64.7, 56.9, 54.8, 35.2.

3,3'-((2-amino-2-((2-cyanoethoxy)methyl)butane-1,4 diyl)bis(oxy))dipropanenitrile (2.39). To a stirred solution of 2-amino-2-(hydroxymethyl)butane-1,4-diol **2.38** (3.65 g, 27.0 mmol) and KOH pellets (0.4 g) in 1,4-dioxane (13 mL) was added acrylonitrile (6.3 mL, 94 mmol) drop wise over a period of 1 h. Once the addition was complete, the mixture was stirred at room temperature for 24 h. The solvent was evaporated under reduced pressure to yield thick liquid residue which was dissolved in CH_2Cl_2 (50 mL)

and washed with H_2O (50 mL). The aqueous layer was re-extracted with additional portions of CH_2Cl_2 (2×30 mL). The combined CH_2Cl_2 fractions were dried over Na_2SO_4 and evaporated under reduced pressure and the residue was purified by column chromatography (SiO_2, 5% EtOH in EtOAc) to give the product as a thick brown oil (3.89 g, 49%): IR (neat) 3371, 3307, 2873, 2245 cm^{-1}; ^1H NMR ($CDCl_3$) δ (ppm) 3.68 (t, *J* = 6.0 Hz, 4H), 3.65 (t, *J* = 6.1 Hz, 2H), 3.62 (t, *J* = 6.2 Hz, 2H), 3.41 (ABq, Δδ = 19.5 Hz, *J* = 8.7 Hz, 4H), 2.60 (t, *J* = 6.0 Hz, 4H), 2.59 (t, *J* = 6.0 Hz, 2H), 1.72 (t, *J* = 6.1 Hz, 2H); ^{13}C NMR ($CDCl_3$) δ (ppm) 118.2 (all three nitrile carbons), 75.1, 67.5, 66.0, 65.8, 54.7, 34.6, 19.1, 19.0; HRMS (FAB) $C_{14}H_{23}N_4O_3$ $[M+H]^+$ calcd 295.17703, found 295.17720.

Dimethyl-3,3'-((2-amino-2-((3-methoxy-3-oxopropoxy)methyl)butane-1,4-diyl)bis(oxy))dipropanoate (2.40). Dry HCl gas was bubbled into a solution of the trinitrile **2.39** (1.43 g, 4.86 mmol) in MeOH (12 ml) until it was saturated (NH_4Cl precipitated out). The resulting mixture was heated at reflux for 10 h. Saturated Na_2CO_3 was added drop wise while stirring the mixture until CO_2 effervescence ceased. The solution was extracted with EtOAc (3×30 mL). The combined organic layers were washed with brine, dried over Na_2SO_4 and evaporated to obtain the product as a liquid (1.41 g, 74%), which was used in the next step without further purification. IR (neat) 2951, 2875, 1732 cm^{-1}; ^1H NMR ($CDCl_3$) δ (ppm) 3.74- 3.63 (m, 15H), 3.53 (t, *J* = 6.5 Hz, 2H), 3.26 (ABq, Δδ = 13.8 Hz, *J* = 8.9 Hz, 4H), 2.55 (t, *J* = 6.3 Hz, 6H), 2.03 (br s, 2H), 1.62 (t, *J* = 6.4 Hz, 2H); ^{13}C NMR ($CDCl_3$) δ (ppm) 172.3, 172.2, 75.1, 67.4, 66.8,

66.3, 54.7, 51.8, 51.7, 35.1, 35.0, 34.5; HRMS (FAB) $C_{17}H_{32}NO_9$ $[M+H]^+$ calcd 394.20770, found 394.20860.

Dimethyl-3,3'-((2-((3-methoxy-3-oxopropoxy)methyl)-2-(4-methylphenylsulfonamido)butane-1,4-diyl)bis(oxy))dipropanoate (2.41). To a stirred solution of the amino triester **2.40** (1.40 g, 3.56 mmol) and TsCl (1.60 g, 8.40 mmol) in CH_2Cl_2 (32 mL) was slowly added Et_3N (1.0 mL, 7.2 mmol) and the resulting mixture was heated at reflux for 20 h. The solvent was evaporated under reduced pressure and the residue was dissolved in CH_2Cl_2 (50 mL), washed with water (2×25 mL), dried over Na_2SO_4 and concentrated under reduced pressure. The crude product was purified by column chromatography (SiO_2, hexanes/EtOAc gradient) to give the tosyl amide as a thick oil (1.42 g, 75%): IR (neat) 3287, 2953, 2876, 1732 cm^{-1} ; ^1H NMR ($CDCl_3$) δ (ppm) 7.73 (d, *J* = 8.3 Hz, 2H), 7.24 (d, *J* = 8.3 Hz, 2H), 5.58 (s, 1H), 3.67 (s, 3H), 3.64 (s, 6H), 3.58 (t, *J* = 6.3 Hz, 2H), 3.50-3.36 (m, 10H), 2.52 (t, *J* = 6.3 Hz, 2H), 2.39 (t, *J* = 6.3 Hz, 4H), 2.38 (s, 3H), 1.88 (t, *J* = 6.0 Hz, 2H); ^{13}C NMR ($CDCl_3$) δ (ppm) 172.1, 172.0, 142.8, 140.6, 129.3, 126.9, 72.1, 66.9, 66.5, 66.2, 61.6, 51.8, 51.7, 34.8, 34.6, 32.6, 21.5; HRMS (FAB) $C_{24}H_{38}NO_{11}S$ $[M+H]^+$ calcd 548.21655, found 548.21570.

3,3'-((2-(2-(3-(hydroxyamino)-3-oxopropoxy)ethyl)-2-(4-methylphenylsulfonamido)propane-1,3-diyl)bis(oxy))bis(N-hydroxypropanamide) (2.28). To a solution of the tosylamido triester **2.41** (0.5 g, 0.91 mmol) in dry MeOH (5.5 mL) was added NH_2OTMS (0.67 mL, 5.48 mmol) and the resulting solution was stirred at room temperature. The reaction was monitored by TLC (50% EtOAc in hexanes). No

reaction was observed after 3 h. KOH (0.3 g) was added and stirring was continued for an additional 45 min. Amberlyst-15 (2.6 g, washed with dry MeOH) was added to the reaction mixture and stirring was continued for 1 h. The mixture was filtered and the filtrate was evaporated under reduced pressure to obtain the ligand **2.28** as a solid (0.44 g, 88%): IR (neat) 3215, 2876, 1638 cm^{-1}; ^{1}H NMR (D_2O) δ (ppm) 7.80 (d, *J* = 8.2 Hz, 2H), 7.47 (d, *J* = 8.2 Hz, 2H), 3.64 (t, *J* = 6.0 Hz, 2H), 3.48-3.52 (m, 6H), 3.39 (s, 4H), 2.44 (s, 3H), 2.40 (t, *J* = 6.0 Hz, 2H), 2.32 (t, *J* = 5.8 Hz, 4H), 1.85 (t, *J* = 6.7 Hz, 2H); ^{13}C NMR (MeOD) δ (ppm) 171.0, 170.9, 144.4, 141.9, 123.5, 127.9, 72.5, 67.6, 67.3, 62.5, 54.9, 34.4, 33.3, 21.5; HRMS (FAB) $C_{21}H_{35}N_4O_{11}S$ $[M+H]^+$ calcd 551.20227, found 551.20260.

tert-butyl (1,7-dihydroxy-4-(3-hydroxypropyl)heptan-4-yl)carbamate (2.44). To a stirred solution of 4-amino-4-(3-hydroxypropyl)heptane-1,7-diol **2.43** (1.65 g, 8.06 mmol) in dry MeOH (33 mL) was added $(Boc)_2O$ (1.86 g, 8.5 mmol) and the mixture was stirred at room temperature for 20 h. The solvent was evaporated under reduced pressure and the residue was purified by column chromatography (SiO_2, CH_2Cl_2/MeOH gradient) to give the product (1.681 g, 68%) which was crystallized from CH_2Cl_2 as white crystals: IR (neat) 3453, 3400, 3307, 3228, 2947, 2872, 1689 cm^{-1}; ^{1}H NMR (MeOD) δ (ppm) 3.43 (t, *J* = 6.6 Hz, 6H), 1.57-1.51 (m, 6H), 1.42-1.35 (m, 6H), 1.32 (s, 9H); ^{13}C (MeOD) δ (ppm) 156.5, 79.3, 63.4, 57.9, 32.4, 28.8, 27.5.

Diethyl 2,2'-((4-((tert-butoxycarbonyl)amino)-4-(3-(2-ethoxy-2-oxoethoxy)propyl)heptane-1,7-diyl)bis(oxy))diacetate (2.45). To a stirred solution of

tert-butyl (1,7-dihydroxy-4-(3-hydroxypropyl)heptan-4-yl)carbamate **2.44** (0.6 g, 1.96 mmol) and $Rh_2(OAc)_4$ (0.043 g, 0.098 mmol) in CH_2Cl_2 (6 mL) was added a solution of ethyl diazoacetate (1.05 ml, 9.98 mmol) in CH_2Cl_2 (50 ml) over a period of 1 h (syringe pump) at room temperature. After the addition was complete, the mixture was stirred for 5 h at room temperature. The solvent was removed under reduced pressure and the crude product was purified by column chromatography (SiO_2, hexane/EtOAc gradient) to give the pure product **2.45** (0.8 g, 73%): IR (neat) 3356, 2952, 2875, 1749, 1729, 1640 cm^{-1}; ^1H NMR ($CDCl_3$) δ (ppm) 4.20 (q, *J* = 7.1 Hz, 6H), 4.05 (s, 6H), 3.49 (t, *J* = 6.3 Hz, 6H), 1.63-1.57 (m, 12H), 1.39 (s, 9H), 1.27 (t, *J* = 7.1 Hz, 9H); ^{13}C ($CDCl_3$) δ (ppm) 170.6, 154.3, 78.7, 72.1, 68.5, 60.9, 56.9, 31.8, 28.6, 23.7, 14.4; HRMS (FAB) $C_{27}H_{49}NO_{11}Na$ $[M+Na]^+$ calcd 586.32037, found 586.31950.

Diethyl 2,2'-((4-amino-4-(3-(2-ethoxy-2-oxoethoxy)propyl)heptane-1,7-diyl)bis(oxy))diacetate (2.46). Compound **2.45** (1.147 g, 2.03 mmol) was mixed with a 1:1 mixture of CF_3CO_2H (2.3 mL, 31 mmol) and CH_2Cl_2 (2.3 mL) and the resulting solution was stirred at room temperature. The reaction was monitored by TLC (50% EtOAc in hexane). When the reaction was complete, the solvent was evaporated under reduced pressure. The residue was dissolved in CH_2Cl_2 (10 mL) and a saturated solution of Na_2CO_3 was added drop wise while cautiously shaking the flask until CO_2 evolution ceased. The layers were separated and the aqueous layer was extracted twice more with CH_2Cl_2 (2×20 mL). The combined organic layers were dried over Na_2SO_4 and evaporated under reduced pressure to give the crude product, which was purified by column chromatography (SiO_2, CH_2Cl_2/MeOH gradient) to give the free amine **2.46** as a colorless

oil (0.683 g, 73%): IR (neat) 3436, 2945, 2864, 1744, 1634, cm^{-1}; ^{1}H NMR ($CDCl_3$) δ (ppm) 4.19 (q, *J* = 7.1 Hz, 6H), 4.05 (s, 6H), 3.52 (t, *J* = 5.7 Hz, 6H), 1.65-1.54 (m, 12H), 1.24 (t, *J* = 7.1 Hz, 9H); ^{13}C ($CDCl_3$) δ (ppm) 170.6, 72.1, 68.5, 61.0, 54.7, 35.2, 23.7, 14.3.

Diethyl 2,2'-((4-(3-(2-ethoxy-2-oxoethoxy)propyl)-4-(4-methylphenylsulfonamido)heptane-1,7-diyl)bis(oxy))diacetate (2.47). To the stirred solution of the free amine **2.46** (0.68 g, 1.46 mmol) and tosyl chloride (0.66 g, 3.5 mmol) in CH_2Cl_2 (13 ml) was added Et_3N (0.40 mL, 2.87 mmol) and the mixture was heated at reflux for 17 h. The solvent was evaporated under reduced pressure and the residue was dissolved in CH_2Cl_2 (25 ml) and washed with water (2×25 mL). The aqueous layer was extracted with CH_2Cl_2 (2×25 mL) and the combined organic layers was dried over Na_2SO_4 and concentrated under reduced pressure. The residue was purified by column chromatography (SiO_2, hexane/EtOAc gradient) to give the product as a gummy solid (0.826 g, 91%): IR (neat) 3278, 2948, 2877, 1747 cm^{-1}; ^{1}H NMR ($CDCl_3$) δ (ppm) 7.68 (d, *J* = 8.2 Hz, 2H), 7.17 (d, *J* = 8.2 Hz, 2H), 4.10 (q, *J* = 7.1 Hz, 6H), 3.88 (s, 6H), 3.24 (t, *J* = 5.9 Hz, 6H), 2.31 (s, 3H), 1.48-1.38 (m, 12H), 1.18 (t, *J* = 7.1 Hz, 9H); ^{13}C ($CDCl_3$) δ (ppm) 170.3, 142.6, 140.7, 129.3, 126.7, 72.4, 68.1, 61.9, 61.0, 32.7, 23.2, 21.3, 14.1; HRMS (FAB) $C_{29}H_{47}NO_{11}SNa$ $[M+Na]^+$ calcd 640.27673, found 640.27700.

2,2'-((4-(3-(2-(hydroxyamino)-2-oxoethoxy)propyl)-4-(4-methylphenylsulfonamido)heptane-1,7-diyl)bis(oxy))bis(N-hydroxyacetamide) (2.29). To a solution of the triester **2.47** (0.54 g, 1.46 mmol) in MeOH (6 mL) was added

NH_2OTMS (1.00 mL, 8.17 mmol) and the mixture was stirred at room temperature for 30 h. The solvent was evaporated under reduced pressure to give a foamy solid. Recrystallization from a 1:1 mixture of EtOH and *i*-PrOH yielded the product **2.29** as a white crystalline solid (0.55 g, 80%): IR (neat) 3256, 2953, 2872, 1642 cm^{-1}; ^1H NMR (D_2O) δ (ppm) 7.81 (d, *J* = 8.3 Hz, 2H), 7.44 (d, *J* = 8.3 Hz, 2H), 3.99 (s, 6 H), 3.35 (t, *J* = 5.9 Hz, 6H), 2.43 (s, 3H), 1.52 (m, 12H); ^{13}C (MeOD) δ (ppm) 169.2, 144.4, 142.7, 130.7, 128.0, 72.9, 70.1, 63.0, 33.7, 24.2, 21.5; HRMS (FAB) $C_{23}H_{39}N_4O_{11}S$ $[M+H]^+$ calcd 579.23358, found 579.23320. The structure of **2.29** was further confirmed X-ray crystallography.

Nonanedial O,O-dibenzyl dioxime (2.55). To a solution of nonanedial **2.54** (3.80 g, 24.3 mmol) and O-benzylhydroxylamine hydrochloride (10.1 g, 63.3 mmol) in EtOH (120 mL) was added pyridine (8.6 g, 108.8 mmol) drop wise. The resulting solution was heated at reflux for 4 h. The solvent was evaporated under reduced pressure and the residue was dissolved in CH_2Cl_2 (200 mL) and washed with water (3×100 mL). The aqueous layer was re-extracted with CH_2Cl_2 (2×100 mL). The combined organic layers were dried over Na_2SO_4, evaporated under reduced pressure, and the residue was purified by column chromatography (SiO_2 hexanes) to give the product as a colorless liquid (6.12 g, 69%) as a 1.5:1 mixture of geometric isomers. IR (neat) 3030, 2925, 2856 cm^{-1}; ^1H NMR ($CDCl_3$) δ (ppm) 7.46 (t, *J* = 6.2 Hz, 0.6H), 7.39-7.31 (m, 5H), 6.69 (t, *J* = 5.4 Hz, 0.4H), 5.13 (s, 0.8 H), 5.08 (s, 1.2H), 2.39 (app q, 0.8H), 2.20 (app q, 1.2H), 1.48 (m 2H), 1.32 (m, 3H); ^{13}C NMR ($CDCl_3$) δ (ppm) 152.6, 151.7, 138.3, 137.8, 128.5 (×2), 128.3,

128.0, 127.9, 127.8, 75.8, 75.6, 29.6, 29.3, 29.1, 29.0, 26.7, 26.2, 25.9; HRMS (FAB) $C_{23}H_{31}N_2O_2$ $[M+H]^+$ calcd 367.23856, found 367.23830.

One of the isomers was isolated and characterized completely. ^{1}H NMR ($CDCl_3$) δ (ppm) 7.39 (t, *J* = 6.2 Hz, 2H), 7.31-7.24 (m, 10H), 5.00 (s, 4H), 2.13 (app q, 4H), 1.41 (quin, *J* = 6.8 Hz, 4H), 1.25 (m, 6H); ^{13}C NMR ($CDCl_3$) δ (ppm) 151.7, 137.9, 128.5, 128.4, 127.9, 75.6, 29.6, 29.1, 29.0, 26.7.

N,N'-(nonane-1,9-diyl)bis(O-benzylhydroxylamine) (2.56). To a solution of **2.55** (0.11 g, 0.3 mmol) and $NaCNBH_3$ (0.042 g, 0.66 mmol) in MeOH (2 mL) was added 2N HCl in MeOH drop wise until the solution pH was between 3 and 4. The resulting mixture was stirred for 3 h at room temperature. The solvent was evaporated under reduced pressure and the solid residue was dissolved in water (2 mL) and 6 N KOH solution was added drop wise to adjust the solution pH to >9. The aqueous solution was extracted with CH_2Cl_2 (3×10 ml), and combined organic extracts were washed with brine (20 mL), dried over Na_2SO_4 and evaporated under reduced pressure. The residue was purified by column chromatography (SiO_2 hexanes/EtOAc gradient) to give the product as a colorless liquid (0.083 g, 76%): IR (neat) 3028, 2924, 2852, 1453, 1363 cm^{-1}; ^{1}H NMR ($CDCl_3$) δ (ppm) 7.30-7.38 (m, 10H), 4.73 (s, 4H), 2.94 (t, *J* = 7.0 Hz, 4H), 1.52 (app quin, *J* =6.7 Hz, 4H), 1.30 (br s, 10H); ^{13}C NMR ($CDCl_3$) δ (ppm) 138.2, 128.5 (×2), 127.9, 76.3, 52.3, 29.6, 27.4, 27.3; HRMS (FAB) $C_{23}H_{34}N_2O_2Na$ $[M+Na]^+$ calcd 393.2518, found 393.2517.

N-(benzyloxy)-N-(9-((benzyloxy)amino)nonyl)acetamide (2.57). To a solution of **2.56** (3.0 g, 8.09 mmol) in CH_2Cl_2 (50 mL) was added a solution of DMAP (0.99 g, 8.10 mmol), and Ac_2O (0.77 mL, 8.14 mmol) in CH_2Cl_2 (50 mL). Finally, pyridine (1.34 mL, 16.56 mmol) was added drop wise and the resulting mixture was stirred at room temperature for 2 h. The mixture was diluted with CH_2Cl_2 (30 mL) and washed with saturated $NaHCO_3$ (50 mL). The organic layer was dried over Na_2SO_4 and evaporated under reduced pressure and the solid residue was purified by column chromatography (SiO_2, hexanes/EtOAc gradient) to give a colorless liquid (1.6 g, 48%): IR (neat) 3031, 2927, 2854, 1660 cm^{-1}; ^1H NMR ($CDCl_3$) δ (ppm) 7.31-7.39 (m, 10H), 5.56 (br s, 1H), 4.82 (s, 2H), 4.71 (s, 2H), 3.63 (t, *J* = 6.9 Hz, 2H), 2.93 (t, *J* = 7.1 Hz, 2H), 2.10 (s, 3H), 1.64 (m, 2H), 1.50 (m, 2H), 1.29 (br s, 10H); ^{13}C NMR ($CDCl_3$) δ (ppm) 154.2, 138.2, 134.7, 129.3, 129.0, 128.9, 128.5 (×2), 127.9, 76.4, 76.3, 52.3, 29.6, 29.4, 27.5, 27.3, 27.0, 26.9, 20.7; HRMS (FAB) $C_{25}H_{37}N_2O_3$ $[M+H]^+$ calcd 413.28040, found 413.2776.

3,3'-((2-methyl-2-(4-methylphenylsulfonamido)propane-1,3-diyl)bis(oxy))dipropanoic acid (2.61). To a solution of bis-ester (**2.60**) (3.00 g, 6.96 mmol) in aqueous THF (1:1, 30 ml) at 0 ^oC, was added $LiOH.H_2O$ (1.17 g, 27.9 mmol) and the resulting mixture was stirred for 1 h. After 1 h, the flask was allowed to warm to room temperature while stirring was continued. When all starting material was consumed (TLC 1:1 EtOAc/hexanes), the reaction was quenched with 2N HCl and the solution pH was adjusted to 1. The mixture was filtered (to remove LiCl) and extracted with CH_2Cl_2 (3×50 mL). The combined organic extracts were washed with brine, dried over Na_2SO_4 and evaporated under reduced pressure to give the di-acid as a white powder (2.67 g,

95%) which was used in the next step without further purification. IR (neat) 3300, 3051, 2925, 2875, 1697 cm $^{-1}$; ^{1}H NMR (D_2O) δ (ppm) 7.84 (d, *J* = 8.3 Hz, 2H), 7.45 (d, *J* = 8.3 Hz, 2H), 3.60-3.53 (m, 4H), 3.37 (ABq, Δδ = 22.8 Hz, *J* = 10 Hz, 4H), 2.53 (t, *J* = 6.0 Hz, 4H), 2.44 (s, 3H), 1.14 (s, 3H); ^{13}C NMR (MeOD) δ (ppm) 175.6, 144.3, 142.5, 130.5, 128.0, 74.8, 68.0, 60.1, 35.7, 21.5, 19.4; HRMS (FAB) $C_{17}H_{26}NO_8S$ $[M+H]^+$ calcd 404.13790, found 404.13880.

3,3'-((2-methyl-2-(4-methylphenylsulfonamido)propane-1,3-diyl)bis(oxy))bis(N-(benzyloxy)-N-(9-(N-(benzyloxy)acetamido)nonyl)propanamide) (2.62). To a solution of **2.57** (0.40 g, 0.97 mmol) and DMAP (0.16 g, 1.31 mmol) in CH_2Cl_2 (10 mL) and pyridine (0.11 mL, 1.4 mmol), was added a solution of **2.61** (0.18 g, 0.45 mmol) and HOBt (0.14 g, 1.03 mmol) in CH_2Cl_2 (10 mL) and the mixture was cooled to 0 ^{o}C. DCC (0.2 g, 0.97 mmol) was added and the mixture was stirred for 1 h at 0 ^{o}C. It was allowed to warm to room temperature and was stirred for an additional 15 h. The solvent was evaporated under reduced pressure and the residue was purified by column chromatography (SiO_2, hexanes/EtOAc gradient) to give the product as a thick colorless oil (0.342 g, 65%): IR (neat) 3033, 2930, 2856, 1650, 1601 cm^{-1}; ^{1}H NMR ($CDCl_3$) δ (ppm) 7.75 (d, *J* = 8.2 Hz, 2H), 7.45-7.33 (m, 20H), 7.17 (d, *J* = 8.2 Hz, 2H), 5.74 (s, 1H), 4.78 (s, 4H), 4.76 (s, 4H), 3.63-3.59 (m, 12H), 3.30 (ABq, Δδ = 52.5 Hz, *J* = 9.2 Hz, 4H), 2.66-2.55 (m, 4H), 2.25 (s, 3H), 2.04 (s, 6H), 1.58 (m, 8H), 1.23 (br s, 20H), 1.08 (s, 3H); ^{13}C NMR ($CDCl_3$) δ (ppm) 172.2, 172.0, 142.4, 140.8, 134.4, 134.3, 129.9, 129.3, 129.2, 129.0, 128.7, 128.6, 128.5, 127.0, 126.7, 126.2, 77.6, 76.2, 76.0, 73.7, 66.7, 58.6,

45.2, 32.5, 29.2, 29.0, 26.7, 26.5, 21.3, 20.4, 18.1; HRMS (FAB) $C_{67}H_{94}N_5O_{12}S$ $[M+H]^+$ calcd 1192.66199, found 1192.66110.

3,3'-((2-methyl-2-(4-methylphenylsulfonamido)propane-1,3-diyl)bis(oxy))bis(N-hydroxy-N-(9-(N-hydroxyacetamido)nonyl)propanamide) (2.49). To a solution of **2.62** (0.34 g, 0.28 mmol) in MeOH (11 mL) was added 10% Pd/C (0.074 g). The flask was then evacuated and flushed with H_2 from two balloons and the mixture was stirred under H_2 at room temperature until the starting material was consumed (TLC, 70% EtOAc in hexanes). The reaction flask was purged with Ar and the mixture was filtered. The filtrate was evaporated under reduced pressure to give the product as a foamy solid (0.22 g, 91%): IR (neat) 3360, 3060, 2928, 2857, 1611 cm^{-1}; ^1H NMR (MeOD) δ (ppm) 7.68 (d, *J* = 8.2 Hz, 2H), 7.23 (d, *J* = 8.2 Hz, 2H), 3.52-3.46 (m, 12H), 3.27-3.17 (m, 4H overlapping with MeOH peak), 2.58 (t, *J* = 6.0 Hz, 4H), 2.31 (s, 3H), 1.99 (s, 6H), 1.51 (br s, 8H), 1.21 (br s, 20H), 1.00 (s, 3H); ^{13}C NMR (MeOD) δ (ppm) 173.6, 173.5, 144.2, 142.6, 130.5, 128.0, 75.0, 68.0, 60.1, 48.9, 33.9, 30.6, 30.4, 27.8, 21.6, 20.3, 19.5; HRMS (FAB) $C_{39}H_{70}N_5O_{12}S$ $[M+H]^+$ calcd 832.4742, found 832.4725.

Dimethyl-3,3'-((2-(((benzyloxy)carbonyl)amino)-2-methylpropane-1,3-diyl)bis(oxy))dipropanoate (2.63). To a stirred solution of **2.59** (2.0 g, 7.2 mmol) in THF (57 mL) was added 10% aqueous Na_2CO_3 (57.0 mL, 53.7 mmol). After 15 minutes at room temperature CbzCl (1.13 mL, 7.93 mmol) was added and stirring was continued for an additional 5 h. The layers were separated and the aq. layer was extracted with EtOAc (2×30 mL). The combined organic extracts were washed with water and brine,

dried over Na_2SO_4 and evaporated under reduced pressure. The residue was purified by column chromatography (SiO_2, hexane/EtOAc gradient) to obtain the product as a colorless oil (1.9 g, 65%): IR (neat) 3366, 2951, 2875, 1731 cm^{-1}; ^1H NMR (300 MHz, $CDCl_3$) δ (ppm) 7.33-7.31 (m, 5H), 5.28 (s, 1H), 5.01 (s, 2H), 3.67 (t, *J* = 6.2 Hz, 4H), 3.64 (s, 6H), 3.47 (ABq, Δδ = 42.9 Hz, *J* = 9.0 Hz, 4H), 2.53 (t, *J* = 6.2 Hz, 4H), 1.29 (s, 3H); ^{13}C NMR (300 MHz, $CDCl_3$) δ (ppm) 172.2, 155.3, 136.8, 128.6, 128.2, 128.1, 73.1, 66.9, 66.1, 55.8, 51.8, 34.9, 19.8; HRMS (FAB) $C_{20}H_{30}NO_8$ $[M+H]^+$ calcd 412.19714, found 412.19750.

3,3'-((2-(((benzyloxy)carbonyl)amino)-2-methylpropane-1,3-diyl)bis(oxy))dipropanoic acid (2.64). To a solution of bis-ester (**2.63**) (7.40 g, 18.0 mmol) in 50% aqueous THF (75 mL) was added LiOH (1.68 g, 70.1 mmol) at 0 ^0C and the resulting mixture was stirred for 1 h. After 1 h, the flask was allowed to warm to room temperature with continued stirring. Once the starting material was consumed (TLC analysis, 1:1 EtOAc/hexanes), the reaction was quenched with 2N HCl to adjust the solution pH to 2. The mixture was extracted with CH_2Cl_2 (3×100 mL) and the combined extracts were washed with brine, dried over Na_2SO_4, and evaporated under reduced pressure to give the product as a colorless gel (6.8 g, quant) which was used in the next step without further purification. IR (neat) 3033, 2939, 2878, 1709 cm^{-1}; ^1H NMR (300 MHz, $CDCl_3$) δ (ppm) 10.28 (br s, 2H), 7.35-7.29 (m, 5H), 5.34 (br s, 1H), 5.04 (s, 2H), 3.68 (t, *J* = 6.2 Hz, 4H), 3.49 (ABq, Δδ = 39.6 Hz, *J* = 8.9 Hz, 4H), 2.57 (t, *J* = 6.2 Hz, 4H), 1.31 (s, 3H); ^{13}C NMR (300 MHz, $CDCl_3$) δ (ppm) 177.7, 155.4, 136.6, 128.6,

128.2, 128.2, 77.3, 72.9, 66.4, 55.7, 34.8, 19.1; HRMS (FAB) $C_{18}H_{26}NO_8$ $[M+H]^+$ calcd 384.1658, found 384.1648.

Benzyl (3,35-diacetyl-13,25-bis(benzyloxy)-19-methyl-14,24-dioxo-1,37-diphenyl-2,17,21,36-tetraoxa-3,13,25,35-tetraazaheptatriacontan-19-yl)carbamate (2.65). To a solution of **2.57** (1.1 g, 2.66 mmol) and DMAP (0.44 g, 3.60 mmol) in CH_2Cl_2 (50 mL) and pyridine (0.29 mL 3.58 mmol), was added a stirred solution of **2.64** (0.47 g, 1.22 mmol) and HOBt (0.37 g, 2.71 mmol) in CH_2Cl_2 (50 mL). The mixture was cooled to 0 ^{0}C and DCC (0.58 g, 2.81 mmol) was added. The mixture was stirred for 1 h at 0 ^{0}C, then allowed to warm to room temperature and stirred for an additional 15 h. The solvent was concentrated under reduced pressure and the solids were removed by filtration (DCC urea) and washed with CH_2Cl_2. The filtrate was evaporated under reduced pressure and the residue was purified by column chromatography (SiO_2, EtOAc/hexanes gradient) to give the product as a white solid product (0.80 g, 56%): IR (neat) 3029, 2930, 2856, 1719, 1649 cm^{-1}; ^{1}H NMR (300 MHz, $CDCl_3$) δ (ppm) 7.36-7.25 (m, 5H), 5.49 (s, 1H), 5.00 (s, 2H), 4.79 (s, 4H), 4.78 (s, 4H), 3.71 (t, *J* = 6.2 Hz, 4H), 3.60-3.55 (m, 8H), 3.49 (ABq, Δδ = 45.8 Hz, *J* = 9.1 Hz, 4H), 2.64 (t, *J* = 5.9 Hz, 4H), 2.07 (s, 6H), 1.60-1.58 (m, 8H), 1.32 (s, 3H), 1.24 (s, 20H); ^{13}C NMR (300 MHz, $CDCl_3$) δ (ppm) 172.4, 172.2, 155.1, 136.8, 134.5, 129.1 (×2), 128.9, 128.8, 128.7, 128.4, 127.9, 127.8, 77.4, 76.3, 76.2, 73.2, 67.1, 65.9, 55.7, 45.3, 33.9, 32.7, 29.4, 29.3, 29.2, 29.1, 26.8, 26.7, 26.6, 20.5, 19.0; HRMS (FAB) $C_{68}H_{94}N_5O_{12}$ $[M+H]^+$ calcd 1172.68994, found 1172.68620.

9,9'-((3,3'-((2-amino-2-methylpropane-1,3 diyl)bis(oxy))bis(propanoyl))bis(hydroxyazanediyl))bis(N-hydroxynonanamide) (2.63). To a solution of **2.65** (0.50 g, 0.43 mmol) in MeOH (16 mL) was added 10% Pd/C (0.11 g) under argon. The flask was evacuated and flushed with H_2 (balloons) and then the mixture was stirred under H_2 at room temperature until the starting material was consumed (TLC analysis, 70% EtOAc in hexanes). The reaction mixture was then flushed with Ar and filtered. The filtrate was evaporated in vacuo to obtain a sticky solid as the product (0.29 g, quant): IR (neat) 3133 (broad), 2927, 2854, 1607 cm^{-1}; ^1H NMR (300 MHz, MeOD) δ (ppm) 3.75 (t, *J* = 6.1 Hz, 4H), 3.60 (t, *J* = 7.1 Hz, 4H), 3.58 (t, *J* = 7.1 Hz, 4H), 3.41 (ABq, Δδ = 26.4 Hz, *J* = 9.6 Hz, 4H), 2.76 (t, *J* = 6.1 Hz, 4H), 2.09 (s, 6H), 1.61 (m, 8H), 1.32 (m, 20H), 1.15 (s, 3H); ^{13}C NMR (300 MHz, MeOD) δ (ppm) 173.5, 173.4, 74.9, 68.3, 56.5, 48.9, 34.8, 33.8, 30.7, 30.4, 27.8, 26.8, 26.2, 20.4 (×2); HRMS (FAB) $C_{32}H_{64}N_5O_{10}$ $[M+H]^+$ calcd 678.46533, found 678.46620.

Methyl 9-((benzyloxy)imino)nonanoate (2.68). To a solution of aldehyde **2.67** (3.40 g, 18.2 mmol) and O-benzylhydroxylamine hydrochloride (3.79 g, 23.7 mmol) in EtOH (73 mL) was added pyridine (3.75 g, 47.4 mmol) drop wise. The resulting solution was heated at reflux for 3 h. The solvent was evaporated under reduced pressure and the residue was triturated with EtOAc (5×20 mL). The EtOAc fractions were combined and filtered, then evaporated under reduced pressure. The residue was purified by column chromatography (SiO_2 hexanes/EtOAc gradient) to give the oxime as a thick colorless liquid (4.7 g, 89%) as the mixture of two geometric isomers: IR (neat) 3027, 2929, 2856, 1736, cm^{-1}; ^1H NMR ($CDCl_3$) δ (ppm) 7.44 (t, *J* = 6.2 Hz, 0.6H), 7.37-7.27 (m, 5H), 6.67

(t, *J* = 5.5 Hz, 0.4H), 5.11 (s, 0.8H), 5.06 (s, 1.2H), 3.67 (s, 3H), 2.37 (m, 0.6H), 2.31 (m, 2H), 2.17 (m, 1.4H), 1.62 (m, 2H), 1.47 (m, 2H), 1.31 (m, 6H); ^{13}C NMR ($CDCl_3$) δ (ppm) 174.4, 152.6, 151.7, 138.3, 137.8, 128.5 (× 2), 128.4, 128.0, 127.9 (× 2), 75.8, 75.6, 51.6, 34.2, 29.6, 29.3, 29.1, 29.0, 26.7, 26.3, 25.9, 25.0.

One of the isomers was isolated and characterized, but isomerized soon on standing: ^{1}H NMR ($CDCl_3$) δ (ppm) 7.44 (t, *J* = 6.2 Hz, 1H), 7.37-7.27 (m, 5H), 5.06 (s, 2H), 3.67 (s, 3H), 2.30 (t, *J* = 7.4Hz, 2H), 2.17 (app q, *J* = 6.4 Hz, 2H), 1.62 (m, 2H), 1.47 (m, 2H), 1.31 (br s, 6H).

Methyl 9-((benzyloxy)amino)nonanoate (2.69). To a solution of oxime **2.68** (4.70 g, 16.1 mmol) and $NaCNBH_3$ (1.12 g, 17.8 mmol) in MeOH (100 mL) was added 2N HCl in MeOH drop wise at room temperature until the solution pH (checked by universal indicator) was adjusted to 4-3, then the solution was stirred for 3 h at room temperature. The solvent was evaporated under reduced pressure to give a solid residue, which was dissolved in water (100 mL). 6 N KOH solution was added drop wise to adjust the solution pH to >9. The aqueous solution was extracted with CH_2Cl_2 (3×100 mL). The combined organic layers were washed with brine, dried over Na_2SO_4 and evaporated under reduced pressure. The residue was purified by column chromatography (SiO_2 2% EtOAc in hexanes) to give the hydroxylamine as a colorless liquid (4.6 g, quant): IR (neat) 3022, 2928, 2854, 1736 cm^{-1}; ^{1}H NMR ($CDCl_3$) δ (ppm) 7.36-7.27 (m, 5H), 4.71 (s, 2H), 3.67 (s, 3H), 2.92 (t, *J* = 7.0 Hz, 2H), 2.30 (t, *J* = 7.4 Hz, 2H), 1.62 (m, 2H), 1.50 (m, 2H), 1.30 (br s, 8H); ^{13}C NMR ($CDCl_3$) δ (ppm) 174.5, 138.1, 128.5, 127.9, 76.3,

52.3, 51.6, 34.2, 29.4, 29.3, 29.2, 27.4, 27.2, 25.1; HRMS (FAB) $C_{17}H_{28}NO_3$ $[M+H]^+$ calcd 294.20691, found 294.20750.

Dimethyl-10,22-bis(benzyloxy)-16-methyl-16-(4-methylphenylsulfonamido)-11,21-dioxo-14,18-dioxa-10,22-diazahentriacontane-1,31-dioate (2.70). To a solution of hydroxylamine **2.69** (0.10 g, 0.34 mmol) and DMAP (0.06 g, 0.49 mmol) in CH_2Cl_2 (4 mL) and pyridine (0.04 mL, 0.49 mmol) was added a solution of dicarboxylic acid **2.61** (0.06 g, 0.15 mmol) and HOBt (0.05 g, 0.37 mmol) in CH_2Cl_2 (4 mL). The mixture was cooled to 0 ^{0}C and DCC (0.07 g, 0.34 mmol) was added. The mixture was stirred for 1 h at 0 ^{0}C, then it allowed to warm to room temperature and stirred for an additional 20 h. The solvent was evaporated under reduced pressure and the liquid residue was purified by column chromatography (SiO_2 hexanes/EtoAc gradient) to give a thick colorless oil (0.142 g, 60%): IR (neat) 3269, 3028, 2930, 2857, 1734, 1653 cm^{-1}; ^{1}H NMR ($CDCl_3$) δ (ppm) 7.77 (d, *J* = 8.2 Hz, 2H), 7.41-7.36 (m, 10H), 7.22 (d, *J* = 8.2 Hz, 2H), 5.65 (s, 1H), 4.82 (s, 4H), 3.66-3.63 (m, 14H), 3.34 (ABq, Δδ = 87 Hz, *J* = 9.2 Hz, 4H), 2.67-2.57 (m, 4H), 2.38 (s, 3H), 2.28 (t, *J* = 7.5 Hz, 4H), 1.62-1.57 (m, 8H), 1.28 (m, 16H), 1.09 (s, 3H); ^{13}C NMR ($CDCl_3$) δ (ppm) 174.4, 172.5, 142.8, 141.0, 134.6, 129.5, 129.3, 129.1, 128.9, 127.0, 76.5, 74.0, 76.1, 58.9, 51.6, 45.6, 34.2, 34.8, 29.3, 29.2, 26.8, 25.0, 21.6, 18.3; HRMS (FAB) $C_{51}H_{76}N_3O_{12}S$ $[M+H]^+$ calcd 954.51495, found 954.51690.

9,9'-(9-methyl-9-(4-methylphenylsulfonamido)-4,14-dioxo-1,17-diphenyl-2,7,11,16-tetraoxa-3,15-diazaheptadecane-3,15-diyl)bis(N-hydroxynonanamide) (2.71). To a solution of **2.70** (2.03 g, 2.13 mmol) in dry MeOH (45 mL) was added KOH (0.80 g, 14.3

mmol), NH_2OTMS (1.22 mL, 9.38 mmol) and the resulting solution was stirred at room temperature for 15 h. Amberlyst-15 (6 g, washed with dry MeOH) was added to the reaction mixture and stirred for an additional 1 h. The mixture was filtered and the filtrate was evaporated under reduced pressure to obtain the white foamy solid product (2.01 g, quant.) which was used without further purification in the next step: IR (neat): 3258, 2927, 2857, 1632, 1454, 1110 cm^{-1}; ^1H NMR (MeOD) δ (ppm) 7.63 (d, *J* = 8.2 Hz, 2H), 7.15 (d, *J* = 8.2 Hz, 2H), 4.76 (s, 4H), 3.55 (app t, *J* = 5.9 Hz, 4H), 3.42 (app t, *J* = 5.8 Hz, 4H), 3.23-3.12 (ABq, 4H over laps with MeOD), 2.47 (app t, *J* = 5.8 Hz, 4H), 2.24 (s, 3H), 2.13 (t, *J* = 7.4 Hz, 1.4H), 1.94 (t, *J* = 7.3 Hz, 2.3H), 1.48 (m, 8H), 1.17 (m, 16H), 0.95 (s, 3H); ^{13}C NMR (MeOD) δ 174.4, 173.1, 144.2, 142.6, 136.2, 130.7, 130.5, 130.1, 129.9, 128.0, 77.4, 75.1, 68.0, 60.1, 46.1, 35.0, 33.9, 30.4, 30.3, 30.2, 27.9, 27.7, 26.8, 26.1, 21.6, 19.6; HRMS (FAB) $C_{49}H_{74}N_5O_{12}S$ $[M+H]^+$ calcd 956.50543, found 956.50500.

9,9'-((3,3'-((2-methyl-2-(4-methylphenylsulfonamido)propane-1,3-diyl)bis(oxy))bis(propanoyl))bis(hydroxyazanediyl))bis(N-hydroxynonanamide) (2.50). To a solution of **2.71** (2.0 g, 2.1 mmol) in MeOH (100 mL) under argon was added 10% Pd/C (0.22 g). The flask was then evacuated, flushed with H_2 (balloons) and the mixture was stirred under H_2 at room temperature for 3 h. The reaction mixture was filtered and the filtrate was evaporated under reduced pressure to give the product as a foamy solid (1.3 g, 81%): IR (neat) 3500-2600 (broad), 2927, 2856, 1613 cm^{-1}; ^1H NMR (MeOD) δ 7.58 (d, *J* = 8.0 Hz, 2H), 7.14 (d, *J* = 8.0 Hz, 2H), 3.44-3.36 (m, 8 H), 3.16-3.09 (m, 4H, overlaps with CD_3OD), 2.47 (t, *J* = 5.7 Hz, 4H), 2.21 (s, 3H), 1.89 (t, *J* = 7.2

Hz, 4H), 1.41 (br. S, 8H), 1.12 (br. S, 16H), 0.89 (s, 3H); ^{13}C NMR (MeOD) δ 173.6, 173.1, 144.3, 142.5, 130.5, 128.0, 74.9, 68.0, 60.1, 52.1, 34.9, 33.8, 30.3, 30.1, 27.8, 27.7, 26.8, 26.1, 21.6, 19.4; HRMS (FAB) $C_{35}H_{62}N_5O_{12}S$ $[M+H]^+$ calcd 776.41150, found 776.41130.

References

[1] Bickel, H.; Fechtig, B.; Hall, G. E.; Keller-Schierlein, W.; Prelog, V. *Helv. Chim. Acta* **1960**, *43*, 2129.

[2] Inomata, T.; Eguchi, H.; Funahashi, Y.; Ozawa, T.; Masuda, H. *Langmuir* **2012**, 28, 1611-1617.

[3] Bergeron, R. J. *Chem. Rev.* **1981**, 64, 587-602

[4] Weizman, H.; Ardon, O.; Mester, B.; Libman, J.; Dwir, O.; Hadar, Y.; Chen, Y.; Shanzer, A. *J. Am. Chem. Soc.* 1996, 118, 12368-12375.

[5] Kalinovskaya, N. I.; Romanenko, L. A.; Irisawa, T.; Ermakova, S. P.; Kalinovsky, A. I. *Microbiological Research* **2011**, 166, 654-661.

[6] (a) Bergeron, R. J.; Pegram, J. J. *J. Org. Chem.* **1988**, 53, 3131-3134. (b) Bergeron, R. J.; Wiegand, J.; McManis, J. S.; Perumal, P. T. *J. Med. Chem.* **1991**, 34, 3182-3187.

[7] Raymond, K. N.; Tufano, T. P. *J. Am. Chem. Soc.* **1981**, 103, 6617-6624. (b) Wong, G. B.; Kappel, M. J.; Raymond, K. N.; Matzanke, B.; Winkelmann, G. *J. Am. Chem. Soc.* **1983**, *105*, 810-815.

[8] (a) Sun, Y.; Martell, A. E.; Motekaitis, R. J. *Inorg. Chem.* **1985**, 24, 4343-4350. (b) Sun, Y.; Martell, A. E. Tetrahedron 1990, 46, 2725-2736.

[9] (a) Miller, M. J.; Maurer, P. J. *J. Am. Chem. Soc.* **1983**, *105*, 240-245. (b) Miller, M. J. *Chem. Rev.* 1989, *89.* 1563-1579.

[10] Neilands, J. B. *Achieves of Biochemistry and Biophysics* **1993**, 302, 1-3.

[11] (a) Tor, Y.; Libman, J.; Shanzer, A. *J. Am. Chem. Soc.* 1987, 109, 6518-6519. (b) Weizman, H.; Ardon, O.; Mester, B.; Libman, J.; Dwir, O.; Hadar, Y.; Chen, Y.; Shanzer, A. *J. Am. Chem. Soc.* **1996,** *118,* 12368-12375. (c) Kornreich-Leshem, H.; Ziv, C.;

Gumienna-Kontecka, E.; Arad-Yellin, R.; Chen, Y.; Elhabiri, M.; Albrecht-Gary, A. M.; Hadar, Y.; Shanzer, A. *J. Am. Chem. Soc.* **2005**, 127, 1137-1145.

[12] (a) Poreddy, A. R.; Schall, O. F.; Osiek, T. A.; Wheatley, J. R.; Beusen, D. D.; Marshall, G. R.; Slomczynska, U. *J. Comb. Chem.* **2004,** *6*, 239-254. (b) Ye, Y.; Liu, M.; Kao, J. L.-K.; Marshall, G. R. *Biopolymers (Peptide Science)* 2003, 71, 489-515. (c) Ye, Y.; Liu, M.; Kao, J. L.-K.; Marshall, G. R. *Biopolymers (Peptide Science)* 2006, 84, 472–489

[13] Bergeron, R. J.; Huang, G.; Weimer, W. R.; Smith, R. E.; Wiegand, J.; McManis, J. S.; Perumal, P. T. *J. Med. Chem.* **2003**, 46, 16-24.

[14] d'Hardemare, A. M.; Torelli, S.; Serratrice, G.; Pierre, J. L. *BioMetals* **2006** 19, 349-366.

[15] Matsumoto, K.; Ozawa, T.; Jitsukawa, K.; Masuda, H. *Inorg. Chem.* **2004**, 43, 8538-8546.

[16] Matsumoto, K.; Ozawa, T.; Jitsukawa, K.; Einaga, H.; Masuda, H. *Inorg. Chem.* **2001**, 40, 190-191.

[17] Matsumoto, K.; Suzuki, N.; Ozawa, T.; Jitsukawa, K.; Masuda, H. *Eur. J. Inorg. Chem.* **2001**, 10, 2481-2484.

[18] Karpishin, T. B.; Dewey, T. M.; Raymond, K. N. *J. Am. Chem. Soc.* **1993**, *115*, 1842-1851.

[19] Lee, B. H.; Miller, M. J., Prody, C. A.; Neilands, J. B. *J. Med. Chem.* **1985**, 28, 317-323.

[20] Dayan, I.; Libman, J.; Agi, Y.; Shanzer, A. *Inorg. Chem.* **1993**, 32, 1467-1475.

[21] Motekaitis, R. J.; Sun, Y.; Martell, A. E. *Inorg. Chem.* **1991**, 30, 1554-1556.

[22] Ouchetto, H.; Dias, M.; Mornet, R.; Lesuisse, E.; Camardo, J. M. *Bioorg. Med. Chem.* **2005**, 13, 1799–1803.

[23] Final report by Dr. Praveen Kommana.

[24] (a) Final report by Dr. Praveen Kommana. (b)Yokel, R. A.; Harris, W. R.; Spilling, C. D. Zhan, C. G. U.S. Patent 7,932,326, **2008**.

[25] Newkome, G. R.; Lin, X. *Macromolecules* **1991**, 24, 1443.

[26] This work was performed in collaboration with Dr. Bruce Hamper.

[27] Cardona, C. M.; Gawley, R. E. *J. Org. Chem.* **2002**, 67, 1411-1413.

[28] Griesser, H.; Ohrlein, R.; Ehrler, R.; Jager, V. *Synthesis* **1999**, 77, 236.

[29] X. A. Dominguez, I. C. Lopez and R. Franco, *J. Org. Chem*. **1961**, **26**, 1625.

[30] Newkome, G. R.; Moorefield, C. N; Theriot, K. J. *J. Org. Chem.* **1988**, 53, 5552.

[31] Evers, A.; Hancock, R. D.; Martell, A. E.; Motekaitis, R. J. *Inorg. Chem.* **1989**, 28, 2189-2195.

[32] Jödicke, T.; Menges, F.; Kehr, G.; Erker, G.; Höweler, U.; Fröhlich, R. *Eur. J. Inorg. Chem.* **2001**, 2097-2106.

[33] Donohoe, T. J.; Fishlock, L. P.; Procopiou, P. A. *Org. Lett*. **2008**, 10, 285.

[34] (a) Borch, R. F.; Bernstein, M. D.; Durst, H. D. *J. Am. Chem. Soc*. **1971**, 93, 2897. (b) Keck, G. E.; Wager, T. T.; McHardy, H. F. *Tetrahedron* **1999**, 55, 11755.

[35] (a) Keck, G. E.; Wager, T. T.; McHardy, H. F. *Tetrahedron* **1999**, 55, 11755. b) Nishino, N.; Yoshikawa, D.; Watanabe, L. A.; Kato, T.; Jose, B.; Komatsu, Y.; Sumida, Y.; Yoshida M. *Bioorg. Med. Chem. Lett*. **2004**, 14, 2427.

[36] Choudry, B. M.; Kantam, M. L.; Kavita, B. *Green Chemistry* **1999**, 289.

[37] Chavez, F.; Sherry, A. D. *J. Org. Chem.* **1989**, 54, 2990-2992.

[38] Kai, K.; Takeuchi, J.; Kataoka, T.; Yokoyama, M.; Watanabe, N. *Tetrahedron* **2008**, 64, 6760.

[39] Srisung, S. Ph. D. Dissertation, University of Missouri-St. Louis, **2007**.

[40] Crisponi, G.; Nurchi, V. M. *J. Inorg. Biochem.* **2011**, 105, 1518-1522.

[41] Yokel, R. A.; Harris, W. R.; Spilling, C. D.; Kuhn, R. J.; Dawadi, S. *U.S. Pat. Appl. Publ.* **2012**, US 2012/0061325 A1.

CHAPTER 3: Synthesis of hydroxamate functionalized chelating resins and aluminum removal studies

3.1 Specific objectives

The objectives of this project were:

(1) Immobilization of hydroxamate chelators 222-THA **2.27**, 223-THA **2.28**, and tetrahydroxamate-B **2.50** on a solid support such as polystyrene resin to obtain hydroxamate functionalized chelating resins. These resins will be applied to remove aluminum from clinical calcium gluconate solutions.

(2) An exploration of linker strategies for the immobilization of chelators via a terminal free amine. The effect of the linker on kinetics of aluminum extraction from calcium gluconate solutions will be studied, and variations in aluminum binding affinities with alternate linkers will be compared.

3.2 Background

A chelating resin is a solid polymeric material containing covalently linked chelating compounds. Chelating resins bind metal ions by forming coordination complexes. Closely related materials, ion exchange resins, bind metals through ionic interactions. Chelating resins are designed to have higher binding affinities and greater selectivity for a certain metal ion or a group of metal ions, as opposed to ion exchange resins which are less selective. This selectivity can be easily understood in terms of the well-known principle of hard and soft acid and base (HSAB) theory. Many of the known chelating resins, such as chelex **3.1** (Figure 3.1), contain immobilized nonspecific ligands. They exhibit high capacity for metal ions but poor selectivity. Chelex, for example, contains iminodiacetic acid as a chelating group and binds most divalent and trivalent metal ions. It is selective, however, for divalent metal ions over monovalent metal ions. Chelex is regularly used for the complexation of divalent metal ions such as

Cu^{2+}, Ni^{2+} and Zn^{2+}.[1] The spherical balls drawn as a part of the structure of chelex **3.1** and all other chelating resins mentioned in this chapter represent the polymeric backbone of the solid support.

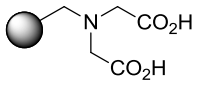

3.1

Figure 3.1 Structure of Chelex

For some applications, immobilized ligands designed to target specific metals can yield superior results. As alkali and alkaline earth metals such as sodium, potassium, calcium, and magnesium are present in relatively high concentrations in natural waters, the chelating resins should possess the ability to selectively bind heavy metals, transition metals or any other toxic metals from such systems for their commercial applications.[2] In this study, we are concerned with the preparation of chelating resins functionalized with trivalent metal selective hydroxamate ligands, and their use in the removal of aluminum from commercial calcium gluconate solutions.

There are relatively few literature examples of synthesis and metal binding studies of hydroxamate functionalized chelating resins. Usually, there are two methods for the synthesis of chelating resins. The first method involves the polymerization of monomers already containing a chelating group of interest or, a group which can be easily converted to the chelating group. In the second method, a chelating group is separately synthesized and then immobilized on a solid support via a chemical reaction between appropriate functional groups present in the chelator group and the solid support. Some of the

relevant examples of hydroxamate based chelating resins and their syntheses are provided below.

Lee and Hong[3] studied the synthetic methods for hydroxamate chelating resin **3.5** and its metal binding properties. The synthesis involved the polymerization of ethyl acrylate **3.2** crosslinked with divinylbenzene **3.3**, which gave ester functionalized resin **3.4**, followed by conversion of ester groups to hydroxamic acids by treatment with hydroxylamine in MeOH to obtain resin **3.5** (Scheme 3.1). The poly(hydroxamic acid) resin **3.5** showed excellent binding capacities for copper, iron, vanadium, and uranyl ions.

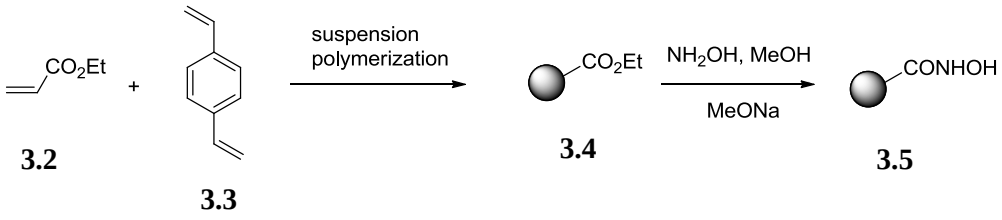

Scheme 3.1 Lee's synthesis of hydroxamate chelating resins

Crumbliss and Garrison reported the synthesis of hydroxamate functionalized Fe(III) selective chelating resins **3.8**, **3.9** (Scheme 3.1), and their iron binding capacity.[2] They used the Amberlite IRC-50 ion exchange resin **3.6** (Rohm and Haas) as the solid support. The synthesis proceeded by converting the carboxylic acid group of amberlite resin **3.6** into acid chloride **3.7** by treatment with thionyl chloride. Resin **3.7** was then treated with hydroxylamine hydrochloride or N-methyl hydroxylamine hydrochloride to obtain the hydroxamate functionalized resins **3.8** and **3.9**, respectively. They reported Fe(III) binding capacities of 1.75 and 1.52 mmol Fe/g dry resin for resins **3.8** and **3.9** at pH 2.5, respectively, and claimed that these numbers are the highest reported values for

any commercially available resins. As expected, these resins are found to be highly selective for Fe^{3+} in the presence of Ca^{2+}.

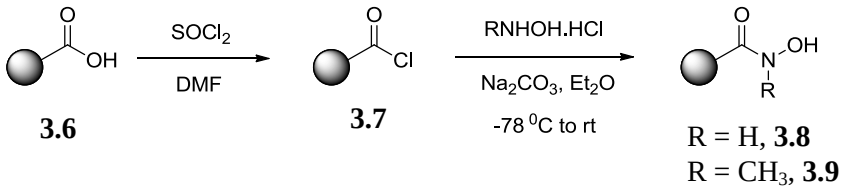

3.6 **3.7**

R = H, **3.8**
R = CH_3, **3.9**

Scheme 3.2 Crumbliss' synthesis of hydroxamate chelating resins

Inspired by the structure of naturally occurring trihydroxamic acids, Liu and coworkers[4] synthesized chelating resins with varying spacing between the hydroxamate groups, i.e., resins **3.12**, **3.16**, and **3.17** (Scheme 3.3). A nitrile functionalized macroporous cross-linked co-polymer **3.10** was prepared by the reaction of acrylonitrile and divinylbenzene. The nitrile groups were hydrolyzed to carboxylic acids to obtain resin **3.11**. The carboxylic acid resin **3.11** was then either converted to the hydroxamate resin **3.12** by treating with hydroxylamine or to the acid chloride resin **3.13** by treating with thionyl chloride. The resin **3.13** was reacted with two amine esters of varying chain lengths to obtain amide ester resins **3.14** and **3.15,** which were converted to hydroxamate resins **3.16** and **3.17** by treating with hydroxylamine. They performed the Cu(II) binding studies on the chelating resins **3.12**, **3.16**, and **3.17** and found that the Cu(II) binding affinities were very similar for all three.

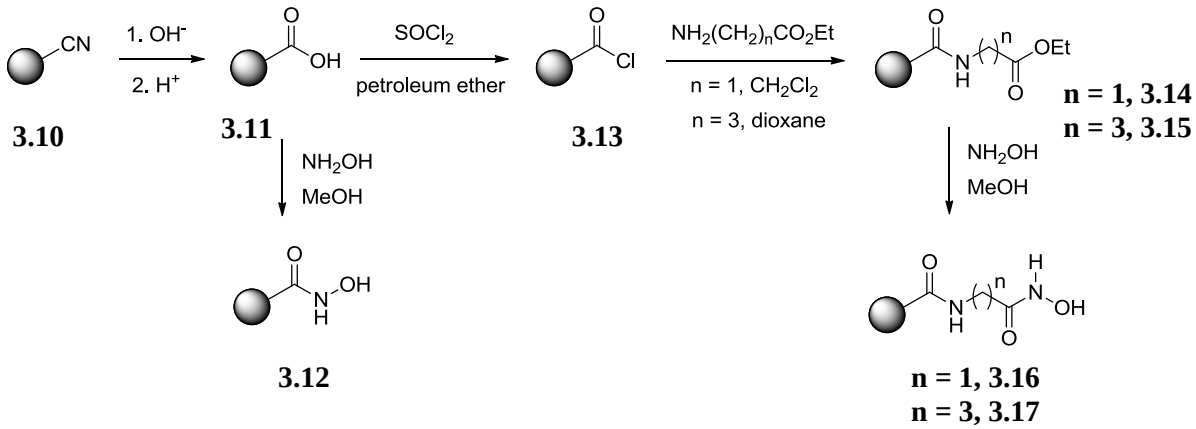

Scheme 3.3 Liu's synthesis of hydroxamate chelating resins

Hutchinson and coworkers reported the synthesis of a macrocyclic tetrahydroxamate ligand based on calix[4]arene and silica immobilized calix[4]arene tetrahydoxamate.[5] Such an immobilized tetrahydroxamate ligand was prepared by the reaction of activated silica with triethoxysilane calyx[4]arene tetrahydroxamate **3.18** (Figure 3.2). They prepared a cartridge packed with chelating silica and used the cartridge for on-line preconcentration of trace metal ions from aqueous samples. The resin removed divalent metal ions Cu(II), Mn(II), and Zn(II) almost quantitatively from such samples.

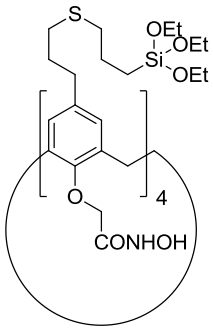

3.18

Figure 3.2 Hutchinson's triethoxysilane derivative of calix[4]arene tetrahydroxamate

In most of the literature examples of hydroxamate based chelating resins, the solid supports are randomly functionalized with hydroxamate groups. We proposed the immobilization of rationally designed hydroxamate chelators containing a proper spacer for the formation of a stable octahedral complex with metal ions. Thus for optimal binding of trivalent metal ions, we proposed the immobilization of hydroxamate ligands such as 222-THA **2.27**, 223-THA **2.28**, and tetrahydroxamate-B **2.50** (Chapter 2).

High affinity natural siderophores such as DFO would be a perfect ligand for such immobilization. DFO has a free amine which can be easily linked to various solid supports. There are previous examples of immobilization of DFO on solid support. Anthone and coworkers[6] prepared a chelating device for the extracorporeal removal of aluminum from blood. The device is made up of high-flux polysulfone F-60 hollow fiber immobilized with DFO. DFO is prohibitively expensive for the preparation of large scale chelating resin, which prevents its use for the current application. Other commercially available chelating resins such as chelex are not strong enough to remove aluminum from calcium gluconate solutions, as indicated by a work performed by Prof. Wesley R. Harris.[7] Thus, there is a need for a chelating resin that can be produced cost effectively and is also strong enough to significantly reduce aluminum contamination from commercial calcium gluconate solutions.

The intermediates in the synthesis of solution phase chelating compounds such as **2.33** and **2.40** described in Chapter 2 include a free primary amine group that allows these intermediates to be covalently linked to polymeric solid supports via various linkages. The ester groups present in these intermediates can be modified to hydroxamates in a single synthetic step. The solid supports of choice in the present study

are macroporous polystyrene divinylbenzene copolymer such as XAD-4 sold by Rohm and Haas and aminomethyl polystyrene resin sold by Sigma-Aldrich. Other solid supports that can be used for the immobilization of these chelating compounds are polymers such as polyacrylate, sepharose, and silica gel.

3.3 Immobilization of 222-THA via sulfonamide linker and aluminum removal studies

3.3.1 Synthesis

Immobilization of trihydroxamate ligand 222-THA via a sulfonamide linkage on polystyrene resin was reported previously (Scheme 3.4).[8] Synthesis of free amine trimethyl ester **2.33** is described in Chapter 2. The free amine **2.33** was treated with the sulfonyl chloride functionalized resin **3.18** in the presence of triethylamine to obtain the sulfonamide trimethyl ester functionalized resin **3.19**. Resin **3.18** was prepared from commercially available macroporous polystyrene resin XAD-4 (from Rohm and Haas) in a single step by treating with chlorosulfonic acid. The ester functional groups in resin **3.19** were converted to hydroxamic acid by treating with trimethylsilyl hydroxylamine and KOH in MeOH followed by aqueous acetic acid treatment to obtain the required resin **3.20**. Complete conversion of ester to hydroxamic acid was confirmed by the disappearance of the ester peak at 1732 cm^{-1} and appearance of a hydroxamic acid peak at 1644 cm^{-1} in the IR spectrum. The loading of ligand on the resin surface was 0.3 mmol ligand per gram of resin as determined by S and N combustion analysis of the resin.

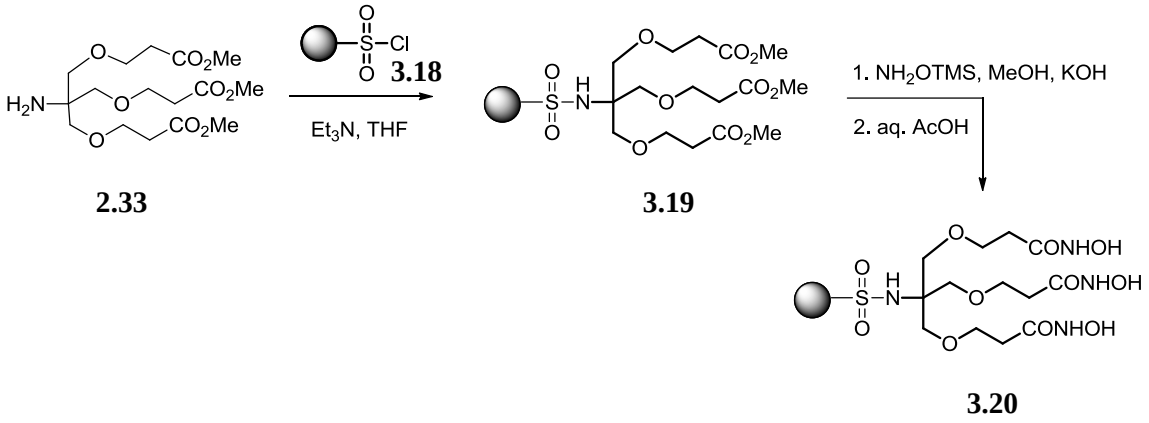

Scheme 3.4 Synthesis of solid supported 222-THA with sulfonamide linker

3.3.2 Removal of aluminum from commercial calcium gluconate solution by resin 3.20

To determine the ability of resin **3.20** to remove aluminum from commercial calcium gluconate solutions, the following experiment was performed.[9] Resin **3.20** (500 mg, 0.15 mmol ligand) was added to 20 ml calcium gluconate solution (6500 ng Al per ml solution, pH 6.2, Abraxis Pharmaceutical Products, calcium gluconate Injection USP 10% lot: 406253, exp 09/10), and the mixture was stirred with a magnetic overhead stirrer. Periodically, a 200 µl aliquot was removed from the mixture and 5 µl concentrated nitric acid was added to the aliquot to stabilize the aluminum ion in solution. Aluminum concentrations in each aliquot were determined by Inductively Coupled Plasma-Mass Spectrometry (ICP-MS). A blank sample was prepared by mixing 200 µl 18 Mohm water and 5 µl concentrated nitric acid. A plot of the fraction of the original aluminum concentration remaining in the extracted solution as a function of extraction time is shown in Figure 3.3. The pH of the extraction mixture at the end of 47 hours of extraction was measured to be 4.5.

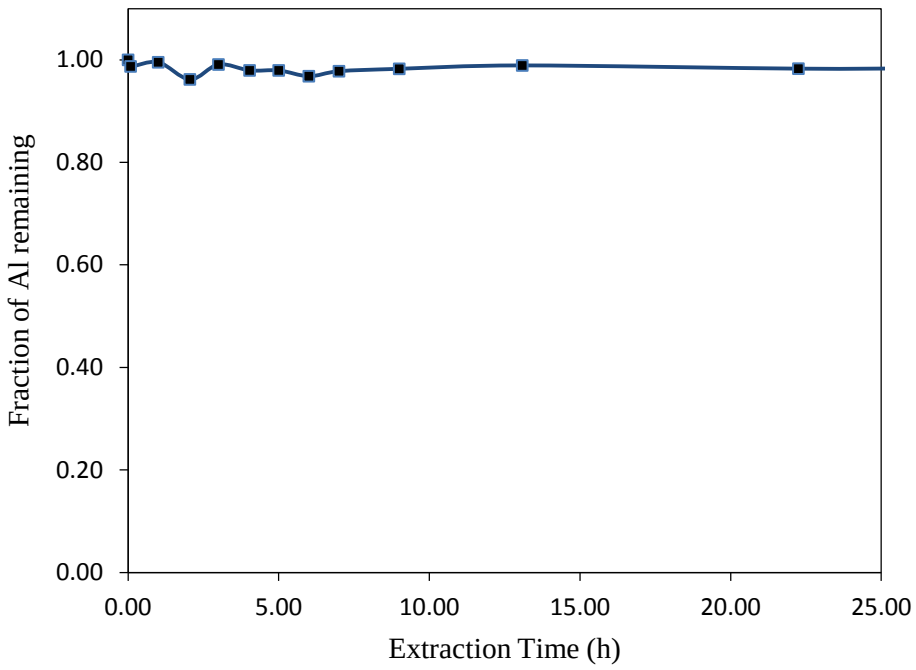

Figure 3.3 Extraction of Al from $Ca(glu)_2$ by resin 3.20

The results shown in Figure 3.3 clearly indicated that resin **3.20** did not remove aluminum from calcium gluconate solution at all. The inability of resin **3.20** to remove aluminum could have been caused by the drastic decrease in the pH of calcium gluconate solution after the addition of resin. It could also be due to the nature of sulfonamide linker which might have interfered with the binding process. However, the resin **3.20** easily removed Al^{3+} from buffered aqueous solutions.[1] Thus, the need of utilizing various linker types and other modified hydroxamate ligand groups for the optimization of aluminum binding was realized.

3.4 Immobilization of 222-THA via urea linker and aluminum removal studies

3.4.1 Synthesis

Synthesis of urea linked 222-THA resin **3.25a** and **3.25b** started with the free amine trimethyl ester **2.33** (Scheme 3.5).[10] The synthesis was accomplished by two slightly different methods. In method 1, the amine group of compound **2.33** was converted to isocyanate **3.21** by treating with triphosgene under Schotten and Baumann conditions. Commercially available macroporous aminomethyl polystyrene resin **3.20** (from Sigma-Aldrich) was treated with the isocyanate **3.21** in the presence of diisopropylethylamine (DIPEA) for 15 h to obtain the urea triester resin **3.24a**. In method 2, the aminomethyl resin **3.22** was first converted to isocyanate resin **3.23** by treating with triphosgene. The isocyannate resin **3.23** was then treated with amine **2.33** to obtain the urea triester resin **3.24b**. The only difference between resins **2.24a** and **2.24b** is the amount of loading of the triester group on the resin surface. Combustion analysis of resins **2.24a** and **2.24b** gave loading values of 1.23 meq/g and 1.22 meq/g respectively based on N analysis. The ester functional groups of resins **3.24a** and **3.24b** were converted to hydroxamic acids by treating with trimethylsilyl hydroxylamine and KOH in methanol followed by aqueous acetic acid treatment separately to obtain resins **3.25a** and **3.25b**. Complete conversion of ester to hydroxamic acid was confirmed by disappearance of the ester peak at around 1735 cm^{-1} and appearance of a hydroxamic acid peak at around 1640 cm^{-1} in the IR spectrum. The loading of ligand on resins **3.25a** and **3.25b** were calculated by N combustion analysis of the resins to be 1.04 and 0.54 meq/g respectively.

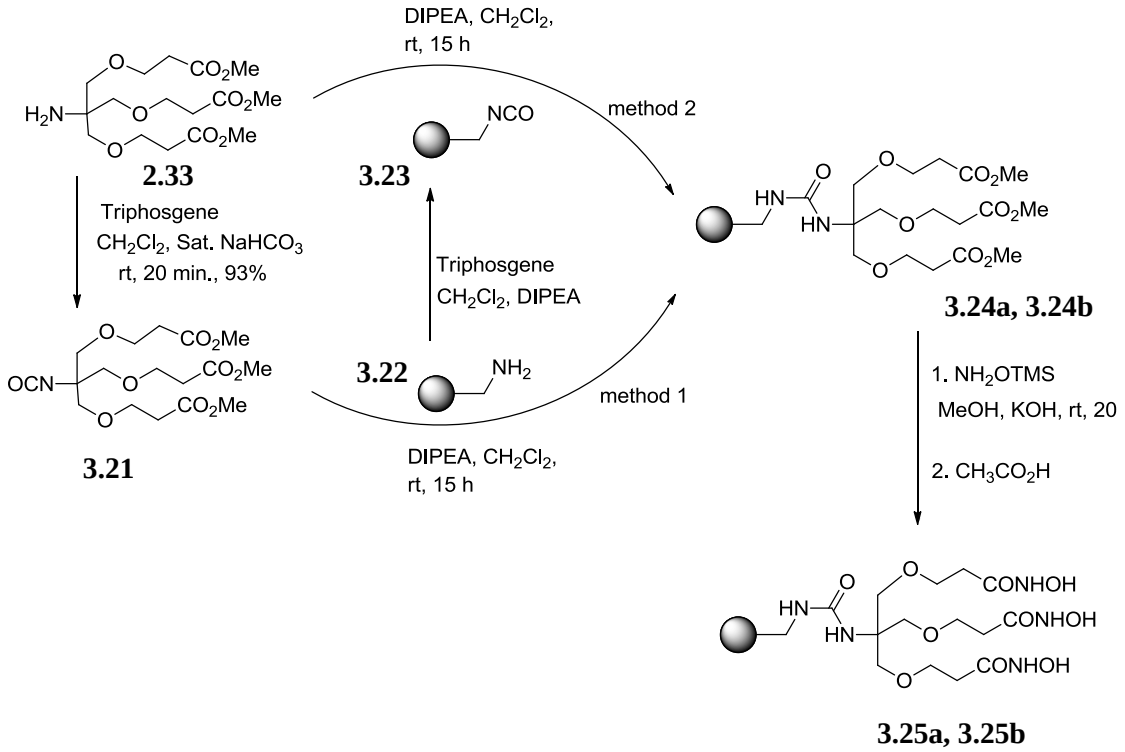

Scheme 3.5 Synthesis of solid supported 222-THA with urea linker

3.4.2 Removal of aluminum from commercial calcium gluconate solution by resin 3.25a

Resin **3.25a** (237 mg, 1.04 meq/g, 0.25 mmol ligand) was added to 10 ml calcium gluconate solution (6500 ng Al per ml solution, pH 6.1, Abraxis Pharmaceutical Products, calcium gluconate Injection USP 10% lot: 406253, exp 09/10), and the mixture was stirred with a magnetic overhead stirrer.[9] Periodically, a 100 µl aliquot was removed from the mixture and 5 µl concentrated nitric acid was added. Aluminum concentrations in each aliquot were determined by ICP-MS. A blank sample was prepared by mixing 100 µl 18 Mohm water and 5 µl concentrated nitric acid. A plot of fraction of original aluminum concentration remaining in the extracted solution as a function of extraction

time is shown in Figure 3.2. After 47 hours, the final pH of the extracted solution was measured to be 5.0.

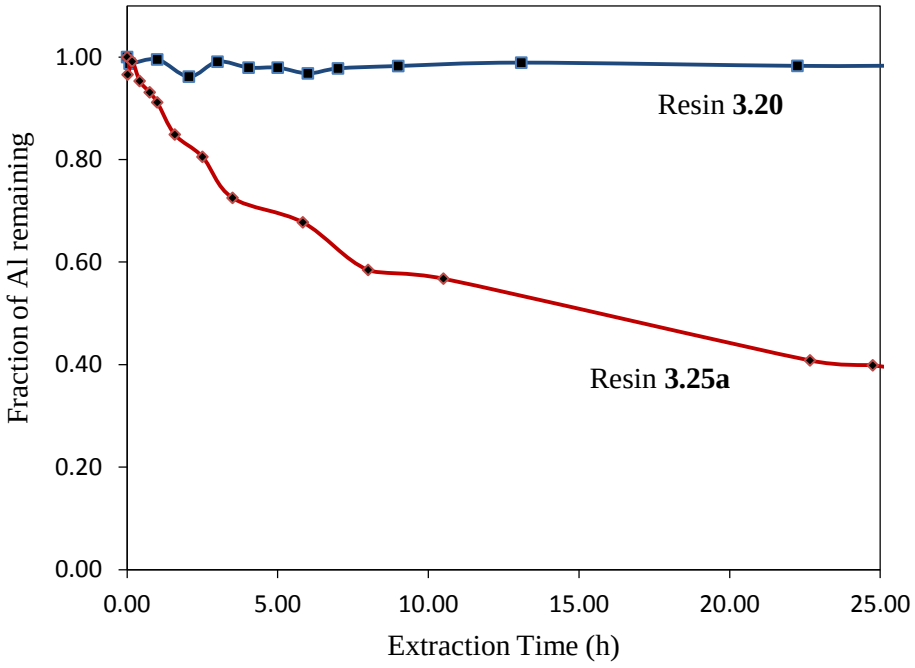

Figure 3.4 Extraction of Al from $Ca(glu)_2$ by resins 3.25a and 3.20

The results provided in Figure 3.4 indicated that resin **3.25a** removed about 60% of the aluminum present in the calcium gluconate solution over a period of 24 hours. This proves that the urea linked resin **3.25a** is much better than the sulfonamide linked resin **3.20** in removing aluminum from calcium gluconate solutions. At this stage, we started considering the immobilization of the slightly better solution phase ligand 223-THA and the much better ligand tetrahydroxamate-B through urea linkages, with the anticipation of improved binding of aluminum.

3.5 Immobilization of 223-THA via urea linker and aluminum removal studies

3.5.1 Synthesis

Synthesis of urea linked 223-THA resin **3.28** started with the free amine trimethyl ester **2.40** (Chapter 2). The free amine group of compound **2.40** was converted to the isocyanate **3.26** (Scheme 3.6) by treating with triphosgene under Schotten and Baumann conditions. Commercially available macroporous aminomethyl polystyrene resin **3.22** (from Sigma-Aldrich) was treated with isocyanate **3.26** in the presence of diisopropylethylamine (DIPEA) for 15 h to obtain the urea triester resin **3.27**. The ester functional groups of resin **3.27** were converted to hydroxamic acids by treating with trimethylsilyl hydroxylamine and KOH in methanol followed by aqueous acetic acid treatment to obtain resin **3.28**. Complete conversion of ester to hydroxamic acid was confirmed by the disappearance of ester peak at 1736 cm^{-1} and appearance of a hydroxamic acid peak at 1641 cm^{-1} in the IR spectrum. The maximum possible loading of ligand on resin **3.28** was determined again by N combustion analysis of the resin to be 0.66 meq/g.

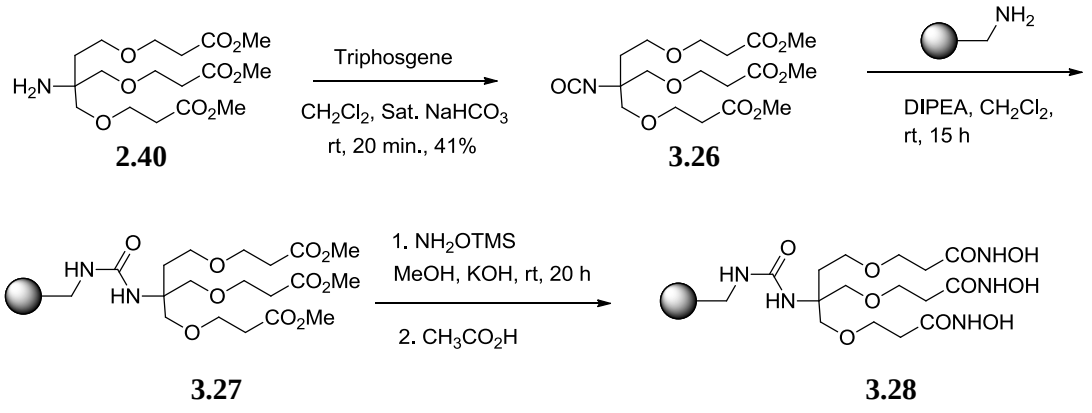

2.40 **3.26** **3.27** **3.28**

Scheme 3.6 Synthesis of solid supported 223-THA with urea linker

3.5.2 Removal of aluminum from commercial calcium gluconate solution by resin 3.28[9]

Resin **3.28** (242 mg, 0.66 meq/g, 0.16 mmol ligand) was added to 10 ml calcium gluconate solution (6136 ng Al per ml solution, pH 6.2, Abraxis Pharmaceutical Products, calcium gluconate Injection USP 10% lot: 6001317, exp 12/12) and the mixture was stirred with a magnetic overhead stirrer. Periodically, a 100 µl aliquot was removed from the mixture and 5 µl concentrated nitric acid was added. Aluminum concentrations in each aliquot were determined by ICP-MS. A blank sample was prepared by mixing 100 µl 18 Mohm water and 5 µl concentrated nitric acid. A plot of fraction of original aluminum concentration remaining in the extracted solution as a function of extraction time is shown in Figure 3.3. The final pH of the extraction mixture at the end of 28 hours of extraction was measured to be 5.3.

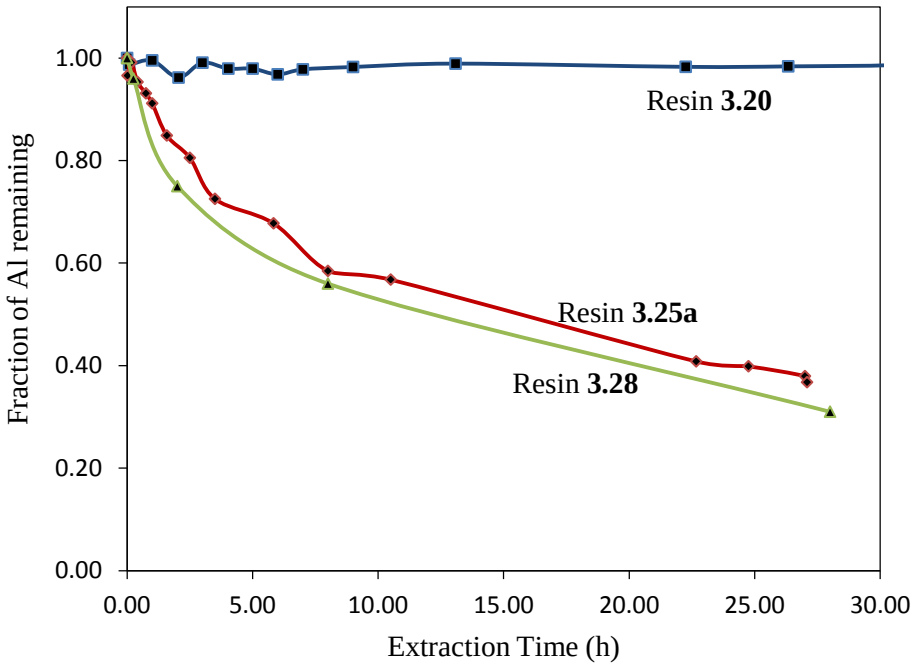

Figure 3.5 Extraction of Al from $Ca(glu)_2$ by resins 3.28, 3.25a and 3.20

The aluminum extraction studies shown in Figure 3.5 suggested that resins **3.25a** and **3.28** were equally effective in removing aluminum from calcium gluconate solutions. These results are reasonable because the aluminum binding affinities of solution phase trihydroxamate ligands 222-THA and 223-THA were about the same. As a reminder, the slightly different 222-THA and 223-THA ligands are the functional groups of resins **3.25a** and **3.28** respectively.

3.6 Immobilization of tetrahydroxamate-B ligand via urea linker

3.6.1 Synthesis

Tetrahydroxamate-B resin was prepared by immobilizing the appropriate isocyanate derivative on an aminomethyl polystyrene resin. This was accomplished via two different methods. The first method (Schemes 3.7, 3.8, and 3.10) involved the immobilization of di-ester on a polystyrene resin at the initial stage of the synthesis, followed by a large number of chemical transformations while on the solid support. The second route (Scheme 3.11) involved the preparation of fully protected tetrahydroxamate-B, selective deprotection of the amine, and immobilization on the resin at the final stage of the synthesis. Both methods are examples of convergent synthesis because two coupling partners are prepared separately.

Method 1:

Amine **2.59** (Chapter 2) was treated with triphosgene in the presence of the aqueous base to produce the isocyanate **3.29** (Scheme 3.7). This reaction was quite vigorous with the evolution of gas. Isocyanate **3.29** was reacted with aminomethyl polystyrene resin beads in the presence of a base to produce the immobilized di-ester

3.30, the immobilization occurring via the formation of a urea linkage. The loading of diester group on resin **3.30** was calculated by N combustion analysis of the resin to be 1.30 meq/g. The ester groups of resin **3.30** were converted to acid groups by alkaline hydrolysis, followed by protonation with a mineral acid to obtain resin immobilized dicarboxylic acid **3.31**. Complete conversion of the ester to carboxylic acid was confirmed by the disappearance of the ester peak at 1736 cm^{-1} and appearance of a carboxylic acid peak at 1713 cm^{-1} in the IR spectrum.

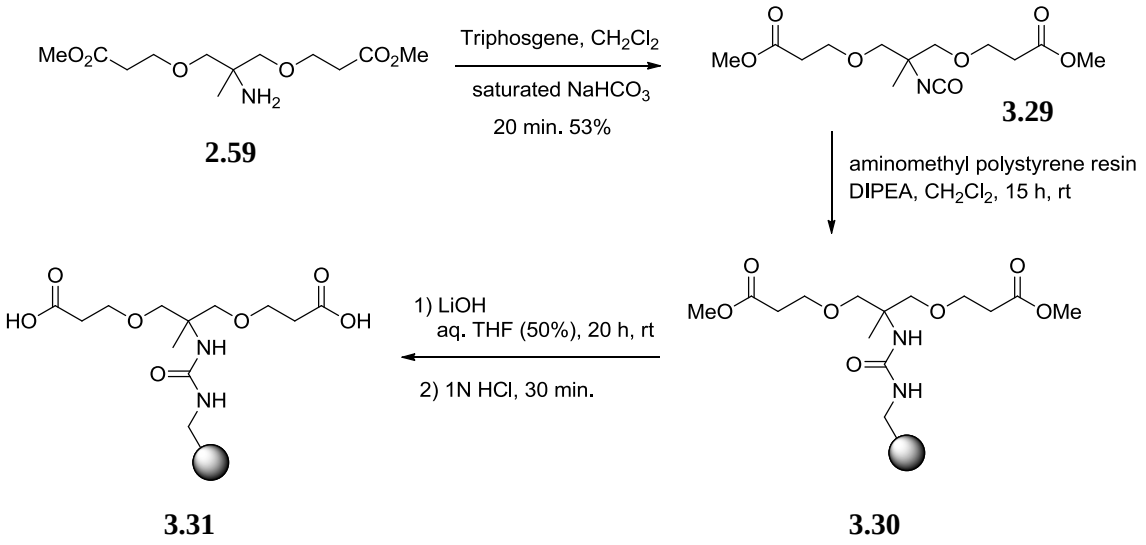

Scheme 3.7 Synthesis of solid supported dicarboxylic acid with urea linker

The aldehyde **2.67** (Chapter 2) was reacted with hydroxylamine hydrochloride and pyridine in refluxing ethanol to produce the oxime **3.32** in 95% yields (Scheme 3.8). Sodium cyanoborohydride reduction of oxime **3.32** afforded unprotected hydroxylamine **3.33** in 60-80% yield. This reduction should be carried out at pH lower than 3 to prevent the formation of the byproduct dialkylhydroxylamine **3.34**. A mechanism for the

formation of this byproduct is given in Scheme 3.9.[11] In the absence of sufficient proton concentration, hydroxylamine **3.33** has the oppertunity to react with oxime **3.32** to give the addition product **3.35**, which loses a molecule of hydroxylamine to form the positively charged species **3.36**. Addition of a hydride to highly electrophilic iminium carbon of **3.36** leads to the formation of dialkylated hydroxylamine **3.34**. Formation of this byproduct can be avoided if the pH is lowered quickly and sufficiently to cause rapid reduction of oxime to hydroxylamine. The formation of this byproduct was a more serious issue while scaling up this reaction. The ratio of product **3.33** to byproduct **3.34** was found to be in the range of 4.4:1 to 1.5:1 solely depending upon the pH of the reaction mixture.

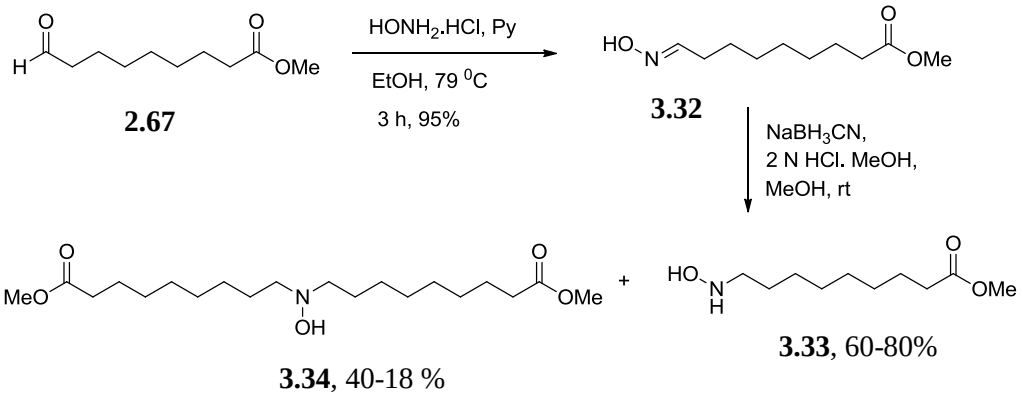

Scheme 3.8 Synthesis hydroxylamine

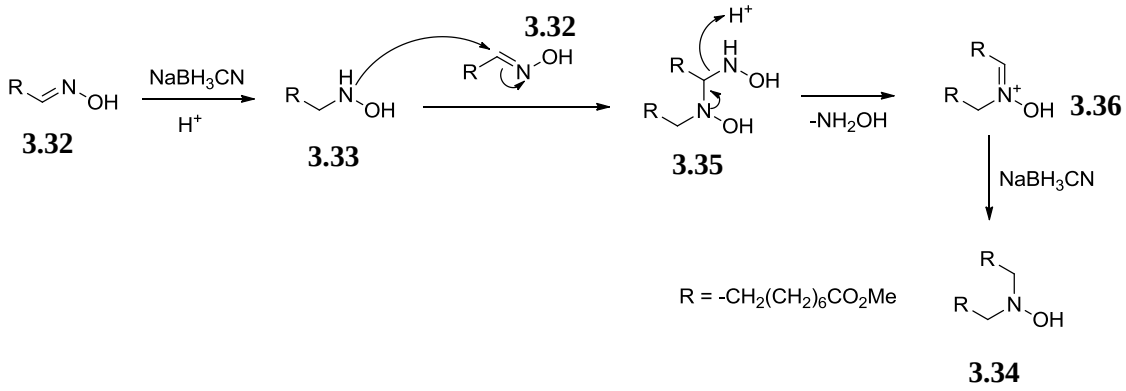

Scheme 3.9 Mechanism for the formation of byproduct dialkylhydroxylamine

Immobilized di-carboxylic acid **3.31** was then coupled with hydroxylamine **3.33** using the coupling agent EDC to afford the product **3.37**. EDC was preferentially used over DCC as a coupling agent because the byproduct of the reaction, EDC urea, was more soluble in common solvents than DCC urea. The ester groups of **3.37** were then converted to the hydroxamic acids by treating with O-trimethylsilyl hydroxylamine to afford the final product **3.38a**. The maximum possible loading of ligand on resin **3.38a** was calculated again by N combustion analysis of the resin to be 0.54 meq/g.

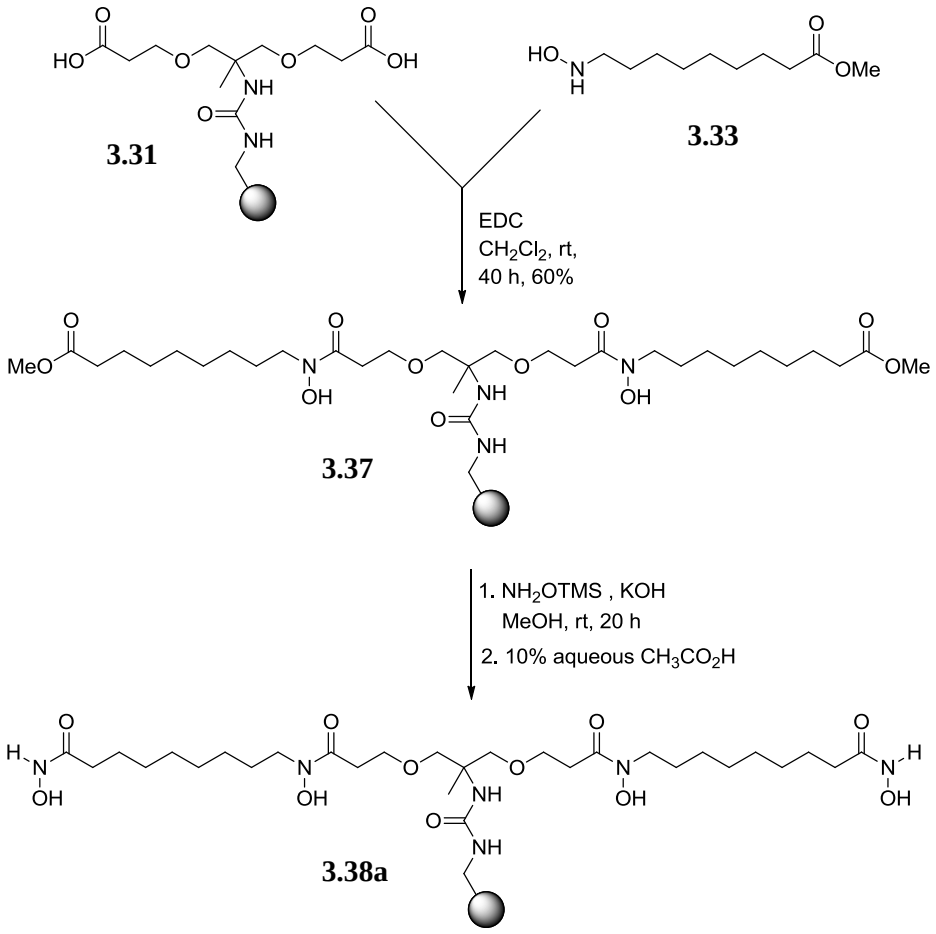

Scheme 3.10 Coupling of resin immobilized dicarboxylic acid and hydroxylamine, and final synthesis of tetrahydroxamate immobilized chelating resin 3.38a (method 1)

Method 2:

-Cbz and -THP were used as a set of orthogonal protecting groups for the amine and the hydoxamic acids, respectively. The -Cbz group can be selectively deprotected by hydrogenolysis in the presence of acid labile -THP group. The -THP protected hydroxamates can be easily deprotected at the last step of synthesis.

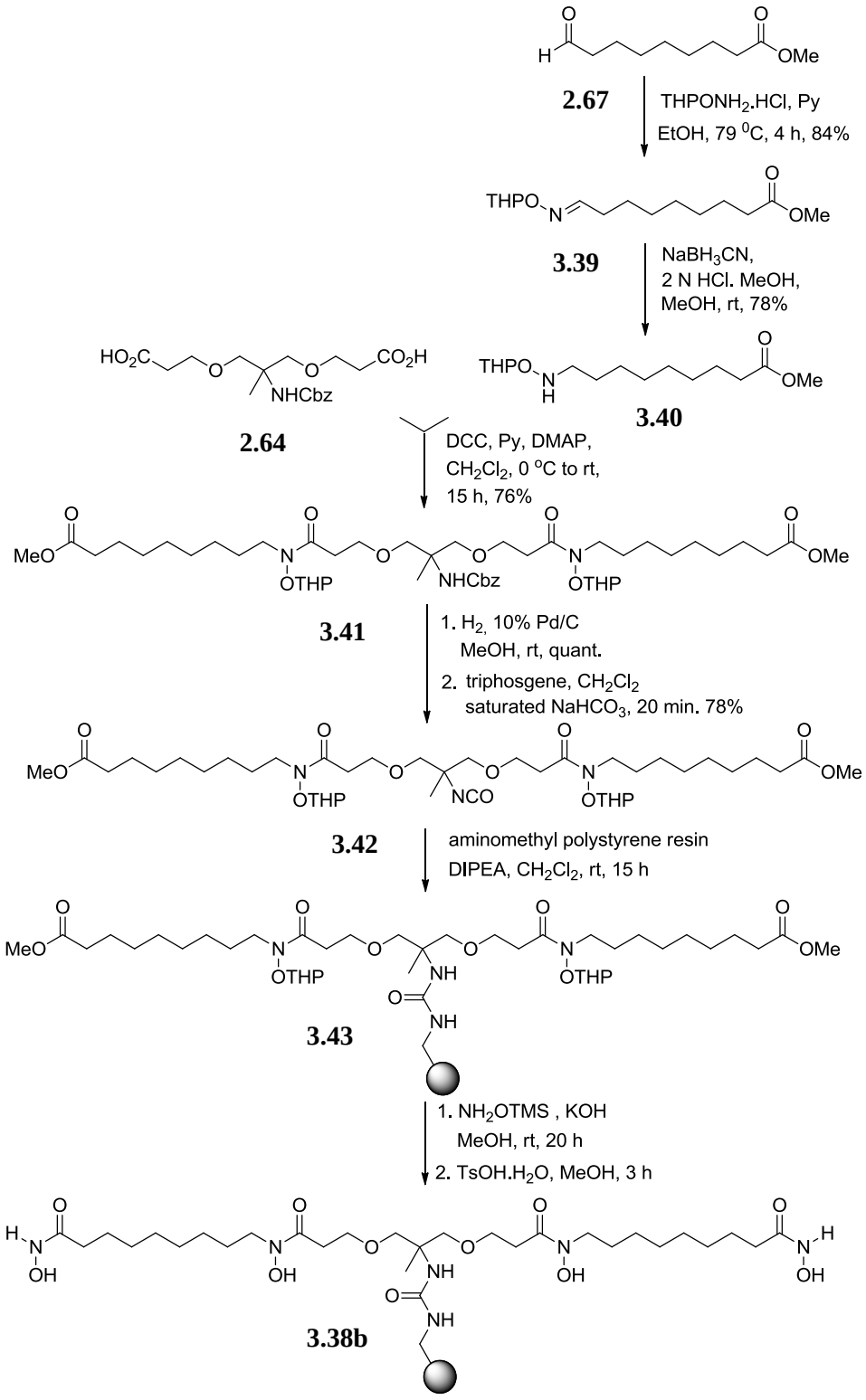

Scheme 3.11 synthesis of tetrahydroxamate immobilized chelating resin 3.38b

(method 2)

The -THP protected oxime **3.39** was prepared from aldehyde **2.67** by reacting with O-THP hydroxylamine hydrochloride and pyridine in refluxing ethanol in 84% yield (Scheme 3.11).[12] Sodium cyanoborohydride reduction of oxime afforded O-THP protected hydroxylamine **3.40** in 78% yield, which was coupled with di-carboxylic acid **2.64** to afford the compound **3.41** in 76% yield. The -Cbz group was selectively deprotected by hydrogenolysis with H_2 over Pd/C to afford the free amine which was treated with triphosgene to form the isocyanate **3.42** in 78% yield over two steps. Isocyanate **3.42** was then treated with aminomethyl polystyrene resin to form the urea linked compound **3.43**. The ester groups of compound **3.43** were converted to hydroxamic acids by reacting with O-trimethylsilyl hydroxylamine. Finally, -THP deprotection was carried out by treating the resin with $TsOH.H_2O$ to obtain the chelating resin **3.38b**. The maximum possible loading of ligand on resin **3.38b** was determined again by N combustion analysis of the resin to be 0.44 meq/g.

3.6.2 Removal of aluminum from commercial calcium gluconate solution by resins 3.38a and 3.38b

To determine the ability of tetrahydroxamate functionalized resins **3.38a** and **3.38b** to remove aluminum from commercial calcium gluconate solution, the following experiments were performed:[9]

Resin **3.38a** (213 mg, 0.54 meq/g, 0.11 mmol ligand) was added to 10 ml calcium gluconate solution (6770 ng Al per ml solution, pH 6.1, Abraxis Pharmaceutical Products, calcium gluconate Injection USP 10% lot: 406253, exp 09/10), and the mixture was stirred with a magnetic overhead stirrer. Periodically, a 100 µl aliquot was removed

from the mixture and 5 µl concentrated nitric acid was added. The aluminum concentration in each aliquot was determined by ICP-MS. A blank sample was prepared by mixing 100 µl 18 Mohm water and 5 µl concentrated nitric acid. A plot of the fraction of original aluminum concentration remaining in the extracted solution as a function of extraction time is shown in Figure 3.6. The final pH of the extracted solution at the end of 24 hours of extraction was measured to be 5.2.

Similarly, resin **3.38b** (410 mg, 0.44 meq/g, 0.18 mmol ligand) was added to 10 ml calcium gluconate solution (4834 ng Al per ml solution, pH 6.1, Abraxis Pharmaceutical Products, calcium gluconate Injection USP 10% lot: 6001317, exp 12/12), and the mixture was stirred with a magnetic overhead stirrer. Periodically, a 100 µL aliquot was removed from the mixture and 5 µL concentrated nitric acid was added. The aluminum concentration in each aliquot was determined by ICP-MS. A blank sample was prepared by mixing 100 µl 18 Mohm water and 5 µl concentrated nitric acid. A plot of the fraction of original aluminum concentration remaining in the extracted solution as a function of extraction time is shown in Figure 3.6. The final pH of the extracted solution at the end of 24 hours of extraction was measured to be 5.4.

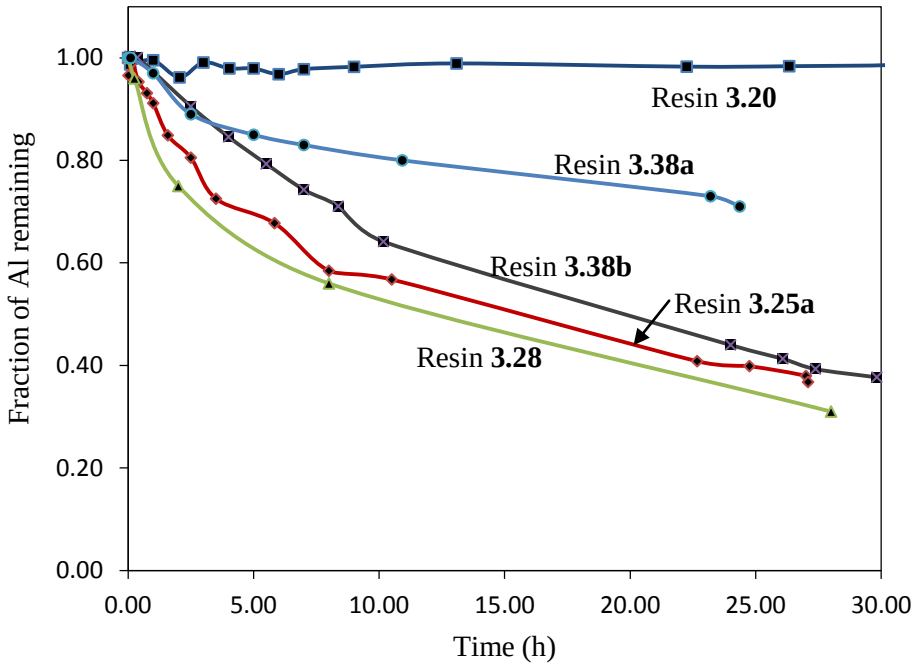

Figure 3.6 Extraction of Al from $Ca(glu)_2$ by resins 3.38a, 3.38b, 3.28, 3.25a and 3.20

The result from above experiments (shown in Figure 3.6) indicated that the tetrahydroxamate functionalized resin **3.38b** (prepared by method 2) was much better than resin **3.38a (**prepared by method 1) in removing aluminum from calcium gluconate solution. Method 1 involved a large number of synthetic steps on solid support, and it was very difficult to monitor the reactions on the solid support. Therefore, the synthesis of resin **3.38a** might not have proceeded as expected.

It was also evident that three resins **3.25a**, **3.28**, and **3.38a**, all containing urea as a linker group and each containing a different hydroxamate functional group, are almost equally effective for aluminum removal from calcium gluconate solution. All three resins removed about 60% aluminum from commercial calcium gluconate solution in a period of about 24 hours. At this stage, it was clear to us that the nature of linker is very

important for the efficiency of resins to bind metal ions. The nature of the linker seems to be much more important in metal binding kinetics than the ligand structure of the chelating resins.

3.7 Effect of nature of linker on kinetics of binding

Results from above experiments suggest that the linker plays a significant and dominating effect on the kinetics of binding metal ions by the chelating resins. To further evaluate the effectiveness of chelating resins to remove aluminum from calcium gluconate solutions, chelating resins were prepared that contain various types of linker groups between the solid support and the ligand.[13] In some cases, the linker was elongated by adding polyethylene glycol units. Among these resins, the one with a secondary amine linker gave the best aluminum binding results and will be described in detail below.

Immobilization of 222-THA on polystyrene resin via a secondary amine linker is presented in Scheme 3.12.[10] The free amine **2.33** was treated with commercially available chloromethylated polystyrene resin **3.44** (Merrifield resin) in the presence of sodium iodide in N-methyl-2-pyrrolidone (NMP) to obtain the secondary amine trimethyl ester functionalized resin **3.45**. The ester functional groups of resin **3.19** were converted to hydroxamic acids by treating with trimethylsilyl hydroxylamine and KOH in MeOH, followed by aqueous acetic acid treatment to obtain resin **3.46**. Complete conversion of the ester to the hydroxamic acid group was confirmed by disappearance of the ester peak at 1739 cm^{-1} and appearance of a hydroxamic acid peak at 1652 cm^{-1} in the IR spectrum.

The loading of ligand on the resin surface was calculated by N combustion analysis of the resin to be 0.46 mmol ligand per gram of resin.

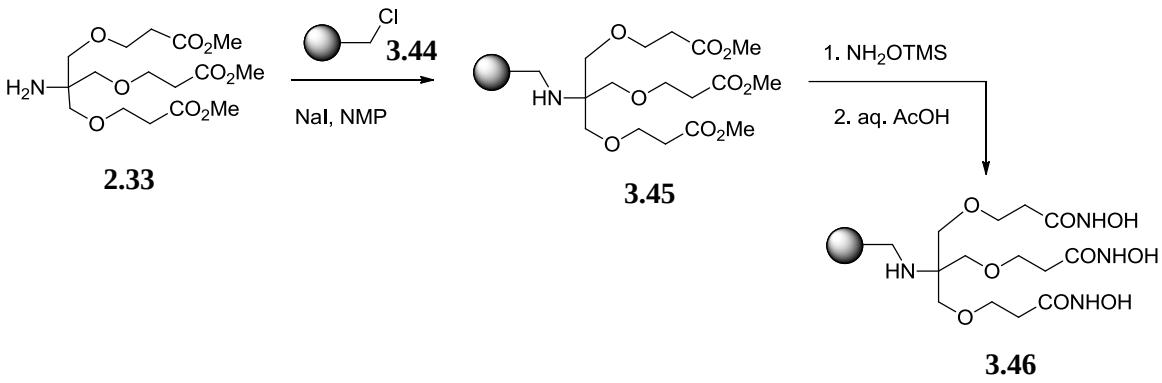

Scheme 3.12 Synthesis of solid supported 222-THA with a secondary amine linker

To determine the ability of resin **3.46** to remove aluminum from commercial calcium gluconate solution, the following experiment was performed.[9] Resin **3.46** (256 mg, 0.46 meq/g, 0.12 mmol ligand) was washed in 100 ml milliQ water for 1 h by argon bubbling agitation, filtered, dried and added to a 10 ml calcium gluconate solution (5970 ng Al per ml solution, pH 6.2, Abraxis Pharmaceutical Products, calcium gluconate Injection USP 10% lot: 6002512, exp 08/13), and the mixture was stirred with a magnetic overhead stirrer. Periodically, a 75 µl aliquot was removed from the mixture and 5 µl concentrated nitric acid was added. The aluminum concentration in each aliquot was determined by ICP-MS. A blank sample was prepared by mixing 75 µl 18 Mohm water and 5 µl concentrated nitric acid. A plot of the fraction of original aluminum concentration remaining in the extracted solution as a function of extraction time is shown in Figure 3.7. An expanded graph for resin **3.46** is shown in Figure 3.8. The final pH of the extracted solution at the end of 4 hours of extraction was measured to be 6.0.

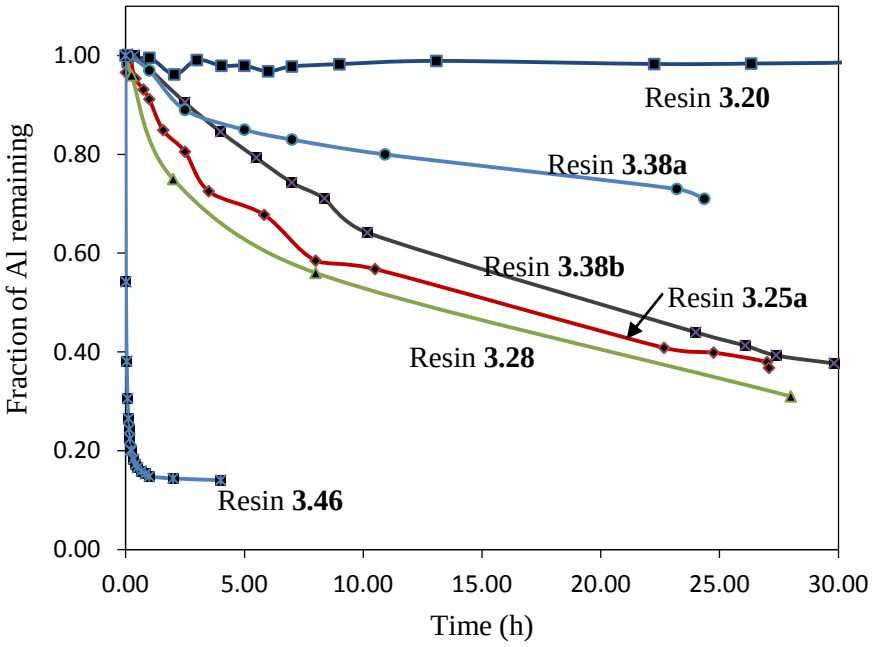

Figure 3.7 Extraction of Al from $Ca(glu)_2$ by resins 3.46, 3.38a, 3.38b, 3.28, 3.25a and 3.20

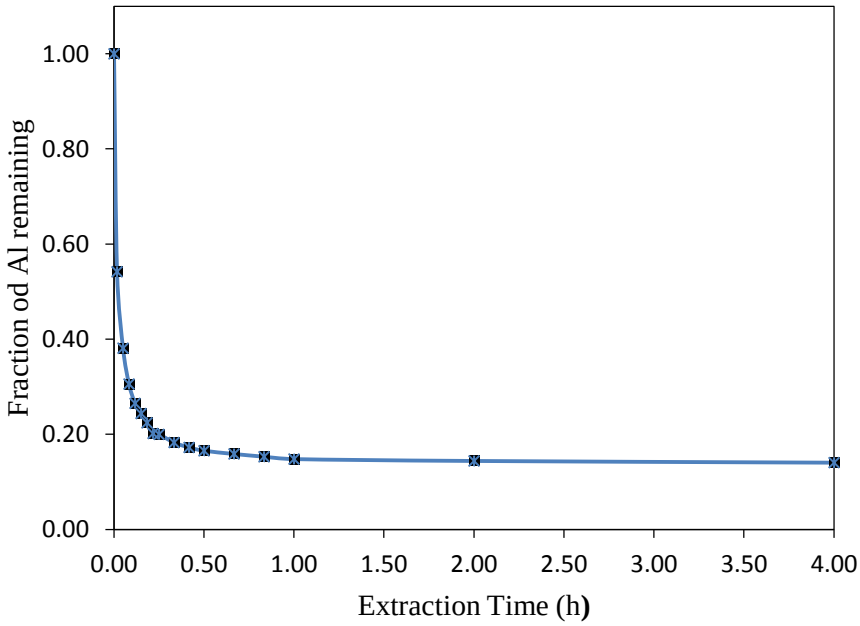

Figure 3.8 Expanded plot of extraction of Al from $Ca(glu)_2$ by resin 3.46

The result provided in Figures 3.7 and 3.8 showed that resin **3.46** containing a secondary amine linker and the 222-THA ligand is the best chelating resin made in our group so far. It removed about 90% of the aluminum from the commercial calcium gluconate solution in about 1 hour. This resin removed 50% aluminum in about 2.5 minutes, which demonstrates its superior kinetic efficiency.

3.8 Summary

A number of hydroxamate functionalized chelating resins were prepared. Various linker groups, which covalently attach ligands to the polymeric solid support, were analyzed. The resin **3.46** (222-THA ligand attached via a secondary amine linker to macroporous polystyrene resin) was found out to be the most efficient resin for the removal of aluminum from calcium gluconate solutions. The resin **3.46** was the best choice for the development of a resin packed cartridge for the in-line depletion of aluminum from commercial calcium gluconate solution. A significant reduction in the pH of calcium gluconate solution after the addition of resins was a serious issue which needs to be fixed before any commercialization of these aluminum binding resins. Multiple aqueous washes of the resin, prior to its use, seemed to address the problem as seen in the case of resin **3.46**.

The design and synthesis of the chelating resins were inspired by the analogy to the complexation behavior of solution phase model ligands described in Chapter 2. However, the analogy was not always perfect in the solid phase. The complexation behavior of ligands covalently bound to the solid support was often very different from those of solution phase ligands. The binding kinetics of chelating resins not only depends

upon the nature of the ligand, but also on the nature of linker and the solid support itself. The nature of linker was found to dictate the kinetics of binding. Changing the linker seemed to have a much more important effect on binding than changing the hydroxamate ligand.

3.9 Experimental section

Dimethyl-3,3'-((2-isocyanato-2-(2-(3-methoxy-3-oxopropoxy)ethyl)propane-1,3-diyl)bis(oxy))dipropanoate (3.26). To a vigorously stirred solution of amine triester **2.40** (12.0 g, 30.5 mmol) in CH_2Cl_2 (100 mL) and saturated $NaHCO_3$ (100 mL) was added triphosgene (3.08 g, 36.0 mmol) in small portions. Once the addition was complete, the mixture was stirred for an additional 15 min., then the layers were separated and the aqueous layer was extracted with CH_2Cl_2 (2×100 mL). The combined organic extracts were dried over Na_2SO_4, evaporated under reduced pressure, and the residue was purified by column chromatography (SiO_2, hexanes/EtOAc gradient) to give the isocyanate **3.26** as a colorless oil (5.14 g, 41%): IR (neat) 2957, 2874, 2244, 1733 cm^{-1}; ^1H NMR (300 MHz, $CDCl_3$) δ (ppm) 3.70 (t, *J* = 6.3 Hz, 4H), 3.64 (s, 9H), 3.63 (t, *J* = 6.3 Hz, 2H), 3.50 (t, *J* = 6.3 Hz, 2H), 3.39 (s, 4H), 2.54 (t, *J* = 6.2 Hz, 4H), 2.52 (t, *J* = 6.2 Hz, 2H), 1.72 (t, *J* = 6.4 Hz, 2H); ^{13}C NMR (300 MHz, $CDCl_3$) δ (ppm) 172.1, 171.9, 126.6, 73.4, 66.8, 66.7, 66.2, 62.7, 51.8, 51.7, 34.9, 34.8, 33.8; HRMS (FAB)) calcd for $C_{18}H_{30}NO_{10}$ $[M + H]^+$: 420.1870. Found 420.1885.

Resin 3.27. To a suspension of aminomethyl polystyrene resin (Aldrich 564095, macroporous 30-60 mesh) (1.84 g, 2.2 meq/g, 4.05 mmol of $–NH_2$), in CH_2Cl_2 (15 mL)

was added diisopropylethyl amine (2.12 ml, 12.2 mmol) followed by the isocyanate **3.26** (5.10 g, 12.2 mmol). The suspension was shaken using orbital shaker overnight at room temperature. The resin was filtered and washed 3 times each with CH_2Cl_2, MeOH, H_2O, saturated $NaHCO_3$, H_2O, MeOH and Et_2O. It was dried under reduced pressure to obtain a pale yellow resin (2.86 g): IR (ATR) 3393, 3026, 2912, 2869, 1736 (C=O), 1673 cm^{-1}; Elemental Analysis C 75.50%, H 7.59%, N 3.35%, loading = 1.19 meq/g (based on %N); %C indicates 76% conversion of available NH_2 groups of the resin.

Resin 3.28. A suspension of the urea triester resin **3.27** (2.68 g, 1.14 meq/g maximum loading, 3.06 mmol) in MeOH (20 mL) was shaken for 15 minutes. A solution of KOH (1.54 g, 27.59 mmol) in MeOH (5 mL) was added followed by NH_2OTMS (3.37 mL, 27.6 mmol) and the mixture was shaken for 20 h using an orbital shaker. The resin was filtered and washed 3 times with MeOH, H_2O. The resin was then suspended in 10% aqueous AcOH (20 mL) and for shaken for 30 minutes. The resin was filtered and washed 3 times with 10 % aqueous AcOH, H_2O, MeOH and Et_2O and dried under reduced pressure to give a light yellow colored resin (2.7 g): IR (ATR) 3221, 3025, 2920, 1641 (C=O hydroxamate, sharp), 1551 cm^{-1}; Elemental Analysis C 71.48%, H 7.36%, N 4.65%, loading = 0.66 meq/g (based on %N).

dimethyl 3,3'-((2-isocyanato-2-methylpropane-1,3-diyl)bis(oxy))dipropanoate (3.29). To a solution of amine **2.59** (30 g, 108.18 mmol) in CH_2Cl_2 (430 ml) was added saturated $NaHCO_3$ (430 ml) and the mixture was stirred. Triphosgene (10.69 g, 36.02 mmol) was added in small portions. A lot of gas was produced during the reaction which stopped 20

min after the complete addition of triphosgene. Layers were separated and the aqueous layer was washed with CH_2Cl_2 (2 × 100 ml). The combined organics were dried over Na_2SO_4 and evaporated to obtain the crude product which was purified by silica gel column chromatography (hexanes/ethyl acetate gradient) to give the product as a colorless oil (17.2 g, 53%): IR (neat) 2954, 2875, 2240 (sharp), 1735 (sharp), 1437, 1111 cm^{-1}; ^1H NMR (300 MHz, $CDCl_3$) δ (ppm) 3.70 (t, *J* = 6.3 Hz, 4H), 3.63 (s, 6H), 3.33 (s, 4H), 2.53 (t, *J* = 6.3 Hz, 4H), 1.14 (s, 3H); ^{13}C NMR (300 MHz, $CDCl_3$) δ (ppm) 171.7, 126.5, 74.7, 66.8, 60.6, 51.1, 34.7, 21.9; HRMS (FAB) $C_{13}H_{22}NO_7$ $[M+H]^+$ calc'd 304.1396, found 304.1391.

Resin 3.30. To a suspension of aminomethyl polystyrene resin (5.0 g, 2.2 meq/g, 11.0 mmol of $–NH_2$, Aldrich 564095, macroporous 30-60 mesh) in CH_2Cl_2 (20 ml) and diisopropylethyl amine (5.8 ml, 33.29 mmol) was added isocyanate **3.29** (10.08 g, 33.23 mmol) and allowed to shake in an orbital shaker overnight at rt. The resin was filtered and washed 3 times each with CH_2Cl_2, MeOH, H_2O, saturated $NaHCO_3$, H_2O, MeOH and Et_2O. It was then dried under reduced pressure to obtain light colored resin (7.6 g): IR (ATR) 3379 (br), 3025, 2921, 2862, 1736 (C=O), 1681, 1540, 1451, 1196, 1108, 699 cm^{-1}; Elemental Analysis C 77.85%, H 7.88%, N 3.65%, Loading value = 1.30 meq/g (based on %N); %C indicates 75% conversion of available NH_2 groups of the resin.

Resin 3.31. To a suspension of resin **3.30** (7.4 g, 0.98 meq/g) in 1:1 mixture of THF (22 ml) and H_2O (22 ml) was added LiOH (1.56 g, 65.1 mmol) in one portion and the mixture was shaken for 20 h at rt. The resin was isolated by filtration and washed 3 times each

with THF, H_2O, MeOH and Et_2O and dried under reduced pressure to give the carboxylate salt which was re-suspended in 1 N HCl (10 ml) and shaken for 30 minutes. The resin was filtered and washed again with H_2O, MeOH and Et_2O and dried under reduced pressure to obtain the product (7.1 g): IR (ATR) 3337, 3024, 2919, 2883, 1713 (C=O), 1635, 1556, 1452, 1109, 698 cm^{-1}.

methyl 9-(hydroxyimino)nonanoate (3.32). To a solution of aldehyde **2.67** (12.0 g, 64.43 mmol) and hydroxylamine hydrochloride (6.3 g, 90.66 mmol) in EtOH (270 ml) was added pyridine (13.6 ml, 168.15 mmol) drop wise and refluxed at 79 ^{0}C for 3 h. The solvent was evaporated and the remaining residue was dissolved in CH_2Cl_2 (300 ml) and washed with water (300 ml). The aqueous layer was extracted with more CH_2Cl_2 (2× 100 ml). Combined organics was dried over Na_2SO_4 and evaporated to obtain a solid crude product which was purified by SiO_2 chromatography (hexanes/EtOAc gradient) to give a white solid (12.1 g, 95%) as the mixture of both geometric isomers of the product: IR (neat) 3205, 3094, 2927, 2854, 1732, 1436, 1172 cm^{-1}; ^{1}H NMR (300 MHz, $CDCl_3$) δ (ppm) 8.43 (br s, 1.72H), 7.41 (t, *J* = 6.2 Hz, 1H), 6.72 (t, *J* = 5.4 Hz, 0.77H), 3.66 (s, 5.55H), 2.37 (td, *J* = 7.5, 7.3 Hz, 1.72H), 2.29 (app t, *J* = 7.3 Hz, 3.70 H), 2.18 (app q, *J* = 6.9 Hz, 2.05H), 1.61 (quintet, *J* = 6.5 Hz, 3.84H), 1.48 (quintet, *J* = 6.1 Hz, 3.79H), 1.31 (br s, 11.42H); ^{13}C NMR (300 MHz, $CDCl_3$) δ (ppm) 174.4, 152.8, 152.2, 51.5, 34.0, 29.4, 29.1, 28.9 (× 2), 28.8, 26.4, 25.9; HRMS (FAB) $C_{10}H_{20}NO_3$ $[M+H]^+$ calc'd 202.14430, found 202.14460.

methyl 9-(hydroxyamino)nonanoate (3.33). To a solution of oxime **3.32** (0.67 g, 3.33 mmol) and $NaCNBH_3$ (0.23 g, 3.66 mmol) in MeOH (27 ml) was added 2N HCl in MeOH drop wise at room temperature until the pH (checked by universal indicator) was adjusted to 3. The pH should be reduced to 3 quickly to prevent the formation of the dialkylhydroxylamine byproduct. The mixture was stirred for 3 h at rt. Solvent was evaporated to obtain solid white residue which was dissolved in water (50 ml). A 6 N KOH solution was added drop wise to increase the pH to >9. This aqueous layer was extracted with CH_2Cl_2 (3 × 50 ml). The organic layers were combined and washed with brine and dried over Na_2SO_4 and evaporated under reduced pressure. The crude product was purified by column chromatography (SiO_2, hexanes/ethyl acetate gradient) to give a white solid product (0.55 g, 80%): IR (neat) 3282, 3142, 2927, 2916, 2850, 1742, 1170 cm^{-1}; ^1H NMR (300 MHz, $CDCl_3$) δ (ppm) 6.47 (br s, 2H), 3.56 (s, 3H), 2.81 (t, *J* = 7.1 Hz, 2H), 2.20 (t, *J* = 7.4 Hz, 2H), 1.53-1.42 (m, 4H), 1.21 (br s, 8H); ^{13}C NMR (300 MHz, $CDCl_3$) δ (ppm) 174.2, 53.7, 51.4, 34.0, 29.2, 29.1, 29.0, 27.0, 26.8, 24.8; HRMS (FAB) $C_{10}H_{22}NO_3$ $[M+H]^+$ calc'd 204.1600, found 204.1602.

dimethyl 9,9'-(hydroxyazanediyl)dinonanoate (3.34). A white solid dialkylated hydroxylamine byproduct **3.34** (0.11 g, 18%) was also isolated from above experiment. IR (neat) 3183, 2930, 2912, 2848, 1733 cm^{-1}; ^1H NMR (300 MHz, $CDCl_3$) δ (ppm) 3.67 (s, 6H), 2.70 (app t, *J* = 7.5 Hz, 4H), 2.30 (t, *J* = 7.7 Hz, 4H), 1.63-1.59 (m, 8H), 1.31 (br s, 16H); ^{13}C NMR (300 MHz, $CDCl_3$) δ (ppm) 174.5, 60.6, 51.6, 34.2, 29.5, 29.3, 29.2, 27.3, 26.8, 25.1; HRMS (FAB) $C_{20}H_{40}NO_5$ $[M+H]^+$ calc'd 374.2906, found 374.2900.

Resin 3.37. To a suspension of dicarboxylic acid resin **3.31** (7.1 g, 0.98 meq/g, if all esters have hydrolysed) in CH_2Cl_2 (150 ml) was added hydroxylamine **3.33** (7.4 g, 36.4 mmol) and EDC (7.08 g, 36.9 mmol) and the mixture was shaken for 40 h in an orbital shaker at rt. The resin was isolated by filtration and washed 3 times each with CH_2Cl_2, MeOH, H_2O, MeOH and Et_2O and dried to obtain the product as light colored resin (8.1 g): IR (ATR) 3347 (br), 3300-2500 (br), 3023, 2922, 2870, 1713 (C=O ester), 1642 (C=O hydroxamate), 1553, 1451, 1105, 699 cm^{-1}; Elemental Analysis C 76.55%, H 7.82%, N 4.81%; Loading value = 0.86 meq/g (based on %N).

Resin 3.38a. To a suspension of resin **3.37** (8.0 g, 0.70 meq/g) in MeOH (90 ml) was added KOH (2.15 g, 38.4 mmol) and NH_2OTMS (4.7 ml, 38.4 mmol) and the mixture was shaken for 20 h in an orbital shaker at rt. The resin was isolated by filtration and washed 3 times each with MeOH, H_2O, 10% aqueous CH_3CO_2H, H_2O, MeOH and Et_2O and dried under reduced pressure to obtain the product as light yellow colored resin (7.6 g): IR (ATR) 3350 (br), 3300-2500 (br), 3028, 2915, 2867, 1717 (some carboxylic acid), 1637 (C=O hydroxamate), 1549, 1451, 1106, 699 cm^{-1}; Elemental Analysis C 75.06%, H 7.75%, N 4.55%; loading value = 0.54 meq/g (maximum loading based on %N).

methyl 9-(((tetrahydro-2H-pyran-2-yl)oxy)imino)nonanoate (3.39). To a solution of aldehyde **2.67** (2.89 g, 15.5 mmol) and O-(tetrahydro-2H- pyran-2-yl)hydroxylamine (2.0 g, 17.1 mmol) in EtOH (62 mL) at room temperature was added pyridine (1.88 mL, 23.3 mmol) drop wise. The resulting solution was heated at reflux for 4 h. The solvent was evaporated under reduced pressure and the residue was dissolved in CH_2Cl_2 (100

mL) and washed with water (2×100 mL). The aqueous layer was re-extracted with CH_2Cl_2 (2×100 mL). The combined organic layers were dried over Na_2SO_4 and evaporated at reduced pressure. The crude product was purified by column chromatography (SiO_2 hexanes) to give the oxime **3.39** as a colorless liquid (3.70 g, 84%) and as a mixture of geometric isomers: IR (neat) 2933, 2856, 1736 cm^{-1}; ^1H NMR ($CDCl_3$) δ (ppm) 7.42 (t, *J* = 6.3 Hz, 0.4H), 6.71 (t, *J* = 5.5 Hz, 0.6H), 5.19 (m, 1.2H), 5.15 (m, 0.8H), 3.89-3.84 (m, 1H), 3.62 (s, 3H), 3.59-3.53 (m, 1H), 2.35 (m, 1.5H), 2.26 (m, 2H), 2.18 (m, 0.5H), 1.90-1.40 (m, 10H), 1.29-1.26 (m, 6H); ^{13}C NMR ($CDCl_3$) δ (ppm) 174.2, 153.5, 152.9, 100.6, 100.5, 63.2, 63.1, 51.4, 34.0, 29.5, 29.1, 29.0, 28.9 (× 3), 26.6, 26.1, 25.8, 25.2(× 2), 24.9, 20.1, 20.0; HRMS (FAB) $C_{15}H_{28}NO_4$ $[M+H]^+$ calcd 286.20184, found 286.20110.

methyl 9-(((tetrahydro-2H-pyran-2-yl)oxy)amino)nonanoate (3.40). To a solution of oxime **3.39** (3.60 g, 12.31 mmol) and $NaCNBH_3$ (0.95 g, 15.1 mmol) in MeOH (100 mL) was added 2N HCl in MeOH drop wise until the solution pH was adjusted to 4 (pH was never allowed to go below 4). The mixture was stirred for 3 h at rt. The solvent was evaporated under reduced pressure to give solid residue which was dissolved in water (100 mL) and then 6 N KOH solution was added drop wise to adjust the solution pH to >9. The aqueous mixture was extracted with CH_2Cl_2 (3×100 mL). The organic layers were combined and washed with brine, dried over Na_2SO_4 and evaporated under reduced pressure. The crude product was purified by column chromatography (SiO_2 hexanes/EtOAc gradient) to give a colorless liquid product (2.80 g, 78%): IR (ATR, neat) 2931, 2854, 1736 cm^{-1}; ^1H NMR ($CDCl_3$) δ (ppm) 5.53 (s, 1H), 4.73-4.71 (m, 1H), 3.89-

3.82 (m, 1H), 3.59 (s, 3H), 3.53-3.46 (m, 1H), 2.96-2.82 (m, 2H), 2.23 (t, *J* = 7.4 Hz, 2H), 1.75-1.39 (m, 10H), 1.25 (m, 8H); ^{13}C NMR ($CDCl_3$) δ (ppm) 174.2, 101.4, 63.1, 52.2, 51.4, 34.0, 29.3, 29.2, 29.1, 29.0, 27.2, 27.1, 25.3, 24.9, 20.2; HRMS (FAB) $C_{15}H_{30}NO_4$ $[M+H]^+$ calcd 288.21747, found 288.21780.

dimethyl 16-(((benzyloxy)carbonyl)amino)-16-methyl-11,21-dioxo-10,22-bis((tetrahydro-2H-pyran-2-yl)oxy)-14,18-dioxa-10,22-diazahentriacontane-1,31-dioate (3.41). To a stirred solution of hydroxylamine **3.40** (2.30 g, 8.00 mmol) and DMAP (1.33 g, 10.9 mmol) in CH_2Cl_2 (70 mL) and pyridine (0.88 mL, 10.9 mmol) was added a solution of dicarboxylic acid **2.64** (1.39 g, 3.63 mmol) in CH_2Cl_2 and the mixture was cooled to 0 ^{0}C. DCC (1.65 g, 8.00 mmol) was added and the mixture was stirred for 1 h at 0 ^{0}C. The mixture was then allowed to warm to room temperature and was stirred for an additional 15 h. The solvent was concentrated under reduced pressure, filtered and washed with CH_2Cl_2. The filtrate was evaporated under reduced pressure and the residue was purified by column chromatography (SiO_2 hexanes/EtOAc gradient) to give the product as a colorless oil (2.50 g, 76%): IR (neat) 3329, 2930, 2856, 1732, 1655 cm^{-1}; ^{1}H NMR ($CDCl_3$) δ (ppm) 7.33-7.24 (m, 5H), 5.51 (s, 1H), 4.99 (s, 2H), 4.87 (s, 2H), 3.92-3.87 (m, 2H), 3.78-3.68 (m, 6H), 3.61 (s, 6H), 3.58-3.37 (m, 8H), 2.65-2.60 (m, 4H), 2.25 (t, *J* = 7.5 Hz, 4H), 1.76-1.54 (m, 20H), 1.29 (s, 3H), 1.24 (br s, 16H); ^{13}C NMR ($CDCl_3$) δ (ppm) 174.1, 172.7, 155.1, 136.7, 136.6, 128.3 (× 2), 127.8, 127.7, 104.3, 77.4, 73.2, 73.1, 67.9, 67.0, 65.8, 63.4, 55.7, 55.6, 51.3, 50.1, 48.6, 48.1, 35.5, 33.9, 32.9, 32.5, 30.6, 29.0 (× 2), 28.9, 28.8 (× 2), 26.6, 26.5, 26.0, 25.6, 25.1, 19.8, 19.1; HRMS (FAB) $C_{48}H_{79}N_3O_{14}Na$ $[M+Na]^+$ calcd 944.5460, found 944.5488.

dimethyl 16-isocyanato-16-methyl-11,21-dioxo-10,22-bis((tetrahydro-2H-pyran-2-yl)oxy)-14,18-dioxa-10,22-diazahentriacontane-1,31-dioate (3.42). To a solution of compound **3.41** (2.50 g, 2.70 mmol) in MeOH (200 mL) under argon was added 10% Pd/C (0.275 g). The flask was evacuated then flushed with H_2 (balloons) and the resulting mixture was stirred under H_2 at room temperature until TLC analysis (75% EtOAc in hexanes) indicated that the starting material was consumed. The reaction flask was then purged with argon and filtered. The filtrate was evaporated under reduced pressure to give the amine as a thick oil (2.1 g, 100%) which was used directly in the next step. To a stirred biphasic mixture of the amine (2.1 g, 2.7 mmol) in CH_2Cl_2 (30 mL) and saturated $NaHCO_3$ (30 mL) was added triphosgene (0.26 g, 0.89 mmol) in small portions. 20 min after the addition of triphosgene, the layers were separated and the aqueous layer was washed with CH_2Cl_2 (2×30 mL). The combined organic layers were dried over Na_2SO_4 and evaporated under reduced pressure to give the isocyanate **3.42** as a thick colorless oil product (1.7 g, 78 %) which was found to be pure enough to use in the next step without further purification. IR (neat) 2932, 2856, 2241, 1736, 1655 cm^{-1}; ^1H NMR ($CDCl_3$) δ (ppm) 4.89 (br s, 2H), 3.96-3.89 (m, 2H), 3.81-3.72 (m, 6H), 3.62 (s, 6H), 3.60-3.53 (m, 4H), 3.41-3.32 (m, 4H), 2.68- 2.61 (m, 4H), 2.26 (t, *J* = 7.4 Hz, 4H), 1.78-1.57 (m, 20H), 1.26 (br s, 16H), 1.18 (s, 3H); ^{13}C NMR ($CDCl_3$) δ (ppm) 174.3, 172.7, 126.8, 104.5, 77.4, 75.3, 75.2, 75.1, 68.2, 67.3, 63.6, 61.2, 61.1, 61.0, 55.0, 51.5, 50.2, 48.3, 35.7, 34.1, 33.1, 32.6, 30.8, 29.5, 29.2, 29.1, 26.9, 26.8, 26.2, 25.5, 25.4, 22.5, 19.8; HRMS (FAB) $C_{41}H_{71}N_3O_{13}Na$ $[M+Na]^+$ calcd 836.48846, found 836.48570.

Resin 3.43. To a suspension of the aminomethyl resin (1.1 g, 2.2 meq/g, 2.42 mmol of –NH_2, Aldrich 564095, macroporous 30-60 mesh) in CH_2Cl_2 (17 mL) and diisopropyl ethyl amine (2.66 mL, 15.3 mmol) was added the isocyanate **3.42** (5.0 g, 6.10 mmol) and the resulting mixture was shaken on an orbital shaker for 24 h at room temperature. The resin was filtered and washed 3 times each with CH_2CH_2, MeOH, H_2O, saturated $NaHCO_3$, H_2O, MeOH and Et_2O. It was then dried under reduced pressure to obtain a light colored resin (1.5 g): IR (ATR) 3377, 3022, 2924, 2848, 1734 (C=O ester), 1655 (C=O hydroxamate) cm^{-1}; Elemental analysis C 81.23%, H 7.96%, N 3.67%, loading = 0.65 meq/g (based on %N); %C indicates 43% conversion of available NH_2 groups of the resin.

Resin 3.38b. To a suspension of the resin **3.43** (1.51 g, 0.30 meq/g, 0.45 mmol) in MeOH (10 mL) was added KOH (0.15 g, 2.7 mmol) and NH_2OTMS (0.33 mL, 2.7 mmol) and the mixture was shaken for 20 h on an orbital shaker. The resin was isolated by filtration and washed 3 times with MeOH. The resin was re-suspended in a solution of $TsOH.H_2O$ (0.52 g, 2.7 mmol) in MeOH (10 mL) and shaken for 3 h. The resin was isolated by filtration and washed 3 times each with MeOH, H_2O, MeOH and Et_2O and dried under reduced pressure to give the product as a pale yellow colored resin (1.73 g): IR (ATR) 3382 (br), 3500-2500 (br), 3024, 2922, 2854, 1646 (C=O hydroxamate) cm^{-1}; Elemental Analysis C 75.74%, H 7.51%, N 3.68%, Loading = 0.44 meq/g (maximum loading based on %N).

References

[1] Srisung, S. Ph. D. Dissertation, University of Missouri-St. Louis, **2007**.

[2] Crumbliss, A. L.; Garrison, J. M. *Inorganica Chimica Acta* **1987**, 133, 281-287.

[3] (a) Lee, T. S.; Hong, S. I. *Polym. Bull.* **1994**, 32, 273. (b) Lee, T. S.; Hong, S. I. *Journal of Polymer science: Part A: Polymer Chemistry* **1995**, 33, 203-210.

[4] Liu, C. Y.; Chen, M. J.; Lee, N. M.; Hwang, H. C.; Jou, S. T.; Hsu, J. C. *Polyhedron* **1992**, 11, 551-558.

[5] Hutchinson, S.; Kearney, G. A.; Horne, E.; Lynch, B.; Glennon, J. D.; McKervey, M. A.; Harris, S. J. *Anal. Chim, Acta* **1994**, 291, 269-275.

[6] Anthone, S.; Ambrus, C. M.; Kohli, R.; Min, I.; Anthone, R.; Stadler, A.; Stadler, I.; Vladutiu, A. *J. Am. Soc. Nephrol.* **1995**, 6, 1271-1277.

[7] Yokel, R. A.; Harris, W. R.; Spilling, C. D.; Kuhn, R. J.; Dawadi, S. *U.S. Pat. Appl. Publ.* **2012**, US 2012/0061325 A, Figure 7, sheet 6.

[8] (a) Final report by Dr. Praveen Khommana. (b) Yokel, R. A.; Harris, W. R.; Spilling, C. D. Zhan, C. G. *U.S. Patent* 7,932,326, **2008**.

[9] All aluminum removal studies were performed in collaboration with Nicholas Bardol (Harris group), Prof. Wesley R. Harris (University of Missouri-St. Louis) and Prof. Robert A. Yokel (University of Kentucky).

[10] (a) This work was performed in collaboration with Prof. Bruce Hamper. (b) Yokel, R. A.; Harris, W. R.; Spilling, C. D.; Kuhn, R. J.; Dawadi, S. *U.S. Pat. Appl. Publ.* **2012**, US 2012/0061325 A1.

[11] Borch, R. F.; Bernstein, M. D.; Durst, H. D. *J. Am. Chem. Soc.* **1971**, 93, 2897-2904.

[12] Kai, K.; Takeuchi, J.; Kataoka, T.; Yokoyama, M.; Watanabe, N. *Tetrahedron* **2008**, 64, 6760.

[13] (a) Yokel, R. A.; Harris, W. R.; Spilling, C. D.; Kuhn, R. J.; Dawadi, S. *U.S. Pat. Appl. Publ.* **2012**, US 2012/0061325 A1. (b) Personal communication with Dr. Bruce Hamper.

CHAPTER 4: Immobilization of citramide based chelators and application in the removal of trivalent metals from water at low pH

4.1 Specific objectives

The objectives of this project were:

(1) Immobilization of citric acid, a common carboxylate based chelating agent, on a solid support such as a polystyrene resin to obtain citramide functionalized chelating resins.

(2) An application of such citramide resins for the removal of trivalent metal ion such as iron from aqueous solutions at low pH. The iron binding affinities of these resins will be determined by difference UV-Vis Spectroscopy.

4.2 Background

Several resins have been prepared in which chelating agents are covalently linked to polymer beads. Compared with simple ion exchange resins, the use of immobilized chelating agents allows one to achieve both higher binding affinity and greater selectivity among different metal ions. This selectivity can be easily understood in terms of the well-known principles of hard-soft acid-base (HSAB) theory.[1] Many of the known chelating resins simply immobilize a nonspecific generic ligand. For some applications, immobilized ligands designed to target specific metals (or groups of metals) could yield superior results.[2]

Citric acid **4.1** (Figure 4.1) has been extensively used as chelating agent for cleaning purposes.[3] Trivalent metal ions such as iron and aluminum form strong complexes with citrates. Carboxylic acids are more acidic than hydroxamic acid, therefore, citrate binds metal ion more strongly than does hydroxamate at low pH. As a hard ligand, citrate coordinates metals via negatively charged oxygen atoms, and prefers to bind hard metal ions such as Fe^{3+} and Al^{3+}. Thus, a citrate immobilized chelating resin

is a good choice for applications that requires removal of such metal ions at low pH. After a thorough literature search, we realized that there are no previous reports of the immobilization of citric acid on a solid surface.

Trivalent metal ions form relatively strong complexes with citrate by binding through its carboxyates and α-hydroxyl groups.[3] Citrate is a tridentate chelator as seen in the structure **4.2** (Figure 4.1). The central carboxylate and α-hydroxyl group first form a perfect five membered chelate with the metal, then, one of the two equivalent terminal carboxylates binds.

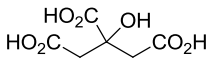

4.1

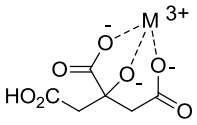

4.2

Figure 4.1 Citric acid and citric acid-trivalent metal complex

Rhizoferrin **4.3** (Figure 4.2), a novel high affinity citrate based natural siderophore,[4] forms a highly stable 1:1 complex with Fe(III). Structure determination of rhizoferrin revealed a diamine backbone symmetrically diacylated by citric acid at its 1-carboxylate.[4] It has two sets of tridentate hydroxy carboxylate chelating groups. The example of rhizoferrin is relevant here, as it further proves the very strong trivalent metal binding properties of the hydroxy carboxylate groups.

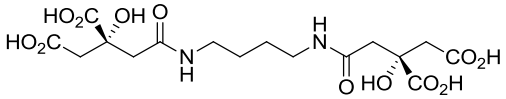

4.3

Figure 4.2 Structure of a citrate based natural siderophore rhizoferrin

4.3 Design of citramide functionalized chelating resins

We recently developed a series of hydroxamate-based chelating resins for the removal of aluminum (and other trivalent metals) from aqueous solutions (Chapter 3).[5] However, the effective binding of trivalent metals to hydroxamates diminishes at low pH. Since waste water streams (and other aqueous solutions) can be acidic, a new system was needed which would operate at low pH. We postulated that immobilized citramide **4.4** or **4.5** (Figure 4.3) would show the desired characteristics. The binding unit of resin **4.4** is very similar to that of natural siderophore rhizofferin **4.3**. The only difference between the resins **4.4** and **4.5** is the type of citrate carboxylate forming the amide linkage. In **4.4**, one of the two equivalent 1-carboxylates of citrate is forming the amide linkage, whereas, in **4.5** the central carboxylate is doing so. Resin **4.4** chelates through an α-hydroxy carboxylate group, whereas, **4.5** binds through a β-hydroxy carboxylate. As mentioned earlier, the α-hydroxy carboxylate is the metal chelating group of citrate as shown in structure **4.2.** Thus, resin **4.4** should be the better binding resin. However, in any synthetic route to resin **4.4**, formation of resin **4.5** in some amount is inevitable.

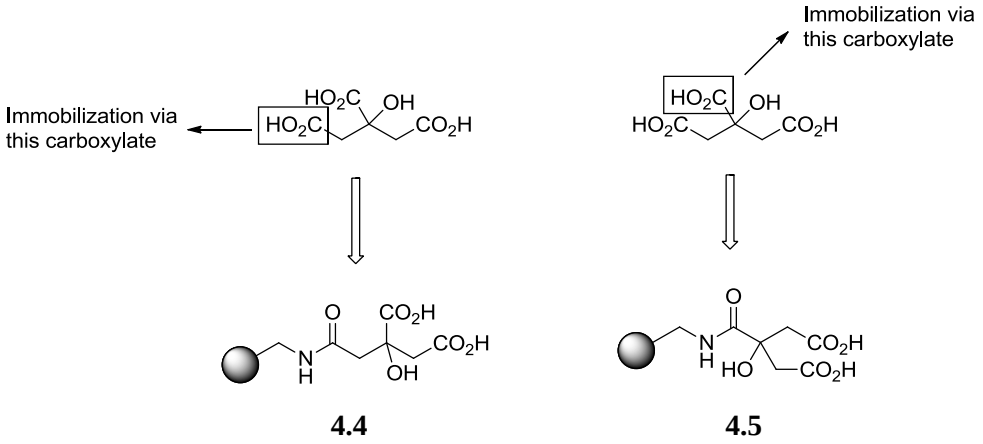

Figure 4.3 Two possible structures of mono-citramide functionalized resin

To demonstrate the ability of citrate functionalized resin **4.4** to bind iron at low pH, the following speciation analysis was performed. An equilibrium model for the mixture of resin **4.4**, Fe^{3+} and acetohydroxamic acid (AHA) was constructed within the speciation software HySS (Hyperquad Simulation and Speciation). The structure of AHA **4.6** is given in Figure 4.4. AHA is a monohydoxamate Fe chelator used in these experiments as a competing ligand. The model included literature values for protonation and Fe binding constants for citrate[6] (assuming the binding of a solution phase citrate is similar to that of a resin immobilized citrate) and AHA (β_{130} = 28.33)[7] as fixed parameters. An effective concentration for the immobilized citrate was calculated by dividing the total mmoles of citrate on the resin by the total sample volume. The concentrations of AHA and citrate were manually varied until the speciation calculation matched about a 50% distribution of Fe^{3+} between the resin and AHA. Concentrations of 10 mM AHA and 45.9 mM citrate gave about a 1:1 distribution of Fe^{3+} (0.1 mM) between these species at pH 6. The predicted speciation of the mixture of Fe^{3+}, resin **4.4** and AHA as a function of pH is shown in Figure 4.5. The result also indicates that the

resin should bind essentially 100% of the Fe^{3+} below pH 5 at above mentioned concentrations. Above pH 5, AHA begins to compete for Fe with the resin, and $Fe(AHA)_3$ is the only species above pH 7.

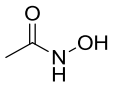

4.6

Figure 4.4 Structure of a hydroxamate chelator Acetohydroxamic acid (AHA)

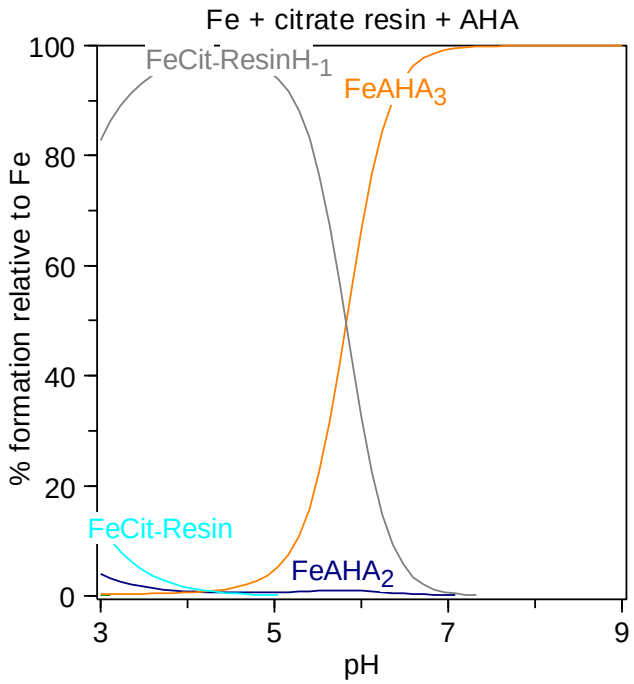

Figure 4.5 Species distribution diagram of Fe^{3+} in a mixture of AHA and the resin 4.4 at pH 3-9

To potentially increase the loading density and provide the opportunity for multiple carboxylates to bind to a single metal, branched polyamine linker scaffolds were studied. Thus, resin **4.7** (Figure 4.6) containing a bis- citramide system immobilized via a tetraamine linker was designed. The ligand on resin **4.7** is a regioisomeric mixture, where two non-eqivalent carboxylates of citric acid are forming amide bonds with the amine groups of resin giving structures **4.7'** and **4.7''**. The structure of resin **4.7** is very close to that of the earlier mentioned natural siderophore rhizoferrin **4.3**. There are 4 carbon atoms between two the amide bonds of rhizoferrin, whereas, there are 4 carbon and 1 nitrogen atoms (total 5 atoms) between two such groups in resin **4.7**. Thus, the iron binding affinity of resin **4.7** was expected to be very close to that of rhizoferrin.

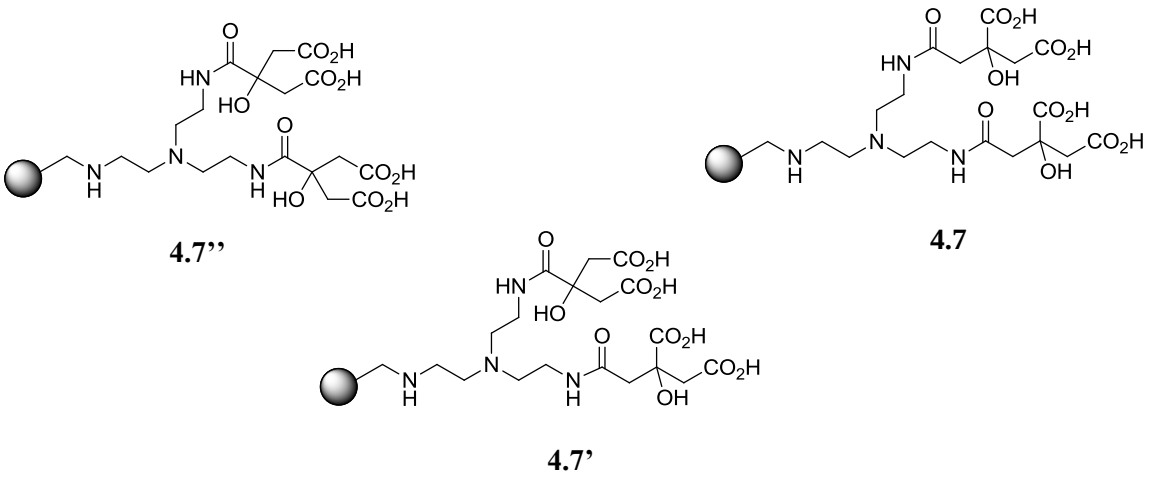

4.7'' **4.7** **4.7'**

Figure 4.6 Possible structures of bis-citramide functionalized resin

An equilibrium model for the mixture of the bis-citramide resin **4.7**, Fe^{3+} and acetohydroxamic acid (AHA) was constructed within the speciation software HySS. As resin **4.7** contains a bis-citramide system, the β_{120}, β_{121} and $\beta_{12\text{-}1}$ constants of citrate[8] were

also included, in addition to the protonation and binding constants of the mono-citrate system. The concentration of AHA was manually varied keeping the concentration of the citrate resin constant until the speciation calculation matched about a 50% distribution of Fe^{3+} between the resin and AHA at pH 6. Concentrations of 30 mM AHA and 45.9 mM citrate gave about a 1:1 distribution of Fe^{3+} (0.1 mM) between these ligands at pH 6. The predicted speciation of the mixture of Fe^{3+}, resin **4.7** and AHA as a function of pH is shown in Figure 4.7. The result also indicates that the resin should bind essentially 100% of the Fe^{3+} below pH 5 at above mentioned concentrations. Above pH 5, AHA begins to compete for Fe with the resin, and $Fe(AHA)_3$ is the only species above pH 7.

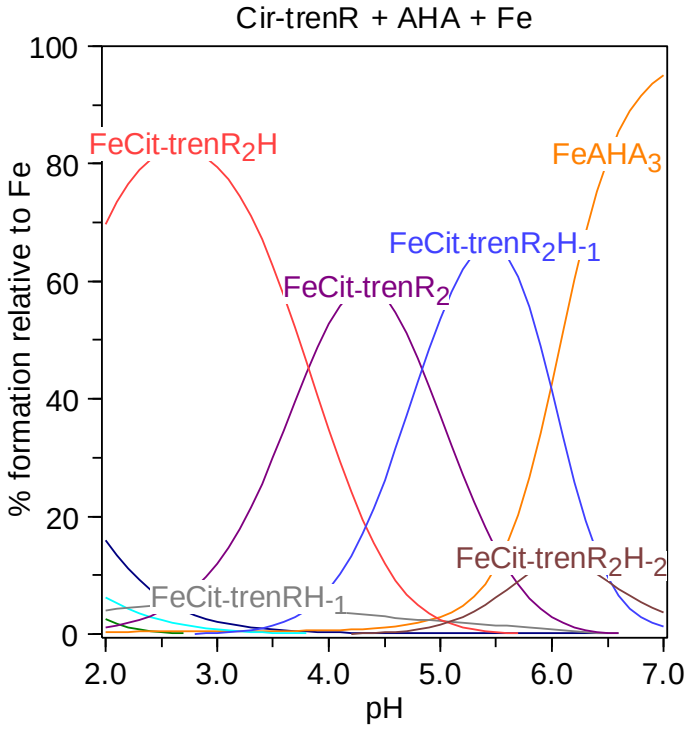

Figure 4.7 Species distribution diagram of Fe^{3+} in a mixture of AHA and the resin 4.6 at pH 2-7

4.4 Synthesis of citric anhydride and solution phase model reactions

Citric anhydride **4.8** was prepared from citric acid **4.1** in a single step following a literature procedure (Scheme 4.1).[9] The spectral characterization data of citric anhydride **4.8** was not provided in the procedure, which is included in the experimental section of this chapter. Before immobilizing citric anhydride **4.8** on an aminomethyl polystyrene resin or any other primary amine functionalized resins, the feasibility of the proposed chemistry was examined in solution. Reaction of benzylamine **4.9** with citric anhydride **4.8** gave the benzyl citramides **4.10** and **4.11** (Scheme 4.1) in a 2:1 ratio, as determined by ^{1}H NMR and reverse phase (C-18 column) HPLC. The citramides were converted to the methyl esters **4.12** and **4.13**. The methyl esters **4.12** and **4.13** were purified by silica gel column chromatography and fully characterized. The 2:1 ratio of ligands **4.10** and **4.11** was further confirmed by the isolated yields of methyl esters **4.12** and **4.13**.

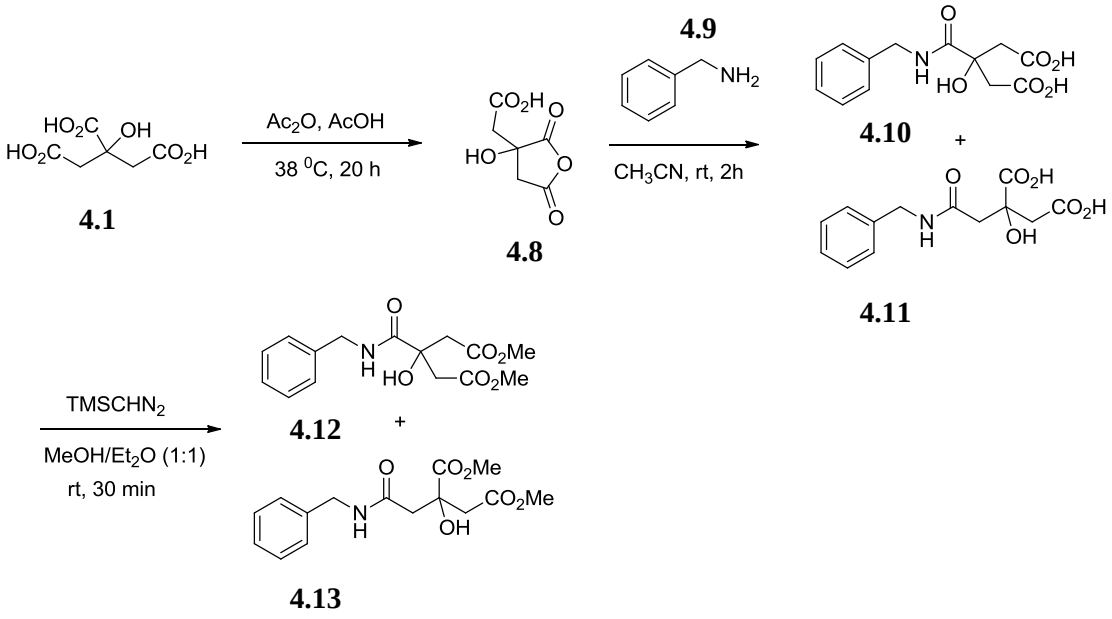

Scheme 4.1 Synthesis of citric acid anhydride and solution phase model reactions

4.5 Immobilization of citric acid anhydride on polystyrene resin

Following the procedures used for the solution phase ligands, aminomethyl polystyrene resin **4.14** (2.2 meq/g, of $-NH_2$, Aldrich 564095, macroporous 30-60 mesh) was reacted with excess citric anhydride **4.8** in acetonitrile to obtain the citramide resins **4.4** and **4.5** (Scheme 4.2). From the solution studies, it is assumed that the resin is a mixture of two regioisomers **4.4** and **4.5**, although the exact ratio of these two regioisomers is unknown in the solid phase. Based on the outcome of solution phase studies, we assumed the ratio of resins **4.4** and **4.5** to be 1:2. The presence of carboxylic acid and amide carbonyl stretching bands at 1720 and 1640 cm^{-1}, respectively in the IR spectrum of the resin, suggested the formation of citamide species. The maximum possible loading of citamide group on the surface of resin was calculated to be 1.53 meq/g based on N combustion analysis. But, some of the nitrogen in this calculation may be unreacted amines of the starting resin. As the resin was treated with HCl during the synthesis, the unreacted amine should be in the form of a hydrochloride salt. For the exact calculation of the loading of citamides, we calculated the ratio of reacted to unreacted amines by converting the hydrochloride salt to hydrobromide salt by treating the resin with 1 M NaBr solution followed by N and Br combustion analysis of the resin. The N to Br ratio of 2.8 suggested that 64% of the amines are acylated. Thus, the loading of citramide groups in resin **4.4** (or **4.5**) was determined to be 0.98 meq/g (64% of 1.53 meq/g).

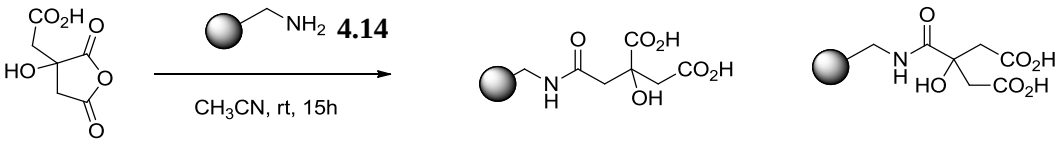

Scheme 4.2 Synthesis of mono-citramide resin

Two different resins with different surface properties were utilized for the synthesis of two different bis-citamide resins **4.7a** and **4.7b** (Scheme 4.3). Two chloromethyl polystyrene resins **4.15a** (ChemPep G20J1233, 0.82 mmol/g Cl, macroporous 100-200 mesh) and **4.15b** (chloromethylated XAD 4, 1.24 mmol/g of Cl) were reacted with tris(2-aminoethyl)amine (TREN) **4.16** in DMF to give the tetra amino resins **4.17a** (0.35 mmol/g tetramine based on N) and **4.17b** (0.65 mmol/g tetramine based on N).[10] Some cross-linking was expected, i.e., the reaction of multiple amine groups of the TREN with multiple chloromethyl groups of the resin. The amino resins were reacted with excess citric anhydride **4.8** in acetonitrile to give **4.7a** and **4.7b**. Their formation was confirmed by the presence of carboxylic acid and amide carbonyl stretching bands in the IR spectrum. Due to the cross linking of TREN and the presence of multiple amines available for acylation, the calculation of exact loading values of citramide groups in the resins **4.7a,b** is extremely problematic. The maximum possible loading of bis-citamide group on the surface of resin **4.7a** and **4.7b** were calculated to be 0.31 and 0.53 meq/g based on N combustion analysis, respectively. These values represent the loading of tetraamine groups in these resins, which is equivalent to the loading of bis-citramide if both primary amines of tetraamine are acylated. As the speciation analysis of bis-citramide resins **4.7a,b** included the species where two citrate

units are bound to one metal, the bis-citramide group was taken as a single binding unit for the calculation of loading values. The resins **4.7a** and **4.7b** are also likely to contain mono-citramide (only one amine of TREN acylated), bis-citramide (as expected), and even tris-citramide (two primary amines and one secondary amine acylated) groups and both citramide regioisomers giving rise to multiple resin species. The loading and the observed binding may be an average of the individual species.

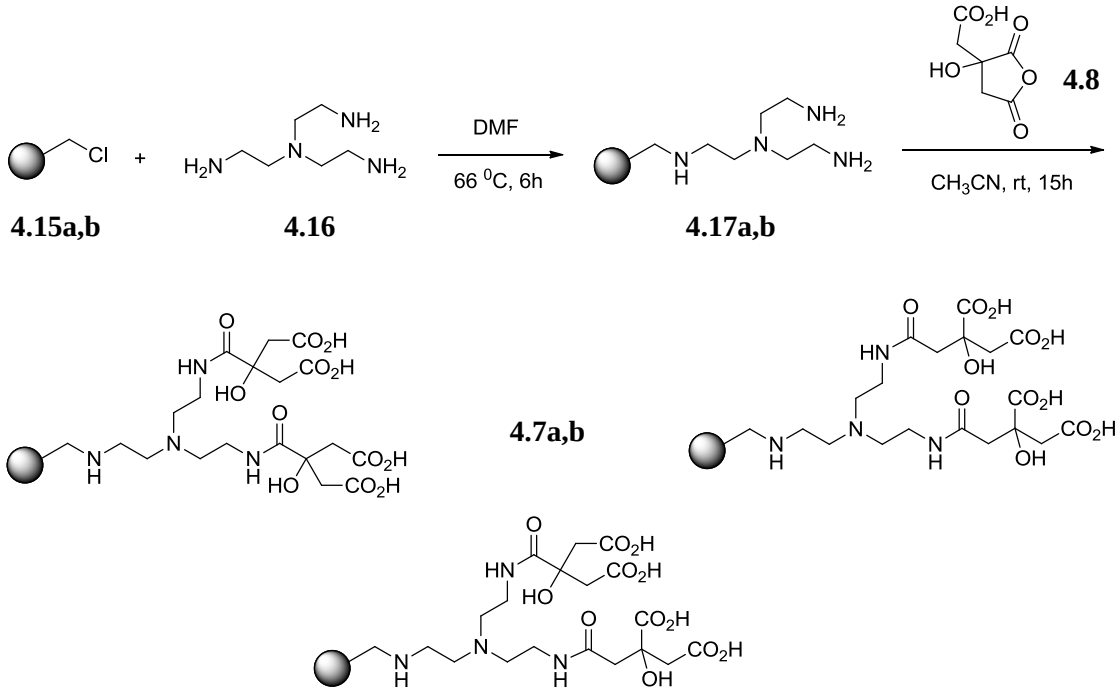

Scheme 4.3 Synthesis of bis-citramide resin

4.6 Fe^{3+} extraction studies of citramide resins by difference UV-Vis Spectroscopy

Mono-citramide resin 4.4 (and 4.5).

A 2 ml mixture of Fe^{3+} (100 μM) and the chelating agent AHA (10 mM) in pH 6.2 MES buffer was prepared, allowed to equilibrate, and the absorbance was recorded. Resin **4.4** (or **4.5**) (60 mg, loading = 0.98 mmol/g, 29.4 mM) was added to the solution,

the mixture was agitated and the absorbance was recorded periodically. The removal of Fe^{3+} from the Fe-AHA complex by the resin was indicated by the decrease in the absorbance band of the Fe-AHA complex at 422 nm, as shown in Figure 4.8. The lowest absorbance in the figure represents an equilibrium distribution of the Fe^{3+} between AHA and the resin. The fraction of Fe^{3+} bound to the resin was calculated by comparing the absorbance at equlibrium to that of the initial Fe-AHA complex before the addition of resin. The results showed that 28% of the Fe^{3+} was bound to the resin **4.4** (and **4.5**) and 72% to AHA when the equilibrium was achieved. After 8 h 20 min, the final pH of the extracted solution was measured to be 5.9.

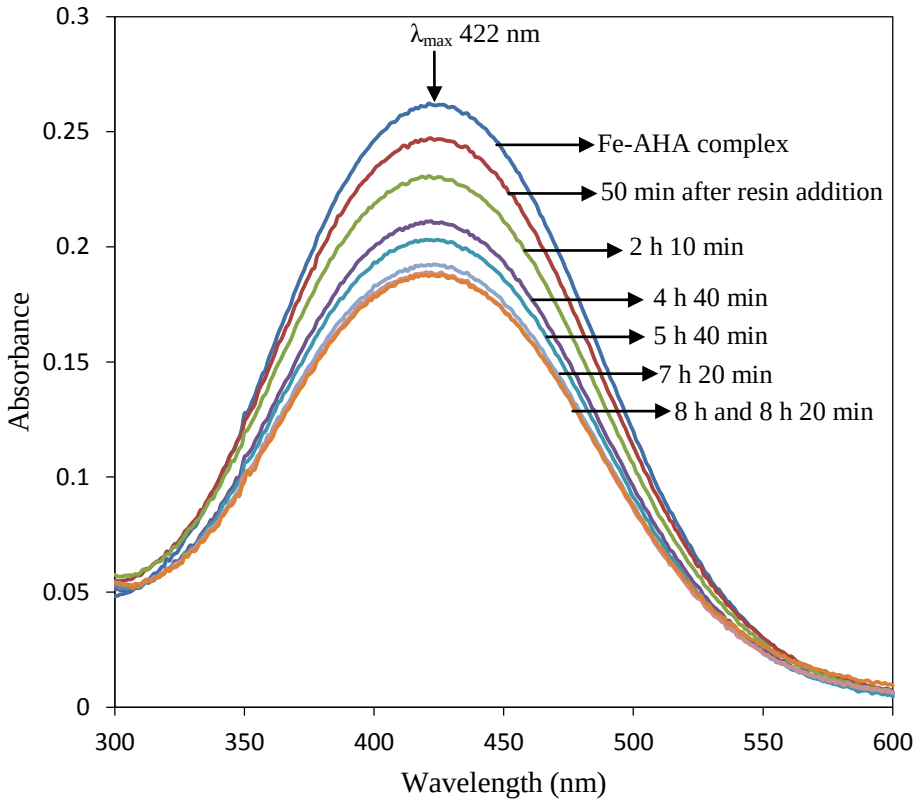

Figure 4.8 Removal of Fe^{3+} from the Fe-AHA complex by mono-citramide resin 4.4 (and 4.5)

Bis-citramide resin 4.7a.

A 2 ml mixture of Fe^{3+} (100 μM) and the chelating agent AHA (40 mM) in pH 6.2 MES buffer was prepared, allowed to equilibrate, and the absorbance was recorded. Resin **4.7a** (65 mg, loading = 0.31 mmol/g, 10 mM) was added to the solution, the mixture was agitated and the absorbance was recorded periodically. The removal of Fe^{3+} from the Fe-AHA complex by the resin was indicated by the decrease in the absorbance band of the Fe-AHA complex at 422 nm, as shown in Figure 4.9. The lowest absorbance in the figure represents an equilibrium distribution of the Fe^{3+} between AHA and the resin. The results showed that 36% of the Fe^{3+} was bound to the resin **4.7a** and 64% to AHA when the equilibrium was achieved. After 3 h 30 min, the final pH of the extracted solution was measured to be 6.0.

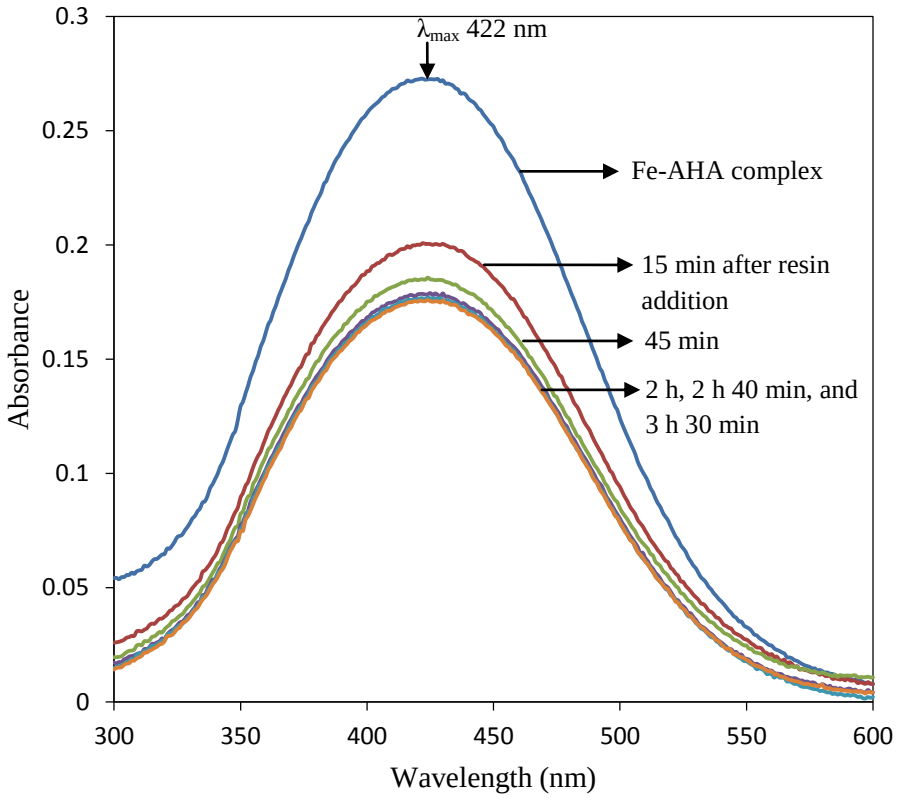

Figure 4.9 Removal of Fe^{3+} from Fe-AHA complex by the bis-citramide resin 4.7a

Bis-citramide resin 4.7b.

A 2 ml mixture of Fe^{3+} (100 μM) and the chelating agent AHA (60 mM) in pH 6.2 MES buffer was prepared, allowed to equilibrate, and the absorbance was recorded. Resin **4.7b** (38 mg, loading = 0.53 mmol/g, 10 mM) was added to the solution, the mixture was agitated and the absorbance was recorded periodically. The removal of Fe^{3+} from the Fe-AHA complex by the resin was again indicated by the decrease in the absorbance band of the Fe-AHA complex at 422 nm, as shown in Figure 4.10. The results showed that 44% of the Fe^{3+} was bound to the resin **4.7b** and 56% to AHA when the equilibrium was achieved. After 3 h 15 min, the final pH of the extracted solution was measured to be 5.9.

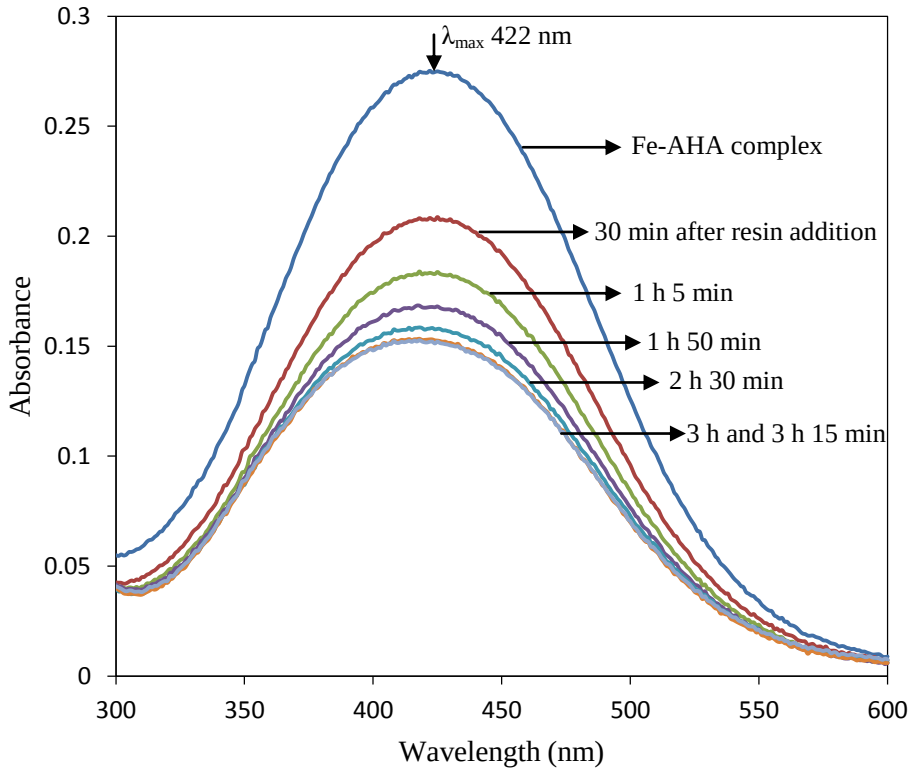

Figure 4.10 Removal of Fe^{3+} from Fe-AHA complex by the bis-citramide resin 4.6b

4.7 Calculation of iron binding affinities of citramide resins

Iron binding constants of these citrate immobilized resins (K_{CitrR}) are calculated using following equations:

$$Fe + CitrR \overset{K_{CitrR}}{\rightleftharpoons} FeCitrR + ?H^{+} \qquad \textbf{Equation 4.1}$$

We don't know how many protons are released in equation 4.1. At least the hydroxyl protons are released and maybe some other protons are released also.

$$K_{CitrR} = \frac{[FeCitrR]}{[Fe][CitrR]} \qquad \textbf{Equation 4.2}$$

As H^{+} is not included in equation 4.2, K_{CitrR} becomes an effective binding constant, a constant which is valid at the pH at which it is measured.

Equation 4.1 represents the equilibrium for the formation of Fe-citramide complex on the resin from free iron and the citramide resins. Charges are omitted for simplicity. The equilibrium constant K_{CitrR} is represented in equation 4.2.

$$Fe + 3AHA \overset{K_{AHA}}{\rightleftharpoons} Fe(AHA)_3 \qquad \textbf{Equation 4.3}$$

$$K_{AHA} = \frac{[Fe(AHA)_3]}{[Fe][AHA]^3} \qquad \textbf{Equation 4.4}$$

Similarly, K_{AHA} (Equation 4.4) represents the equilibrium constant for the formation of the Fe-AHA complex from the free iron and acetohydroxamic acid (AHA), which is shown in equation 4.3.

$$Fe(AHA)_3 + CitrR \underset{}{\overset{K_x}{\rightleftharpoons}} FeCitrR + 3AHA \qquad \textbf{Equation 4.5}$$

$$K_x = \frac{[FeCitrR][AHA]^3}{[Fe(AHA)_3][CitrR]} = \frac{[FeCitrR]}{[Fe][CitrR]} \cdot \frac{[Fe][AHA]^3}{[Fe(AHA)_3]} = \frac{K_{CitrR}}{K_{AHA}} \qquad \textbf{Equation 4.6}$$

$$\log K_{CitrR} = \log K_{AHA} + \log K_x \qquad \textbf{Equation 4.7}$$

In above discussed difference UV-Vis Spectroscopy experiments, the fully formed $Fe(AHA)_3$ complex was treated with citramide resins, which led to the redistribution of Fe between the AHA and resin. This equilibrium is represented in equation 4.5. One can define an exchange constant, K_x, as shown in equation 4.6, which is equal to the ratio of K_{CitrR} (equation 4.2) and K_{AHA} (equation 4.4). Equation 4.7 is the logarithm form of equation 4.6.

Values of K_x have been calculated from difference UV-Vis absorption experiments and using equations 4.8-4.12. The concentration of Fe bound to AHA at equilibrium was calculated from the experiment using equation 4.8. Total Fe used in the experiment was distributed between Fe-AHA and Fe-citramide resin (equation 4.9). As the total Fe concentation was known, and as the concentration of Fe-AHA complex was obtained from equation 4.8, the concentration of Fe bound citramide resin was calculated from equation 4.9. The total citramide used in the experiment (which is known) was equal to the sum of free citramide concentration and the concentration of Fe-citramide complex when the equilibrium has been reached (equation 4.10). Thus, the concentration of free citramide resin at equilibrium was calculated using equation 4.10. Also, as the total AHA concentration was known, the concentration of free AHA at equilibrium was

calculated using equation 4.11. The value α is defined by equation 4.12. When all the required concentrations were obtained, *Kx* was calculated using equation 4.13.

$$[Fe(AHA)_3] = \frac{Abs}{\epsilon} \qquad \textbf{Equation 4.8}$$

$$Fe_{tot} = [Fe(AHA)_3] + [FeCitrR] \qquad \textbf{Equation 4.9}$$

$$CitrR_{tot} = [CitrR] + [FeCitrR] \qquad \textbf{Equation 4.10}$$

$$AHA_{tot} = \alpha[AHA] + 3[Fe(AHA)_3] \qquad \textbf{Equation 4.11}$$

$$\alpha = 1 + K\,[H] \qquad where\ K = \frac{[HAHA]}{[H][AHA]} \qquad \textbf{Equation 4.12}$$

$$K_x = \frac{[FeCitrR][AHA]^3}{[Fe(AHA)_3][CitrR]} \qquad \textbf{Equation 4.13}$$

Therefore, as logK_{AHA} is known (28.33)[7] and logK_x was obtained from the experiment, logK_{CitrR} has been calculated using equation 4.7. The logK_{CitrR} values of mono-citramide resin 4.4 and bis-citramide resins 4.6a and 4.6b are listed in Table 4.1.

Table 4.1 Fe binding constants of citrate immobilized resins 4.4, 4.7a and 4.7b

Resin	pH	logK_{CitrR}
4.4 (and **4.5)**	5.9	13.15
4.7a	6.0	15.81
4.7b	5.9	16.20

4.8 Summary

The present study involved the design, synthesis and use of citramide functionalized chelating resins for the removal of trivalent metals such as iron at low pH. Citric anhydride was prepared in a single step from citric acid by a known procedure. Citric anhydride was then reacted with various amine functionalized polystyrene resins for the preparation of citramide resins. Three different citramide resins were prepared by this method, mono-citramide resin **4.4**, and bis-citramide resins **4.7a** and **4.7b**. The iron binding affinities of these resins were determined by difference UV-Vis Spectroscopy. Binding studies suggested that the bis-citramide resins have about a 3 log unit higher iron binding affinities than mono-citramide resins. There are many directions this project could head in the future, including the study of differences in binding affinities of solution phase citramide chelators, **4.10** and **4.11**. The result from such experiment may further establish a well-known concept that the strongest binding group of citric acid is the α-hydroxyl carboxylate.

4.9 Experimental section

Citric anhydride (4.8). IR (neat) 3454, 3186, 1856, 1772, 1731, 1692, 1179 cm^{-1}; ^{1}H NMR (acetone-d_6) δ (ppm) 3.26 (ABq, Δδ = 119.4 Hz, *J* = 19.0 Hz, 2H), 3.17 (ABq, Δδ = 21.3 Hz, *J* = 17.6 Hz, 2H),; ^{13}C NMR (acetone-d6) δ (ppm) 174.6, 172.1, 169.7, 74.9, 42.2, 41.3; HRMS (FAB) $C_6H_5O_6$ $[M-H]^+$ calcd 173.0086, found 173.0083.

3-(benzylcarbamoyl)-3-hydroxypentanedioic acid (4.10) and 2-(2-(benzylamino)-2-oxoethyl)-2-hydroxysuccinic acid (4.11). To a solution of the citric anhydride **4.8** (0.50

g, 2.9 mmol) in dry CH_3CN (25 mL) was added benzylamine (0.47 mL, 4.3 mmol) drop wise and the resulting solution was stirred at room temperature. The reaction was fast and exothermic. The reaction mixture turned cloudy and finally oiled out at the bottom of the reaction flask. The reaction was allowed to stir for additional 2 h. After 2 h, 1N HCl (25 mL) was added and the stirred mixture was extracted with EtOAc. The combined organic layers were dried over Na_2SO_4 and evaporated under reduced pressure to give the crude product as the regioisomeric mixture of **4.10** and **4.11** (0.71 g combined, 86%). The ratio of **4.10** and **4.11** was calculated to be 2:1 from ^{1}H NMR and reversed phase (C-18 column) HPLC experiments of the crude product. The carboxylic acids **4.10** and **4.11** were converted to methyl esters without any further purification.

dimethyl 3-(benzylcarbamoyl)-3-hydroxypentanedioate (4.12) and dimethyl 2-(2-(benzylamino)-2-oxoethyl)-2-hydroxysuccinate (4.13). To a solution of the mixture of carboxylic acid regioisomers **4.10** and **4.11** (0.60 g, 2.13 mmol) in a 1:1 mixture of dry MeOH and Et_2O (20 mL) was added $TMSCHN_2$ (0.95 mL, 6.40 mmol) and the resulting solution was stirred at room temperature for 30 min. The solvent was evaporated under reduced pressure and the residue was purified by column chromatography (SiO_2, hexane/EtOAc gradient) to give the products **4.12** (0.28 g, 43%) as the major and **4.13** (0.13 g, 20%) as the minor regioisomers.

Compound **4.12**: IR (neat) 3393 (br), 2953, 1735, 1655, 1529, 1201 cm^{-1}; ^{1}H NMR ($CDCl_3$) δ (ppm) 7.26-7.15 (m, 5H), 4.87 (br s, 1H), 4.36 (d, J = 6.0 Hz, 2H), 3.57 (s, 6H), 2.81 (ABq, $\Delta\delta$ = 47.6 Hz, J = 15.7 Hz, 4H); ^{13}C NMR (CDCl3) δ (ppm) 173.0,

171.7, 138.0, 128.7, 127.8, 127.5, 74.5, 52.1, 43.5, 41.7; HRMS (FAB) $C_{15}H_{20}NO_6$ $[M+H]^+$ calcd 310.1291, found 310.1286.

Compound **4.13**: IR (neat) 3359 (br), 2954, 1736, 1648, 1541, 1211 cm^{-1}; ^1H NMR ($CDCl_3$) δ (ppm) 7.26-7.15 (m, 5H), 6.39 (br s, 1H), 4.34 (d, *J* = 5.8 Hz, 2H), 3.69 (s, 3H), 3.59 (s, 3H), 2.77 (ABq, Δδ = 37.6 Hz, *J* = 15.8 Hz, 2H), 2.63 (ABq, Δδ = 34.3 Hz, *J* = 14.7 Hz, 2H); ^{13}C NMR (CDCl3) δ (ppm) 174.1, 170.7, 169.2, 138.0, 128.8, 127.8, 127.7, 73.9, 53.3, 52.2, 44.4, 43.7, 42.9; HRMS (FAB) $C_{15}H_{20}NO_6$ $[M+H]^+$ calcd 310.1291, found 310.1282. The MS fragmentation pattern of compound **4.13** was different from that of compound **4.12**.

Polymer-supported mono citramide 4.4 (or 4.5). To a suspension of aminomethyl resin (2.0 g, 2.2 meq/g, 4.4 mmol of $–NH_2$, Aldrich 564095, macroporous 30-60 mesh) in CH_3CN (10 ml) was added anhydride **4.8** (2.3 g, 13.2 mmol) and the mixture was allowed to shake in an orbital shaker for 15 h at rt. The resin was filtered and washed 3 times each with CH_3CN, H_2O, 1N HCl, H_2O, MeOH and Et_2O. It was then dried under reduced pressure to obtain a light colored resin (2.6 g). IR (ATR): 3420-2500 (br), 3380, 3027, 2920, 1720 (C=O acid), 1640, 1597, 1180, 698 cm^{-1}. Elemental Analysis: C 78.21%, H 7.03%, N 2.62%. Maxium loading value = 1.53 meq/g (based on %N). Corrected loading = 0.98 meq/g.

Polymer-supported tris(2-aminomethyl)amine (4.17a,b).

Resin 4.17a. To a suspension of chloromethyl polystyrene resin (3.0 g, 0.82 mmol/g, 2.46 mmol of Cl, ChemPep G20J1233, macroporous 100-200 mesh) in DMF (10 ml) and

was added tris(2-aminoethyl)amine (1.45 ml, 9.89 mmol) and the mixture was allowed to shake in an orbital shaker for 6 h at 65 ^{0}C. The resin was filtered and washed 3 times each with DMF, MeOH, Et_3N, MeOH and Et_2O. It was then dried under reduced pressure to obtain a white colored resin (3.0 g). IR (ATR) 3023, 2921, 1597, 1493, 1452, 697 cm^{-1}. Elemental Analysis: C 87.96%, H 7.77%, N 1.97%, Cl 0.65%. Loading of tetraamine = 0.35 mmol/g (based on %N).

Resin 4.17b. To a suspension of chloromethyl polystyrene resin (3.0 g, 1.24 mmol/g, 3.72 mmol of Cl, chloromethylated XAD 4) in DMF (10 ml) and was added tris(2-aminoethyl)amine (2.17 ml, 14.88 mmol) and the mixture was allowed to shake in an orbital shaker for 6 h at 65 ^{0}C. The resin was filtered and washed 3 times each with DMF, MeOH, Et_3N, MeOH and Et_2O. It was then dried under reduced pressure to obtain a white colored resin (3.1 g). IR (ATR) 3370 (br), 3019, 2922, 1603, 1447, 708 cm^{-1}. Elemental Analysis: C 77.48%, H 8.01%, N 3.64%, Cl 3.70%. Loading of tetraamine = 0.65 mmol/g (based on %N).

Polymer-supported bis-citramides 4.7a,b.

Resin 4.7a: To a suspension of polymer-supported tris(2-aminomethyl)amine **4.17a** (1.50 g, 0.35 mmol/g, 0.52 mmol of $–NH_2$) in CH_3CN (8 ml) was added the citric anhydride **4.8** (0.54 g, 3.12 mmol) and the mixture was allowed to shake in an orbital shaker for 15 h at rt. The resin was filtered and washed 3 times each with CH_3CN, H_2O, 1N HCl, H_2O, MeOH and Et_2O. It was then dried under reduced pressure to obtain off-white colored resin (1.65 g). IR (ATR): 3400-2500 (br), 3025, 2921, 1724 (C=O acid), 1650, 1601,

1452, 697 cm^{-1}. Elemental Analysis: C 82.20%, H 7.48%, N 1.75%. Loading of tetraamine = 0.31 meq/g (based on %N).

Resin 4.7b: To a suspension of Polymer-supported tris(2-aminomethyl)amine **4.17b** (1.50 g, 0.65 mmol/g, 0.97 mmol of $–NH_2$) in CH_3CN (8 ml) was added the citric anhydride **4.8** (1.02 g, 5.85 mmol) and the mixture was allowed to shake in an orbital shaker for 15 h at rt. The resin was filtered and washed 3 times each with CH_3CN, H_2O, 1N HCl, H_2O, MeOH and Et_2O. It was then dried under reduced pressure to obtain a light colored resin (1.86 g). IR (ATR): 3400-2500 (br), 2925, 1724 (C=O acid), 1653, 1604, 1444, 1190, 708 cm^{-1}. Elemental Analysis: C 70.02%, H 6.98%, N 2.97%. Loading of tetraamine = 0.53 meq/g (based on %N).

References

[1] Huheey J. E. *Inorganic Chemistry*, third ed. New York: Harper & Row, 1983.

[2] Spilling, C. D.; Harris, W. R.; Dawadi, S.; Hamper, B. "Immobilized citrate chelators for removal of trivalent metals at low pH." *US Provisional Patent Application*, 13UMS005, filed Feb. 22, 2013.

[3] Zhou, Y.; Harris, W. R.; Yokel, R. A. *J. Inorg. Biochem.* **2008**, 102, 798-808.

[4] (a) Dxechsel, H.; Metzger, J.; Freund, S.; Jung, G.; Boelaert, J. R.; Winkelmann, G. *Biol. Met.* **1991**, 4, 238-243. (b) Bergeron, R. J.; Xin, M. G.; Smith, R. E.; Wollenweber, M.; McManis, J. S.; Ludit, C.; Abboud, K. A. *Tetrahedron* **1997**, 53, 427-434.

[5] Yokel, R. A.; Harris, W. R.; Spilling, C. D.; Kuhn, R. J.; Dawadi, S. *U.S. Pat. Appl. Publ.* **2012**, US 2012/0061325 A1.

[6] Konigsberger, L. C.; Konigsberger, E.; May, P. M.; Hefter G. T. *J. Inorg. Biochem.* **2000**, 78, 175-184.

[7] Schwarzenback, G.; Schwarzenback, K. *Helv. Chim. Acta* **1963**, 46, 1390.

[8] (a) Konigsberger, L. C.; Konigsberger, E.; May, P. M.; Hefter G. T. *J. Inorg. Biochem.* **2000**, 78, 175-184. (b) Silva, A. M. N.; Kong, X. L.; Parkin, M. C.; Cammack, R.; Hider, R. C. *Dalton Trans.* **2009**, 40, 8616-8625.

[9] Repta, A. J.; Higuchi, T. *Journal of Pharmaceutical Sciences* **1969**, 58, 1110-1114.

[10] Hodges, J. C.; Booth, R. J. *J. Am. Chem. Soc.* **1997**, 119, 4882.

CHAPTER 5: Immobilization of dithio-succinamide based chelators and application in the removal of lead from water

5.1 Specific objectives

The objectives of this project were:

(1) Immobilization of dimercaptosuccinic acid (DMSA), a common heavy metal chelating agent in clinical practice, on a solid support such as polystyrene resin to obtain dithiolate functionalized chelating resins.

(2) An application of such dithiolate resins for the removal of soft metals such as lead from aqueous solutions. The lead binding capacities of these resins will be determined by Atomic Absorption Spectroscopy (AAS).

5.2 Background and Introduction

Several soft metals (Pb, Hg, Cd, As) are high priority environmental contaminants. Their presence in environmental waters is due to discharges from residential dwellings, groundwater infiltration and industrial discharges.[1] The discharge of wastewater containing high concentrations of soft metals into ground water systems has serious adverse environmental effects. The 1997 Comprehensive Environmental Response, Compensation, and Liability Act (CERCLA) priority list of hazardous substances includes arsenic, lead, mercury, and cadmium within the first 10 positions. Arsenic, lead and mercury are ranked 1, 2, and 3 on the CERCLA list[2] and are some of the most widely recognized environmental hazards. Unlike organic pollutants, heavy metals are not biodegradable and accumulate in the environment due to their recirculation. Thus, soft metal pollution of ground water has become a major problem worldwide.

Since the mid-seventies, the average blood lead level in the United States has fallen from 17 µg/dL to 6 µg/dL, due in large part to the reduction in the use of leaded gasoline.[3] As the United States has reduced the exposure to environmental lead, the perceived "safe" level for blood lead has also dropped. In 1991, the Centers for Disease Control reduced the recommended maximum blood lead level from 25 µg/dL to 10 µg/dL.[3] One concern is that chronic exposure of children to even low lead levels has been associated with subtle reductions in cognitive abilities, and no clear threshold for these effects has been established.[4]

To achieve unpolluted drinking water distribution and wastewater discharge, several technologies and processes for heavy metal remediation are currently in use. The most commonly used methods for heavy metal treatment of wastewater are physicochemical methods such as chemical precipitation, ion exchange, and reverse osmosis; and bioremediation such as phytoremediation, and microbial remediation.[1] Currently, all of the existing technologies for heavy metal remediation (chemical remediation, or bioremediation) have pros and cons.[1] The precipitates of heavy metals formed during the chemical precipitation method are usually in the form of light, tiny flocks and occupy a large volume and require additional waste disposal costs. The membranes used in reverse osmosis methods are expensive to produce and operate and are very sensitive to rupture. Bioremediation is an extremely time consuming process and is limited to those compounds that are degradable. Not all compounds are susceptible to rapid and complete degradation. There are some concerns that the products of biodegradation may be more persistent or toxic than the parent compound.[1] There have been recent developments in the ion exchange resins capable of removing soft metals, but

a significant drawback associated with ion exchange resins is the lack of selectivity towards soft metals in the presence of other metal ions. This lack of selectivity can lead to a rapid saturation of the resin.

There are numerous applications for chelating resins capable of removing hazardous metal ions from water, including treatment of runoff and waste water and the purification of drinking water. An ideal chelating resin would also bind toxic soft metals selectively in the presence of harmless and beneficial metals. The binding should be very strong, and at the same time, metals should be easily released for the rejuvenation of the resin. An effective resin would allow one to produce large volumes of purified water, while concentrating the metals into a small volume for recycling or disposal.

Several thiol based resins have been developed over the years for the selective chelation of soft metals. Sulfur containing soft ligands strongly coordinate soft acids such as Hg, and Pb. Mercury is especially thiophilic.

Lezzi and coworkers[5] reported the synthesis of a series of thiol functionalized chelating resins derived from a copolymer bead of styrene-divinylbenzene. Merifield resin **5.1** was reacted with various polyethylene glycols of 4, 9, and 13 methylene units in the presence of tetra n-butyl ammonium hydrogen sulfate to obtain a series of compounds shown in structure **5.2**. The hydroxyl groups of **5.2** were substituted with bromides to obtain resins **5.3** which were reacted with thiourea followed by hydrolysis with piperidine to obtain thiol immobilized resins **5.4**. The complexation behavior of these thiol resins with Hg(II), Cu(II), and Pb(II) ions was studied by batch equilibration techniques. The authors found that polyethylene units improved the hydrophilic behavior of resins, and binding was strongest for the resin with 13 polyethylene units. The binding affinity of

these resins with metals followed the order Hg(II) >> Cu(II) > Pb(II). The thiol resins can be regenerated by washing them with a solution of HCl (6N) and a 10% aqueous solution of thiourea.

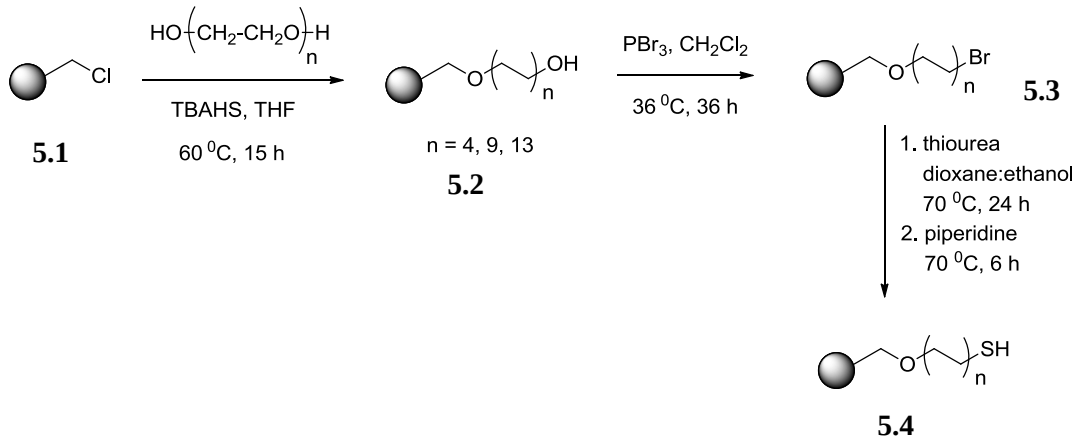

5.1 **5.2** **5.3** **5.4**

Scheme 5.1 Lezzi's synthesis of thiol functionalized chelating resins

5.3 Design of dithiolate functionalized chelating resins

As mentioned earlier, thiol ligands form very stable metal complexes with soft metals,[6] but their use can be limited by the tendency to air-oxidize to disulfide.[7] The dithiolate ligand dimercaptosuccinic acid (DMSA or succimer) is unusually air-stable. DMSA is present in two stereoisomeric forms, *meso* DMSA **5.5**, and *dl* pair DMSA **5.6** (Figure 5.1). *meso* DMSA **5.5** has been studied extensively for use in chelation therapy for the treatment of lead and cadmium poisoning,[8] and is approved as an oral drug for treating lead toxicity in children.[9] At neutral pH, DMSA binds lead through its two thiol groups, and forms a very stable 1:1 complex as shown in structure **5.7** (Figure 5.2). No 2:1 complex forms even in the presence of a modest excess of ligand.[10]

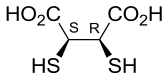

meso-**DMSA 5.5**

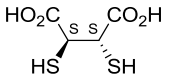

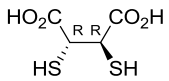

dl pair-**DMSA 5.6**

Figure 5.1 Dimercaptosuccinic acid (DMSA)

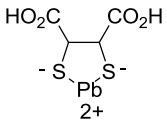

5.7

Figure 5.2 A DMSA Pb(II) complex

DMSA has been chosen as the ligand for this study because it can easily be attached to the resin, it is an air-stable dithiolate, and it forms a stable 1:1 complex with Pb^{2+}. There have been previous examples of dithiol functionalized solid supports. Bruce and coworkers[11] reported the immobilization of *meso*-DMSA **5.5** on silica gel via an amide bond linkage, and the evaluation of binding capacities of this material with Hg, Cd, and Pb. The attachment of DMSA to silica was accomplished in two steps (Scheme 5.2). The silica **5.8** was first reacted with (3-aminopropyl)dimethylethoxysilane (APDMES) **5.9** to obtain primary amino group functionalized silica **5.10**. The *meso*-DMSA **5.5** was then anchored to the surface via formation of amide linkages between the carboxylic acid groups of DMSA and surface amino groups of silica **5.10**, forming DMSA-[silica] **5.11**. This method of attachment of DMSA on silica provides a greater chance for two amine groups on the surface to react with one DMSA molecule to produce the silica with structure **5.12**, thereby significantly increasing the ratio of thiolate to carboxylate in the final product compared to the ratio of such groups in solution phase

DMSA. When equal molar concentrations of the three metals are allowed to react simultaneously with DMSA-[silica] (as a mixture of **5.11** and **5.12**) for 2 h, Hg(II) preferentially binds (99%) compared to Cd(II) (13%) or Pb(II) (0.4%). The increase in the thiol to carboxylic acid ratio over free DMSA appears to be the major factor in enhancing the preference of DMSA-[silica] for mercury. They concluded that the presence of a carboxylate group along with a dithiolate group is essential for strong lead binding.

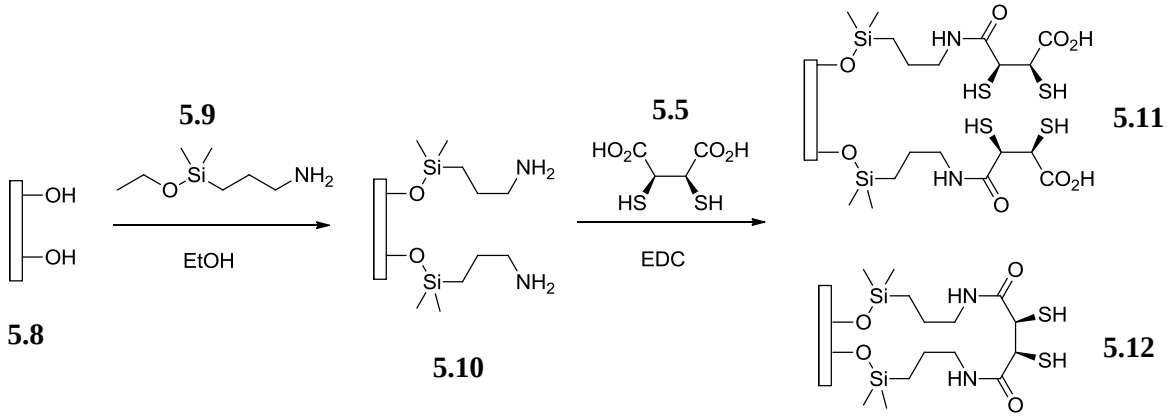

Scheme 5.2 Bruce's method of immobilization of DMSA on silica

Herein, we report the design and synthesis of chelating resins functionalized with the chelating groups present in DMSA, dithiolate and carboxylate, and the sequestration of lead from aqueous solutions. We propose the synthesis of mono-ditholate and bis-dithiolate carboxylate resins **5.13** and **5.14** (Figure 5.3). To increase the loading density and provide the opportunity for multiple dithiols to bind to a single metal, the branched polyamine linker scaffold of resin **5.14** was designed.

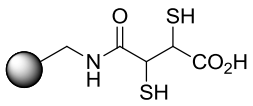

5.13

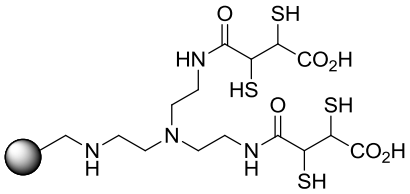

5.14

Figure 5.3 Structures of mono-dithiolate resin 5.13 and bis-dithiolate resin 5.14

5.4 Synthesis of 2,3-diacetylthio-succinic anhydride

To prevent the reaction of two amine groups of the resin with two carboxylic acids of a single DMSA molecule, we propose the synthesis of diacetylthio succinic anhydride. The benefit associated with the anhydride is that when an amine group opens the anhydride, no further reaction can occur. Dithioacetyl succinic anhydride **5.17** (Scheme 5.3) was prepared by following a literature procedure.[12] The potassium salt of acetylene dicarboxylic acid **5.15** was treated with HCl (5N in EtOAc) followed by thioacetic acid to obtain a diastereomeric mixture of *meso* and *dl* dithioacetyl succinic acid **5.16**. The diastereomeric ratio of dithioacetyl succinic acid **5.16** was determined by ^{1}H NMR to be 45:55 (*meso*:*dl*). The anhydride **5.17** was prepared by refluxing the dithioacetyl succinic acid **5.16** in acetyl chloride. The procedure provides a process for the enrichment of both the *dl* pair and the *meso* diastereomers of dithioacetyl succinic acid **5.16** and a process for the preparation of pure *dl* pair of anhydride **5.17**. Spectral characterization data for both the dithioacetyl succinic acid **5.16** and the anhydride **5.17** were not provided, so are included in the present study.

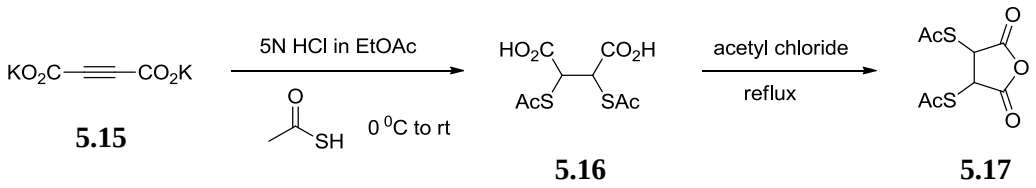

Scheme 5.3 Synthesis of dithioacetyl succinic anhydride

5.5 Synthesis of solution phase dithiol ligands

Before immobilizing dithiol succinic acid (via the anhydride **5.17**) on aminomethyl polystyrene resin or any other primary amine functionalized resins, the feasibility of the proposed chemistry was examined in solution. Reaction of the benzylamine **5.18** with the *dl* pair dithioacetyl succinic anhydride **5.17** gave the acetyl protected hemisuccinamide **5.19** (Scheme 5.4), which was characterized as the methyl ester **5.20**. The methyl ester **5.20** was prepared by reaction with $TMSCHN_2$, purified by silica gel column chromatography and fully characterized. The IR spectrum of compound **5.20** showed peaks at 3380, 1733, 1693, 1665 cm^{-1}, confirming the presence of N-H, ester carbonyl, thioester carbonyl, and amide carbonyl groups, respectively. Deacetylation[13] of the acetyl protected thiol groups of hemisuccinamide **5.19** with ammonium hydroxide in methanol gave the dithiol ligand **5.21**. The deacetylation was confirmed by the loss of acetyl protons in the ^1H NMR of the crude product. The reaction sequence work equally well with *meso* and *dl* enriched diastereomer mixtures. The solution phase ligand **5.22** was obtained by the reaction of *meso* anhydride **5.17**.

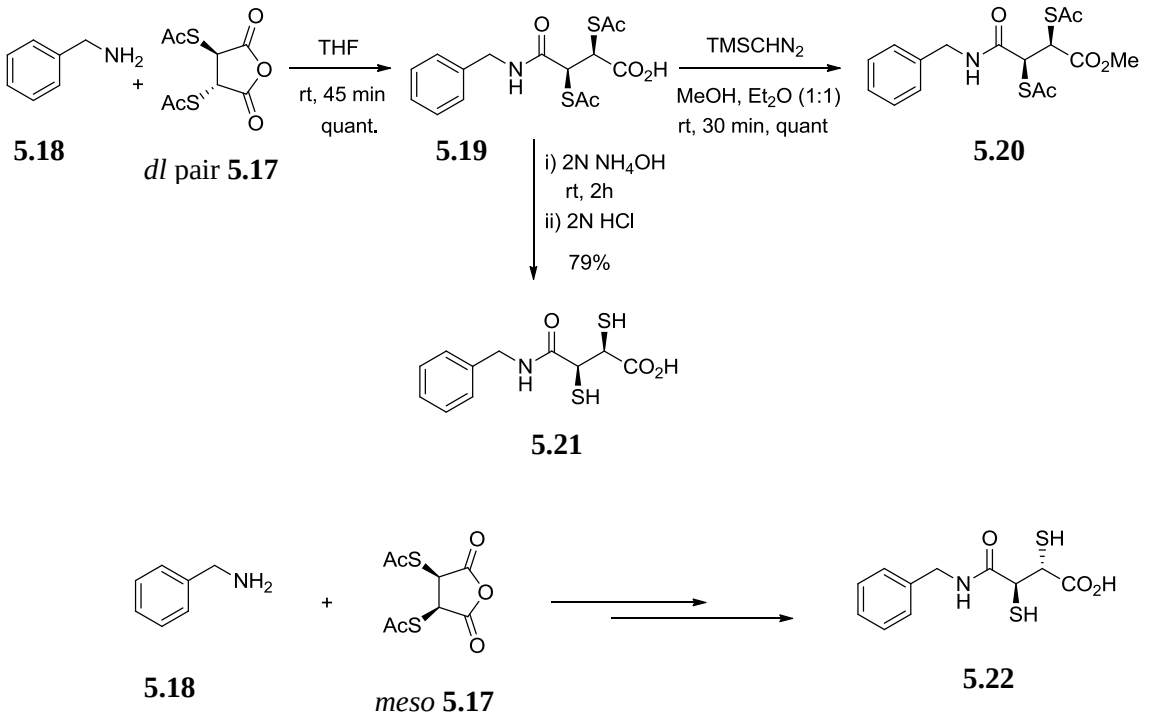

Scheme 5.4 Synthesis of solution phase dithiol ligands

5.6 Immobilization on polystyrene resin

Following the procedures used for the solution phase ligand, aminomethyl polystyrene **5.23** (2.2 meq/g, 3.52 mmol of $-NH_2$, Aldrich 564095, macroporous 30-60 mesh) was reacted with pure *dl* pair dithioacetyl succinic anhydride **5.17** to give the hemisuccinamide resin **5.24**. The IR spectrum of the powdered resin **5.24** showed peaks at 1715, 1681, 1660 cm^{-1}, confirming the presence of acid carbonyl, thioester carbonyl, and amide carbonyl groups, respectively. The ligand loading was calculated to be 0.68 meq/g (based on S combustion analysis, 4.39% S = 1.38 mmol/g S). Deacetylation of the hemisuccinamide **5.24** with ammonium hydroxide in methanol gave the mono-dithiolate resin **5.13** with a ligand loading of 0.61 meq/g (based on S). Hydolysis of thioester groups is confirmed by the loss of the thioester carbonyl stretching band at 1681 cm^{-1}. As

SH stretching bands are usually weak, they are not observed in the IR spectra of dithiolated resins. The S to N ratio was 1:1.5 (from elemental analysis of resin **5.13**), indicating that approximately 33% of the available amines had reacted. If the reaction was complete, the expected S:N ratio would be 2:1.

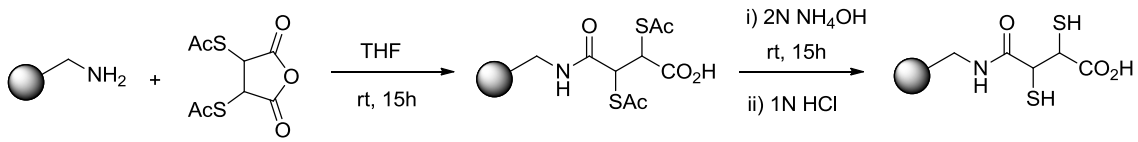

5.23 *dl* pair **5.17** **5.24** **5.13**

Scheme 5.5 Synthesis of mono-dithiolate resin

The synthesis of bis-dithiolate resins **5.14** started with branched tetra-amine resins **4.17a** and **4.17b** (Chapter 4). The two tetra-amine functionalized resins **4.17a** and **4.17b** differ in the nature of resin particles (ChemPep medium versus XAD-4). The resins **4.17a**, and **4.17b** were each reacted with excess *dl* and *meso* enriched dithioacetyl succinic anhydride **5.17** in THF to give **5.25a-d** (0.28 meq/g, 0.22 meq/g, 0.64 meq/g and 0.50 meq/g of dithioacetyl based on %S) (Scheme 5.6). Deacetylation of the hemisuccinamides **5.25a-d** with ammonium hydroxide in methanol gave the dithiol resins **5.14a-d** (0.20 meq/g, 0.16 meq/g, 0.36 meq/g and 0.32 meq/g of dithiol based on %S). Both the anhydride opening and deacetylation reactions on solid phase were monitored by IR spectroscopy, and the results were analogous to the IR of solution phase compounds.

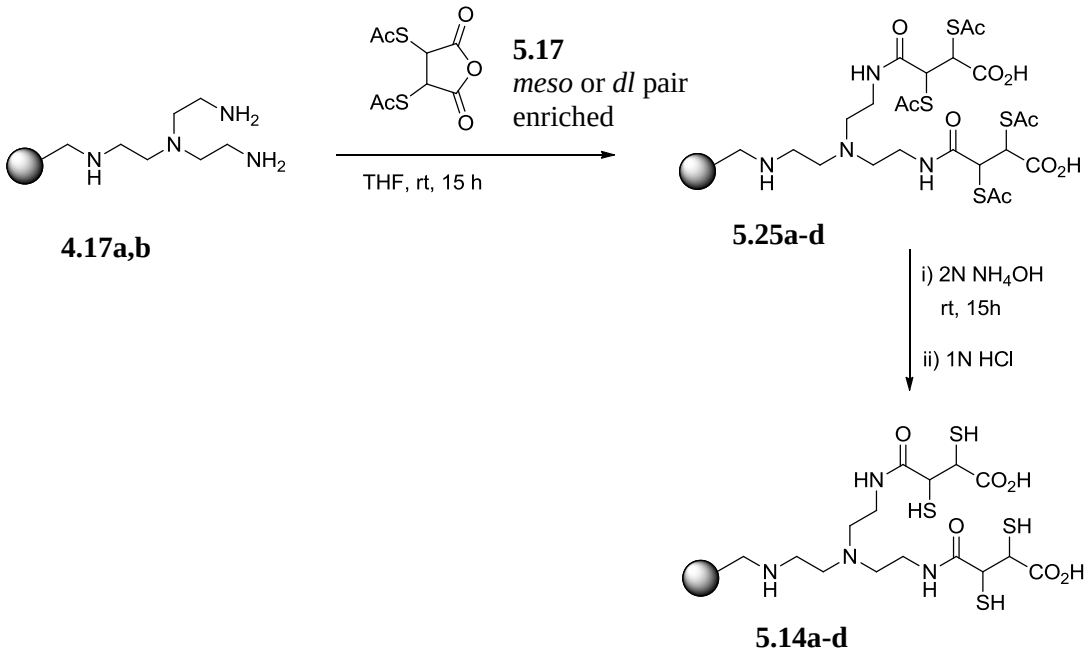

Scheme 5.6 Synthesis of bis-dithiolate resins

Using **5.14a** as an example, a comparsion of the % of S and N show that the tetraamines are 60% acylated (or 30% of the available primary amines have been acylated). Similar calculations were performed for all the resins and the loading values are listed in Table 5.1.

Table 5.1 Loading of various dithiolate resins

Resin	%S	mmol S	mmol dithiol	% N	mmol N	mmol tetramine	% NH_2 acylation
5.13	3.89	1.22	0.61	2.56	1.83	N/A	33%
5.14a	1.25	0.39	0.19	1.80	1.28	0.32	30%
5.14b	0.99	0.31	0.16	1.81	1.28	0.32	24%
5.14c	2.33	0.73	0.36	3.05	2.18	0.54	33%
5.14d	2.04	0.64	0.32	3.10	2.21	0.55	29%

5.7 Study of Pb^{2+} extraction by flame Atomic Absorption Spectroscopy (AAS)

To determine the ability of resin **5.13** to remove lead from aqueous lead nitrate solutions, the following batch extraction experiment was performed. A 10 ml solution of $Pb(NO_3)_2$ (300 μM, 62.1 μg/ml Pb^{2+}) in pH 6.7 MES buffer was prepared. Resin **5.13** (25 mg) was added to the solution and allowed to equilibrate completely by shaking in an orbital shaker for about 22 h. The final pH of the mixture after 22 h was measured to be 6.61. Resin beads were removed by filtration, and the amount of Pb remaining in the solution was measured by flame AAS. The instrument was calibrated with five Pb standard solutions (10, 20, 30, 40, and 50 ppm) each time before the Pb measurement was performed. The results showed that 68.1 μM (14.1 μg/ml) Pb^{2+} remained in the solution after 24 h. 77% of the Pb^{2+} was bound to the resin and 23% remained in the solution when the equilibrium was achieved. The experiment was performed at various pH values to understand the influence of pH on extraction capacity of resins, and the results are summarized in Table 5.2.

Table 5.2 Pb concentration before and after resin 5.13 (pure *dl* pair) treatment at various pH

pH	Weight of resin	Pb concentration before resin treatment	Pb concentration after 22 h resin treatment	% Pb remaining in solution
5.80	25.0 mg	480 μM	289 μM	60
6.58	25.0 mg	300 μM	72 μM	24
6.61	25.0 mg	300 μM	68 μM	23

Similarly, Pb removal capacities of bis-dithiolate functionalized resins **5.14a-d** are summarized in Tables 5.3-5.6.

Table 5.3 Pb concentration before and after resin 5.14a (71% *dl* pair) treatment at various pH

pH	Wt. of resin	Pb concentration before resin treatment	Pb concentration after 22 h resin treatment	% Pb remaining in solution
5.84	45.0 mg	300 μM	127 μM	42
6.56	45.0 mg	300 μM	5 μM	1.7
6.61	33.0 mg	300 μM	26 μM	13

Table 5.4 Pb concentration before and after resin 5.14b (80% *meso*) treatment at various pH

pH	Wt. of resin	Pb concentration before resin treatment	Pb concentration after 22 h resin treatment	% Pb remaining in solution
5.85	56.0 mg	300 μM	122 μM	41
6.56	56.0 mg	300 μM	3 μM	1
6.61	41.0 mg	300 μM	17 μM	6

Table 5.5 Pb concentration before and after resin 5.14c (71% *dl* pair) treatment at various pH

pH	Wt. of resin	Pb concentration before resin treatment	Pb concentration after 22 h resin treatment	% Pb remaining in solution
5.84	25.0 mg	300 μM	52 μM	17
5.97	25.0 mg	300 μM	28 μM	9
6.54	25.0 mg	300 μM	2 μM	0.7
6.60	18.3 mg	300 μM	4 μM	1.3

Table 5.6 Pb concentration before and after resin 5.14d (80% *meso*) treatment at various pH

pH	Wt. of resin	Pb concentration before resin treatment	Pb concentration after 22 h resin treatment	% Pb remaining in solution
5.84	28.0 mg	300 μM	45 μM	15
6.55	28.0 mg	300 μM	1 μM	0.3
6.61	20.5 mg	300 μM	3 μM	1

5.8 Summary

The present study involving the design, synthesis and use of chelating resins functionalized with dithiolate ligands for soft metal remediation has shown great promise. Dithiol ligands such as dimercapto succinic acid (DMSA) are ideal soft metal chelators. The immobilization of DMSA on a polystyrene resin via an amide linkage presented a challenge. Diacetylthio succinic anhydride, in which thiols are protected with acetyl groups, was synthesized and reacted with aminomethylated polystyrene resins to obtain acetyl protected dithiol resins. Finally, the acetyl groups were deprotected to obtain the dithiolate resins. Lead binding studies of these resins showed that, depending on the pH of solution, they very efficiently remove lead from aqueous solutions. At pH 6.5, when excess resin was used, bis-dithiolate functionalized resin **5.14d** removed more than 99% of lead from the lead nitrate solution. There are many directions this project could head in the future, including the study of the difference in binding affinities of pure *meso* versus pure *dl* pair solution phase dithiolate chelators **5.21** and **5.22**, the study of binding

capacities of the resins with other soft metals, and the study of binding capacities of the resins with metals in the presence of competing ligands.

5.9 Experimental section

2,3-bis(acetylthio)succinic acid (5.16). It was obtained as a mixture of 55% *dl* pair and 45% *meso* isomers. IR (neat) 3400-2500 (br.), 2908, 1698, 1654, 1412, 1125 cm^{-1}; *meso*: ^{1}H NMR (MeOD) δ (ppm) 4.85 (s, 1H), 2.37 (s, 3H); ^{13}C (MeOD) δ (ppm) 194.8, 172.5, 48.2, 29.8; *dl* pair: ^{1}H NMR (MeOD) δ (ppm) 4.61 (s, 1H), 2.38 (s, 3H); ^{13}C (MeOD) δ (ppm) 194.1, 172.9, 47.7, 29.9; HRMS (FAB) $C_8H_{11}O_6S_2$ $[M+H]^+$ calcd 266.9997, found 267.0006.

2,5-dioxotetrahydrofuran-3,4-diyl diethanethioate (5.17). IR (neat) 2993 (broad), 2905, 1723, 1696, 1649, 1405, 1210 cm^{-1}; *meso*: ^{1}H NMR ($CDCl_3$) δ (ppm) 4.91 (s, 1H), 2.43 (s, 3H); ^{13}C ($CDCl_3$) δ (ppm) 194.5, 168.1, 45.4, 29.7; *dl* pair: ^{1}H NMR ($CDCl_3$) δ (ppm) 4.21 (s, 1H), 2.45 (s, 3H); ^{13}C ($CDCl_3$) δ (ppm) 194.4, 166.9, 47.8, 30.0; HRMS (FAB) $C_8H_9O_5S_2$ $[M+H]^+$ calcd 248.9891, found 248.9889.

methyl 4-(benzylamino)-2,3-dimercapto-4-oxobutanoate (5.20). To a solution of anhydride **5.17** (pure *dl* pair, 0.31 g, 1.24 mmol) in THF was added benzylamine (0.15 ml, 1.38 mmol) drop wise and the mixture was stirred at rt. Progress of the reaction was monitored by TLC (50% EtOAc in hexane). Reaction was complete in 45 minutes. To the reaction mixture was added 1N HCl (5 ml) and the mixture was stirred for about 5 minutes. The mixture was extracted with CH_2Cl_2 and the combined organics was dried

over Na_2SO_4 and evaporated under reduced pressure to obtain the carboxylic acid **5.19** (0.43 g, quant.) as a foamy solid. To a solution of compound **5.19** (0.09 g, 0.25 mmol) in a 1:1 mixture of MeOH and Et_2O (4 ml) was added trimethylsilyl diazomethane (2M in Et_2O, 0.19 ml, 0.38 mmol) drop wise at rt. The reaction was vigorous with the evolution of gas and was completed immediately after the complete addition of trimethylsilyl diazomethane. The reaction mixture was stirred for a total of 30 min. The solvent was removed under reduced pressure and the crude product was purified by column chromatography (SiO_2, hexane/EtOAc gradient) to give a colorless oil product **5.20** (0.09 g, quant) as a mixture of geometrical isomers around the amide bond. IR (neat) 3380, 2952, 1733, 1693, 1665, 1525 cm^{-1}; ^1H NMR ($CDCl_3$) δ (ppm) 7.28-7.14 (m, 5H), 6.47 (app t, 1H), 4.80 (ABq, Δδ = 42.2 Hz, *J* = 4.3 Hz, 0.7H) + 4.58 (ABq, Δδ = 68.3 Hz, *J* = 8.2 Hz, 1.3H), 4.34 (t, *J* = 5.9 Hz, 2H), 3.66 (s, 3H), 2.32 (s, 2.1H) + 2.31 (s, 3.9H); ^{13}C ($CDCl_3$) δ (ppm) 195.86 + 195.81, 193.51 + 192.60, 170.40 +170.19, 169.05 + 168.99, 137.88 + 137. 86, 128.87 + 128.86, 127.68 + 127.66, 127.65, 53.41 + 53.38, 47.39 + 47.35, 45.87 + 45.40, 43.93, 30.42, 30.21 + 30.05 ; HRMS (FAB) $C_{16}H_{20}NO_5S_2$ $[M+H]^+$ calcd 370.0782, found 370.0786.

General process I (reaction of anhydride 5.17 with amine functionalized resins). To a suspension of resin in THF (6 ml/g of resin) was added anhydride **5.17** (3 equiv. per –NH_2 of resin) and the mixture was allowed to shake in an orbital shaker for 15 h at rt. The resin was filtered and washed 3 times each with THF, MeOH, H_2O, MeOH and Et_2O. It was then treated with 1N HCl and the mixture was shaken for 20 min. The resin was

filtered and washed 3 times each with H_2O, MeOH and Et_2O. It was dried under reduced pressure to obtain the product resin.

General process II (Conversion of thioacetate to thiol). To a thioacetate functionalized resin was added 2N NH_4OH (7-35 ml per mmol of –SAc) and the mixture was allowed to shake in an orbital shaker for 15 h at rt. The resin was filtered and washed 3 times with H_2O. It was then treated with 1 N HCl (~7 ml per mmol of –SAc) and the mixture was shaken for 1 h. The resin was filtered and washed 3 times each with H_2O, MeOH and Et_2O. It was dried under reduced pressure to obtain the thiol functionalized resin.

Resin 5.24. Following the general process I, aminomethyl resin (1.6 g, 2.2 meq/g, 3.52 mmol of $–NH_2$, Aldrich 564095, macroporous 30-60 mesh) was treated with anhydride **5.17** (pure *dl* pair, 2.60 g, 10.47 mmol). Product was obtained as dark brown resin beads (2.27 g). IR (ATR): 3400-2500 (br), 3051, 2914, 1715 (C=O acid), 1681, 1660, 1602, 1493, 698 cm^{-1}. Elemental Analysis: C 76.47%, H 7.07%, N 2.32%, S 4.39%. Loading value = 0.68 meq/g (based on %S).

Mono-dithiolated resin 5.13. Following the general process II, resin **5.24** (2.2 g, 0.68 meq/g, 3.00 mmol of –SAc) was treated with 2N NH_4OH (23 ml) to produce dark brown resin beads (1.9 g). IR (ATR): 3400-2500 (br), 3025, 2921, 1720 (C=O acid), 1655, 1602, 1493, 698 cm^{-1}. Elemental Analysis: C 77.95%, H 7.22%, N 2.56%, S 3.89%. Loading value = 0.61 meq/g (based on %S).

Resin 5.25a. Following the general process I, resin **4.16a** (0.68 g, 0.35 mmol/g, 0.47 mmol of $-NH_2$) was treated with anhydride **5.17** (71% *dl* pair, 0.35 g, 1.43 mmol) to obtain light brown colored resin beads (0.74 g). IR (ATR): 3399 (br), 3023, 2922, 1695, 1642 (br, acid carbonyl imbedded inside), 1602, 1493, 1452, 698 cm^{-1}. Elemental Analysis: C 82.32%, H 7.47%, N 1.72%, S 1.80%. Loading value = 0.14 meq/g (based on %S).

Resin 5.25b. Following the general process I, resin **4.16a** (0.68 g, 0.35 mmol/g, 0.47 mmol of $-NH_2$) was treated with anhydride **5.17** (80% *meso*, 0.35 g, 1.43 mmol) to produce light brown colored resin beads (0.73 g). IR (ATR): 3378 (br), 3027, 2922, 1650 (br, acid carbonyl imbedded inside), 1602, 1493, 1451, 698 cm^{-1}. Elemental Analysis: C 83.24%, H 7.75%, N 1.82%, S 1.43%. Loading value = 0.11 meq/g (based on %S).

Resin 5.25c. Following the general process I, resin **4.16b** (0.78 g, 0.65 mmol/g, 1.01 mmol of $-NH_2$) was treated with anhydride **5.17** (71% *dl* pair, 0.76 g, 3.04 mmol) to produce dark brown colored resin beads (0.95 g). IR (ATR): 3401 (br), 2923, 1695, 1638, 1604, 1444, 1115, 707 cm^{-1}. Elemental Analysis: C 70.21%, H 7.14%, N 2.91%, S 4.05%. Loading value = 0.32 meq/g (based on %S).

Resin 5.25d. Following the general process I, resin **4.16b** (0.78 g, 0.65 mmol/g, 1.01 mmol of $-NH_2$) was treated with anhydride **5.17** (80% *meso*, 0.76 g, 3.04 mmol) to produce dark brown colored resin beads (0.94 g). IR (ATR): 3385 (br), 2924, 1695, 1633,

1605, 1444, 1115, 707 cm^{-1}. Elemental Analysis: C 71.28%, H 7.26%, N 2.91%, S 3.25%. Loading value = 0.25 meq/g (based on %S).

Bis-dithiolated resin 5.14a. Following the general process II, resin **5.25a** (0.70 g, 0.14 meq/g, 0.39 mmol of –SAc) was treated with 2N NH_4OH (14 ml) to produce beige colored resin beads (0.49 g). IR (ATR): 3403 (br), 3025, 2922, 1715 (C=O acid), 1650, 1602, 1493, 1451, 698 cm^{-1}. Elemental Analysis: C 83.50%, H 7.45%, N 1.80%, S 1.25%. Loading value = 0.10 meq/g (based on %S).

Bis-dithiolated resin 5.14b. Following the general process II, resin **5.25b** (0.70 g, 0.11 meq/g, 0.31 mmol of –SAc) was treated with 2N NH_4OH (14 ml) to produce beige colored resin beads (0.52 g). IR (ATR): 3403 (br), 3025, 2922, 1715 (C=O acid), 1650, 1602, 1493, 1452, 698 cm^{-1}. Elemental Analysis: C 83.99%, H 7.47%, N 1.81%, S 0.99%. Loading value = 0.08 meq/g (based on %S).

Bis-dithiolated resin 5.14c. Following the general process II, resin **5.25c** (0.91 g, 0.32 meq/g, 1.16 mmol of –SAc) was treated with 2N NH_4OH (18 ml) to produce brown resin beads (0.79 g). IR (ATR): 3384 (br), 3018, 2923, 1705 (C=O acid), 1634, 1445, 708 cm^{-1}. Elemental Analysis: C 70.51%, H 7.21%, N 3.05%, S 2.33%. Loading value = 0.18 meq/g (based on %S).

Bis-dithiolated resin 5.14d. Following the general process II, resin **5.25d** (0.90 g, 0.25 meq/g, 0.90 mmol of –SAc) was treated with 2N NH_4OH (18 ml) to produce brown resin

beads (0.78 g). IR (ATR): 3396 (br), 3018, 2924, 1705 (C=O acid), 1636, 1445, 708 cm^{-1}. Elemental Analysis: C 70.74%, H 7.66%, N 3.10%, S 2.04%. Loading value = 0.16 meq/g (based on %S).

References

[1] Akpor, O. B.; Muchie, M. *Int. J. Phys. Sci.* **2010**, 5, 1807-1817.

[2] http://www.atsdr.cdc.gov/spl/previous/97list.html

[3] (a) Little, D. N. *Primary Care* **1995**, 22, 69-79. (b) Graeme, K. A.; Pollack, C. V. *J. Emerg. Med.* **1998**, 16, 171-177.

[4] (a) Finkelstein, Y.; Markowitz, M. E.; Rosen, J. F. *Brain Res. Rev.* **1998**, 27, 168-176. (b) Wasserman, G. A.; Liu, X.; Lolacono, N. J.; Factor-Litvak, P.; Kline, J. K.; Popovac, D.; Morina, N.; Musabegovic, A.; Vrenezi, N.; Capuni-Paracka, S.; Lekic, V.; Preteni-Redjepi, E.; Hadzialjevic, S.; Slavkovich, V.; Graziano, J. H. *Env. Health Persp.* **1997**, 105, 956-962. (c) Burns, J. M.; Baghurst, P. A.; Sawyer, M. G.; McMichael, A. J.; Tong, S. *Am. J. Epidem.* **1999**, 149, 740-749.

[5] Lezzi, A.; Cobianco, S.; Roggero, A. *Journal of Polymer Science: Part A: Polymer Chemistry* **1994**, 32, 1877-1883.

[6] Martell, A. E.; Smith R. M. *Critical Stability Constants*, New York: Plenum, **1974**.

[7] Bertini, V.; Lucchesini, F.; Pocci, M.; De Munno, A. *Tet. Lett.* **1998**, 39, 9266.

[8] Aposhian, H. V.; Aposhian, M. M. *Ann. Rev. Pharmacol. Toxicol.* **1990**, 30, 279-306.

[9] Jorgensen, F. M. *Am. Fam. Physician* **1993**, 48, 1496-1502.

[10] Harris, W. R.; Chen, Y.; Stenback, J.; Shah, B. *J. Coord. Chem.* **1991**, 23, 173-186.

[11] Abdel Hamid, A. A.; Tripp, C. P.; Bruce, A. E.; Bruce, M. R. M. *J. Coord. Chem.* **2010**, 63, 731-741.

[12] (a) Gerecke, M.; Friedheim E. A. H; Brossi, A. *Helv. Chim. Acta* **1961**, 44, 953-960. (b) Owen, L. N.; Sultanbawa, M. S. *J. Chem. Soc.* **1949**, 3109-3113. (c) Sulphur-

containing dicarboxylic acids and derivatives thereof and a process for the manufacture of same', *patent specification application in Switzerland*, **1961**, 6911/61.

[13] Zervas, L.; Photaki, I.; Ghelis, N. *J. Am. Chem. Soc.* **1963**, 85, 1337-1341.

APPENDIX

Structure determination summary

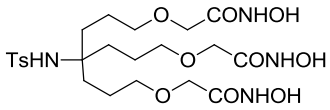

333-THA **2.29**

2,2'-((4-(3-(2-(hydroxyamino)-2-oxoethoxy)propyl)-4-(4-methylphenylsulfonamido)heptane-1,7-diyl)bis(oxy))bis(N-hydroxyacetamide)

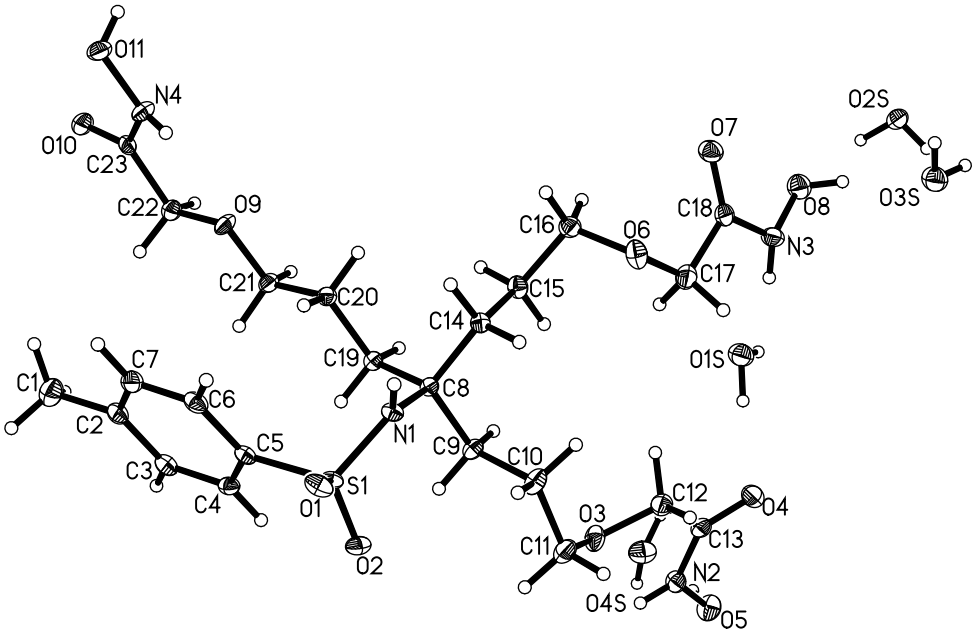

Table A. Crystal data and structure refinement for **2.29**

Identification code	s17309/lt/SD39	
Empirical formula	$C_{23} H_{46} N_4 O_{15} S$	
Formula weight	650.70	
Temperature	100(2) K	
Wavelength	0.71073 Å	
Crystal system	Triclinic	
Space group	P $\bar{1}$	
Unit cell dimensions	a = 7.7871(7) Å	□= 84.734(4)°.
	b = 11.0372(9) Å	□= 78.950(5)°.
	c = 18.3093(17) Å	□ = 80.446(4)°.
Volume	1520.1(2) $Å^3$	
Z	2	
Density (calculated)	1.422 Mg/m^3	
Absorption coefficient	0.183 mm^{-1}	
F(000)	696	
Crystal size	0.439 x 0.195 x 0.068 mm^3	
Theta range for data collection	1.875 to 26.574°	
Index ranges	$-9\leq h\leq 9$, $-13\leq k\leq 13$, $-22\leq l\leq 22$	
Reflections collected	39310	
Independent reflections	6260 [R(int) = 0.0339]	
Completeness to theta = 25.000°	99.8 %	
Absorption correction	Semi-empirical from equivalents	
Max. and min. transmission	0.9877 and 0.9240	
Refinement method	Full-matrix least-squares on F^2	
Data / restraints / parameters	6260 / 10 / 440	
Goodness-of-fit on F^2	1.031	
Final R indices [I>2sigma(I)]	R1 = 0.0350, wR2 = 0.0811	
R indices (all data)	R1 = 0.0501, wR2 = 0.0895	
Extinction coefficient	n/a	
Largest diff. peak and hole	0.401 and -0.338 $e.Å^{-3}$	

Table B. Atomic coordinates (x 10^4) and equivalent isotropic displacement parameters ($Å^2$x 10^3) for **2.29**. U(eq) is defined as one third of the trace of the orthogonalized U^{ij} tensor.

	x	y	z	U(eq)
S(1)	5080(1)	7838(1)	5029(1)	12(1)
O(1)	3889(1)	8917(1)	4839(1)	17(1)
O(2)	4367(2)	6862(1)	5501(1)	16(1)
O(3)	6051(2)	5760(1)	8011(1)	20(1)
O(4)	7746(2)	5590(1)	9687(1)	21(1)
O(5)	6438(2)	3449(1)	9767(1)	23(1)
O(6)	9894(2)	9747(1)	7365(1)	21(1)
O(7)	12856(2)	9974(1)	7932(1)	21(1)
O(8)	13660(2)	8720(1)	9170(1)	24(1)
O(9)	12089(2)	7546(1)	3378(1)	16(1)
O(10)	15098(2)	7140(1)	1667(1)	20(1)
O(11)	14184(2)	9633(1)	1660(1)	21(1)
N(1)	6472(2)	8356(1)	5419(1)	12(1)
N(2)	6311(2)	4348(1)	9191(1)	17(1)
N(3)	12028(2)	8723(1)	8944(1)	19(1)
N(4)	13578(2)	8825(1)	2246(1)	17(1)
C(1)	9025(3)	5562(2)	2178(1)	25(1)
C(2)	8039(2)	6127(2)	2884(1)	17(1)
C(3)	7470(2)	5392(1)	3515(1)	16(1)
C(4)	6556(2)	5905(1)	4167(1)	14(1)
C(5)	6181(2)	7182(1)	4188(1)	13(1)
C(6)	6702(2)	7931(1)	3559(1)	16(1)
C(7)	7639(2)	7404(2)	2918(1)	18(1)
C(8)	7932(2)	7679(1)	5789(1)	11(1)
C(9)	7196(2)	6824(1)	6445(1)	13(1)
C(10)	5835(2)	7466(2)	7056(1)	18(1)
C(11)	4895(2)	6568(2)	7602(1)	20(1)
C(12)	6595(2)	6317(2)	8576(1)	19(1)
C(13)	6934(2)	5376(2)	9202(1)	16(1)
C(14)	8718(2)	8709(1)	6060(1)	13(1)

C(15)	10336(2)	8252(2)	6417(1)	16(1)
C(16)	11024(2)	9283(2)	6708(1)	17(1)
C(17)	10206(2)	9047(2)	8022(1)	23(1)
C(18)	11842(2)	9300(1)	8288(1)	16(1)
C(19)	9326(2)	6897(1)	5238(1)	12(1)
C(20)	10230(2)	7629(1)	4570(1)	13(1)
C(21)	11372(2)	6798(1)	3998(1)	15(1)
C(22)	13176(2)	6829(2)	2819(1)	16(1)
C(23)	14023(2)	7624(2)	2185(1)	15(1)
O(1S)	1088(2)	6356(1)	9214(1)	25(1)
O(2S)	7437(2)	7768(1)	427(1)	24(1)
O(3S)	12715(2)	10036(1)	10358(1)	26(1)
O(4S)	9310(2)	1918(1)	9190(1)	29(1)

Table C. Bond lengths [Å] and angles [°] for **2.29**

S(1)-O(2)	1.4355(11)
S(1)-O(1)	1.4417(11)
S(1)-N(1)	1.6093(13)
S(1)-C(5)	1.7667(16)
O(3)-C(12)	1.413(2)
O(3)-C(11)	1.427(2)
O(4)-C(13)	1.244(2)
O(5)-N(2)	1.3856(18)
O(5)-H(5)	0.8400
O(6)-C(17)	1.408(2)
O(6)-C(16)	1.429(2)
O(7)-C(18)	1.230(2)
O(8)-N(3)	1.4093(19)
O(8)-H(8)	0.8400
O(9)-C(22)	1.4094(19)
O(9)-C(21)	1.4213(19)
O(10)-C(23)	1.2346(19)
O(11)-N(4)	1.3927(17)

O(11)-H(11)	0.8400	C(12)-H(12B)	0.9900
N(1)-C(8)	1.494(2)	C(14)-C(15)	1.522(2)
N(1)-H(1)	0.830(11)	C(14)-H(14A)	0.9900
N(2)-C(13)	1.310(2)	C(14)-H(14B)	0.9900
N(2)-H(2)	0.832(11)	C(15)-C(16)	1.512(2)
N(3)-C(18)	1.329(2)	C(15)-H(15A)	0.9900
N(3)-H(3A)	0.832(11)	C(15)-H(15B)	0.9900
N(4)-C(23)	1.323(2)	C(16)-H(16A)	0.9900
N(4)-H(4A)	0.831(11)	C(16)-H(16B)	0.9900
C(1)-C(2)	1.504(2)	C(17)-C(18)	1.523(2)
C(1)-H(1C)	0.9800	C(17)-H(17A)	0.9900
C(1)-H(1D)	0.9800	C(17)-H(17B)	0.9900
C(1)-H(1E)	0.9800	C(19)-C(20)	1.524(2)
C(2)-C(3)	1.393(2)	C(19)-H(19A)	0.9900
C(2)-C(7)	1.396(2)	C(19)-H(19B)	0.9900
C(3)-C(4)	1.384(2)	C(20)-C(21)	1.508(2)
C(3)-H(3)	0.9500	C(20)-H(20A)	0.9900
C(4)-C(5)	1.393(2)	C(20)-H(20B)	0.9900
C(4)-H(4)	0.9500	C(21)-H(21A)	0.9900
C(5)-C(6)	1.390(2)	C(21)-H(21B)	0.9900
C(6)-C(7)	1.381(2)	C(22)-C(23)	1.505(2)
C(6)-H(6)	0.9500	C(22)-H(22A)	0.9900
C(7)-H(7)	0.9500	C(22)-H(22B)	0.9900
C(8)-C(14)	1.537(2)	O(1S)-H(1SA)	0.891(18)
C(8)-C(9)	1.539(2)	O(1S)-H(1SB)	0.890(18)
C(8)-C(19)	1.540(2)	O(2S)-H(2SA)	0.885(19)
C(9)-C(10)	1.522(2)	O(2S)-H(2SB)	0.886(19)
C(9)-H(9A)	0.9900	O(3S)-H(3SA)	0.921(17)
C(9)-H(9B)	0.9900	O(3S)-H(3SB)	0.920(17)
C(10)-C(11)	1.515(2)	O(4S)-H(4SA)	0.913(18)
C(10)-H(10A)	0.9900	O(4S)-H(4SB)	0.912(18)
C(10)-H(10B)	0.9900		
C(11)-H(11A)	0.9900	O(2)-S(1)-O(1)	118.88(7)
C(11)-H(11B)	0.9900	O(2)-S(1)-N(1)	109.42(7)
C(12)-C(13)	1.506(2)	O(1)-S(1)-N(1)	104.58(7)
C(12)-H(12A)	0.9900	O(2)-S(1)-C(5)	106.31(7)

O(1)-S(1)-C(5)	107.65(7)	C(6)-C(5)-S(1)	120.33(12)
N(1)-S(1)-C(5)	109.83(7)	C(4)-C(5)-S(1)	119.28(12)
C(12)-O(3)-C(11)	114.46(13)	C(7)-C(6)-C(5)	119.58(15)
N(2)-O(5)-H(5)	109.5	C(7)-C(6)-H(6)	120.2
C(17)-O(6)-C(16)	113.29(13)	C(5)-C(6)-H(6)	120.2
N(3)-O(8)-H(8)	109.5	C(6)-C(7)-C(2)	121.08(15)
C(22)-O(9)-C(21)	111.54(12)	C(6)-C(7)-H(7)	119.5
N(4)-O(11)-H(11)	109.5	C(2)-C(7)-H(7)	119.5
C(8)-N(1)-S(1)	130.00(10)	N(1)-C(8)-C(14)	103.71(12)
C(8)-N(1)-H(1)	117.9(13)	N(1)-C(8)-C(9)	110.59(12)
S(1)-N(1)-H(1)	110.8(13)	C(14)-C(8)-C(9)	111.44(13)
C(13)-N(2)-O(5)	120.16(14)	N(1)-C(8)-C(19)	111.26(12)
C(13)-N(2)-H(2)	122.6(14)	C(14)-C(8)-C(19)	111.28(12)
O(5)-N(2)-H(2)	117.1(14)	C(9)-C(8)-C(19)	108.55(12)
C(18)-N(3)-O(8)	116.27(14)	C(10)-C(9)-C(8)	115.10(13)
C(18)-N(3)-H(3A)	120.1(15)	C(10)-C(9)-H(9A)	108.5
O(8)-N(3)-H(3A)	114.1(15)	C(8)-C(9)-H(9A)	108.5
C(23)-N(4)-O(11)	119.62(14)	C(10)-C(9)-H(9B)	108.5
C(23)-N(4)-H(4A)	122.2(13)	C(8)-C(9)-H(9B)	108.5
O(11)-N(4)-H(4A)	113.6(13)	H(9A)-C(9)-H(9B)	107.5
C(2)-C(1)-H(1C)	109.5	C(11)-C(10)-C(9)	112.49(13)
C(2)-C(1)-H(1D)	109.5	C(11)-C(10)-H(10A)	109.1
H(1C)-C(1)-H(1D)	109.5	C(9)-C(10)-H(10A)	109.1
C(2)-C(1)-H(1E)	109.5	C(11)-C(10)-H(10B)	109.1
H(1C)-C(1)-H(1E)	109.5	C(9)-C(10)-H(10B)	109.1
H(1D)-C(1)-H(1E)	109.5	H(10A)-C(10)-H(10B)	107.8
C(3)-C(2)-C(7)	118.42(15)	O(3)-C(11)-C(10)	113.14(14)
C(3)-C(2)-C(1)	120.90(15)	O(3)-C(11)-H(11A)	109.0
C(7)-C(2)-C(1)	120.67(15)	C(10)-C(11)-H(11A)	109.0
C(4)-C(3)-C(2)	121.27(15)	O(3)-C(11)-H(11B)	109.0
C(4)-C(3)-H(3)	119.4	C(10)-C(11)-H(11B)	109.0
C(2)-C(3)-H(3)	119.4	H(11A)-C(11)-H(11B)	107.8
C(3)-C(4)-C(5)	119.25(15)	O(3)-C(12)-C(13)	109.91(13)
C(3)-C(4)-H(4)	120.4	O(3)-C(12)-H(12A)	109.7
C(5)-C(4)-H(4)	120.4	C(13)-C(12)-H(12A)	109.7
C(6)-C(5)-C(4)	120.38(15)	O(3)-C(12)-H(12B)	109.7

C(13)-C(12)-H(12B)	109.7	C(20)-C(19)-C(8)	114.64(12)
H(12A)-C(12)-H(12B)	108.2	C(20)-C(19)-H(19A)	108.6
O(4)-C(13)-N(2)	123.86(16)	C(8)-C(19)-H(19A)	108.6
O(4)-C(13)-C(12)	121.03(15)	C(20)-C(19)-H(19B)	108.6
N(2)-C(13)-C(12)	115.11(15)	C(8)-C(19)-H(19B)	108.6
C(15)-C(14)-C(8)	113.93(13)	H(19A)-C(19)-H(19B)	107.6
C(15)-C(14)-H(14A)	108.8	C(21)-C(20)-C(19)	111.82(13)
C(8)-C(14)-H(14A)	108.8	C(21)-C(20)-H(20A)	109.3
C(15)-C(14)-H(14B)	108.8	C(19)-C(20)-H(20A)	109.3
C(8)-C(14)-H(14B)	108.8	C(21)-C(20)-H(20B)	109.3
H(14A)-C(14)-H(14B)	107.7	C(19)-C(20)-H(20B)	109.3
C(16)-C(15)-C(14)	112.49(13)	H(20A)-C(20)-H(20B)	107.9
C(16)-C(15)-H(15A)	109.1	O(9)-C(21)-C(20)	108.38(12)
C(14)-C(15)-H(15A)	109.1	O(9)-C(21)-H(21A)	110.0
C(16)-C(15)-H(15B)	109.1	C(20)-C(21)-H(21A)	110.0
C(14)-C(15)-H(15B)	109.1	O(9)-C(21)-H(21B)	110.0
H(15A)-C(15)-H(15B)	107.8	C(20)-C(21)-H(21B)	110.0
O(6)-C(16)-C(15)	112.19(13)	H(21A)-C(21)-H(21B)	108.4
O(6)-C(16)-H(16A)	109.2	O(9)-C(22)-C(23)	111.39(13)
C(15)-C(16)-H(16A)	109.2	O(9)-C(22)-H(22A)	109.4
O(6)-C(16)-H(16B)	109.2	C(23)-C(22)-H(22A)	109.4
C(15)-C(16)-H(16B)	109.2	O(9)-C(22)-H(22B)	109.4
H(16A)-C(16)-H(16B)	107.9	C(23)-C(22)-H(22B)	109.4
O(6)-C(17)-C(18)	113.11(14)	H(22A)-C(22)-H(22B)	108.0
O(6)-C(17)-H(17A)	109.0	O(10)-C(23)-N(4)	124.63(15)
C(18)-C(17)-H(17A)	109.0	O(10)-C(23)-C(22)	119.79(14)
O(6)-C(17)-H(17B)	109.0	N(4)-C(23)-C(22)	115.53(14)
C(18)-C(17)-H(17B)	109.0	H(1SA)-O(1S)-H(1SB)	104(2)
H(17A)-C(17)-H(17B)	107.8	H(2SA)-O(2S)-H(2SB)	106(2)
O(7)-C(18)-N(3)	124.43(16)	H(3SA)-O(3S)-H(3SB)	107(2)
O(7)-C(18)-C(17)	123.06(15)	H(4SA)-O(4S)-H(4SB)	114(2)
N(3)-C(18)-C(17)	112.51(14)		

Table D. The nisotropic displacement parameters ($Å^2 x\ 10^3$) for **2.29**. The anisotropic displacement factor exponent takes the form: $-2\pi^2[h^2 a^{*2} U^{11} + ... + 2 h k a^* b^* U^{12}]$

	U^{11}	U^{22}	U^{33}	U^{23}	U^{13}	U^{12}
S(1)	10(1)	9(1)	17(1)	0(1)	-3(1)	-2(1)
O(1)	13(1)	12(1)	26(1)	-1(1)	-8(1)	0(1)
O(2)	14(1)	13(1)	21(1)	-1(1)	1(1)	-4(1)
O(3)	29(1)	17(1)	13(1)	1(1)	-3(1)	-4(1)
O(4)	21(1)	21(1)	22(1)	-4(1)	-6(1)	-5(1)
O(5)	29(1)	18(1)	19(1)	6(1)	-6(1)	-2(1)
O(6)	20(1)	22(1)	20(1)	-6(1)	-7(1)	4(1)
O(7)	24(1)	20(1)	21(1)	3(1)	-7(1)	-8(1)
O(8)	24(1)	27(1)	22(1)	-1(1)	-7(1)	-5(1)
O(9)	18(1)	16(1)	12(1)	-1(1)	4(1)	-4(1)
O(10)	19(1)	24(1)	16(1)	-5(1)	3(1)	-6(1)
O(11)	20(1)	25(1)	18(1)	8(1)	-5(1)	-11(1)
N(1)	12(1)	7(1)	15(1)	2(1)	-4(1)	-2(1)
N(2)	22(1)	17(1)	14(1)	3(1)	-6(1)	-4(1)
N(3)	20(1)	23(1)	18(1)	2(1)	-6(1)	-10(1)
N(4)	16(1)	18(1)	14(1)	1(1)	3(1)	-4(1)
C(1)	25(1)	28(1)	19(1)	-2(1)	-1(1)	-2(1)
C(2)	13(1)	22(1)	17(1)	-1(1)	-6(1)	-4(1)
C(3)	14(1)	13(1)	21(1)	-2(1)	-7(1)	-1(1)
C(4)	13(1)	13(1)	16(1)	3(1)	-4(1)	-4(1)
C(5)	11(1)	13(1)	16(1)	-1(1)	-6(1)	-3(1)
C(6)	18(1)	12(1)	20(1)	2(1)	-9(1)	-5(1)
C(7)	18(1)	21(1)	16(1)	4(1)	-7(1)	-6(1)
C(8)	10(1)	12(1)	11(1)	1(1)	-2(1)	-1(1)
C(9)	14(1)	12(1)	13(1)	2(1)	-1(1)	0(1)
C(10)	19(1)	18(1)	14(1)	1(1)	0(1)	2(1)
C(11)	17(1)	26(1)	16(1)	0(1)	1(1)	-2(1)
C(12)	22(1)	16(1)	18(1)	-1(1)	-1(1)	-5(1)
C(13)	12(1)	19(1)	17(1)	-3(1)	1(1)	-2(1)
C(14)	14(1)	11(1)	13(1)	-1(1)	-3(1)	-1(1)
C(15)	15(1)	17(1)	16(1)	-2(1)	-4(1)	0(1)

C(16)	14(1)	20(1)	17(1)	0(1)	-4(1)	-3(1)
C(17)	20(1)	34(1)	16(1)	-4(1)	-2(1)	-7(1)
C(18)	18(1)	14(1)	16(1)	-4(1)	-2(1)	-1(1)
C(19)	12(1)	12(1)	12(1)	0(1)	-3(1)	0(1)
C(20)	12(1)	14(1)	13(1)	0(1)	-3(1)	-3(1)
C(21)	15(1)	16(1)	13(1)	1(1)	-1(1)	-4(1)
C(22)	16(1)	18(1)	15(1)	-3(1)	1(1)	-4(1)
C(23)	12(1)	22(1)	12(1)	-3(1)	-3(1)	-5(1)
O(1S)	27(1)	26(1)	25(1)	2(1)	-8(1)	-10(1)
O(2S)	27(1)	22(1)	21(1)	-3(1)	4(1)	-8(1)
O(3S)	30(1)	27(1)	22(1)	2(1)	-9(1)	-10(1)
O(4S)	27(1)	26(1)	34(1)	1(1)	-3(1)	-7(1)

Table E. Hydrogen coordinates (x 10^4) and isotropic displacement parameters (Å^2 x 10^3) for **2.29**.

	x	y	z	U(eq)
H(5)	7361	2940	9654	34
H(8)	13490	9101	9561	36
H(11)	15156	9810	1717	31
H(1C)	8179	5340	1899	37
H(1D)	9828	4821	2301	37
H(1E)	9710	6155	1873	37
H(3)	7713	4522	3498	19
H(4)	6189	5393	4595	17
H(6)	6416	8801	3571	19
H(7)	8016	7918	2492	22
H(9A)	6649	6205	6248	16
H(9B)	8198	6376	6670	16
H(10A)	6435	7951	7331	22
H(10B)	4949	8045	6825	22
H(11A)	3954	7036	7956	24
H(11B)	4320	6070	7324	24

H(12A)	5663	6995	8768	22
H(12B)	7688	6670	8367	22
H(14A)	9048	9290	5630	15
H(14B)	7796	9169	6426	15
H(15A)	10026	7644	6835	19
H(15B)	11285	7828	6045	19
H(16A)	12220	8977	6820	20
H(16B)	11128	9961	6316	20
H(17A)	10349	8162	7932	27
H(17B)	9161	9230	8420	27
H(19A)	10243	6442	5510	14
H(19B)	8747	6281	5054	14
H(20A)	9317	8176	4335	16
H(20B)	10970	8152	4742	16
H(21A)	12339	6285	4217	18
H(21B)	10656	6246	3837	18
H(22A)	12456	6313	2627	20
H(22B)	14110	6274	3036	20
H(1)	6470(20)	9104(11)	5310(10)	20(5)
H(2)	5770(20)	4221(18)	8863(9)	23(5)
H(3A)	11580(30)	8090(14)	9084(11)	30(6)
H(4A)	12664(18)	9127(16)	2525(9)	18(5)
H(1SA)	30(30)	6100(20)	9344(14)	52(7)
H(1SB)	1760(30)	5880(20)	9505(14)	67(9)
H(2SA)	6620(30)	7700(30)	832(12)	69(9)
H(2SB)	7470(40)	7110(20)	177(14)	72(9)
H(3SA)	12790(30)	10813(18)	10135(13)	54(7)
H(3SB)	13400(30)	9920(20)	10722(12)	61(8)
H(4SA)	10350(30)	2020(20)	9317(13)	49(7)
H(4SB)	9020(40)	1149(18)	9308(15)	68(9)

Table F. Torsion angles [°] for **2.29**

O(2)-S(1)-N(1)-C(8)	46.05(15)
O(1)-S(1)-N(1)-C(8)	174.43(13)
C(5)-S(1)-N(1)-C(8)	-70.29(15)
C(7)-C(2)-C(3)-C(4)	-1.2(2)
C(1)-C(2)-C(3)-C(4)	-179.75(15)
C(2)-C(3)-C(4)-C(5)	0.8(2)
C(3)-C(4)-C(5)-C(6)	0.7(2)
C(3)-C(4)-C(5)-S(1)	-177.91(12)
O(2)-S(1)-C(5)-C(6)	166.74(13)
O(1)-S(1)-C(5)-C(6)	38.33(15)
N(1)-S(1)-C(5)-C(6)	-74.98(14)
O(2)-S(1)-C(5)-C(4)	-14.65(15)
O(1)-S(1)-C(5)-C(4)	-143.06(12)
N(1)-S(1)-C(5)-C(4)	103.63(13)
C(4)-C(5)-C(6)-C(7)	-1.8(2)
S(1)-C(5)-C(6)-C(7)	176.81(12)
C(5)-C(6)-C(7)-C(2)	1.4(2)
C(3)-C(2)-C(7)-C(6)	0.1(2)
C(1)-C(2)-C(7)-C(6)	178.65(16)
S(1)-N(1)-C(8)-C(14)	-178.59(11)
S(1)-N(1)-C(8)-C(9)	-59.02(18)
S(1)-N(1)-C(8)-C(19)	61.70(17)
N(1)-C(8)-C(9)-C(10)	-59.55(17)
C(14)-C(8)-C(9)-C(10)	55.24(18)
C(19)-C(8)-C(9)-C(10)	178.13(13)
C(8)-C(9)-C(10)-C(11)	168.39(14)
C(12)-O(3)-C(11)-C(10)	74.43(18)
C(9)-C(10)-C(11)-O(3)	63.84(19)
C(11)-O(3)-C(12)-C(13)	150.15(14)
O(5)-N(2)-C(13)-O(4)	4.1(2)
O(5)-N(2)-C(13)-C(12)	-175.61(14)
O(3)-C(12)-C(13)-O(4)	165.87(14)
O(3)-C(12)-C(13)-N(2)	-14.4(2)
N(1)-C(8)-C(14)-C(15)	-176.10(13)

C(9)-C(8)-C(14)-C(15)	64.90(17)
C(19)-C(8)-C(14)-C(15)	-56.40(17)
C(8)-C(14)-C(15)-C(16)	-177.39(13)
C(17)-O(6)-C(16)-C(15)	83.23(16)
C(14)-C(15)-C(16)-O(6)	72.55(17)
C(16)-O(6)-C(17)-C(18)	77.58(17)
O(8)-N(3)-C(18)-O(7)	-11.8(2)
O(8)-N(3)-C(18)-C(17)	168.83(13)
O(6)-C(17)-C(18)-O(7)	-5.4(2)
O(6)-C(17)-C(18)-N(3)	174.03(14)
N(1)-C(8)-C(19)-C(20)	60.34(17)
C(14)-C(8)-C(19)-C(20)	-54.77(17)
C(9)-C(8)-C(19)-C(20)	-177.75(13)
C(8)-C(19)-C(20)-C(21)	-171.56(13)
C(22)-O(9)-C(21)-C(20)	-179.92(13)
C(19)-C(20)-C(21)-O(9)	176.96(12)
C(21)-O(9)-C(22)-C(23)	-176.44(13)
O(11)-N(4)-C(23)-O(10)	7.5(2)
O(11)-N(4)-C(23)-C(22)	-174.88(13)
O(9)-C(22)-C(23)-O(10)	175.80(14)
O(9)-C(22)-C(23)-N(4)	-1.9(2)

Table G. Hydrogen bonds for **2.29** [Å and °]

D-H...A	d(D-H)	d(H...A)	d(D...A)	<(DHA)
O(5)-H(5)...O(4S)	0.84	1.85	2.6726(19)	167.2
O(8)-H(8)...O(3S)	0.84	1.81	2.6440(18)	169.1
O(11)-H(11)...O(7)#1	0.84	1.84	2.6662(17)	166.2
O(11)-H(11)...O(8)#1	0.84	2.36	2.8218(17)	115.4
C(12)-H(12A)...O(8)#2	0.99	2.33	3.318(2)	174.5
C(16)-H(16A)...O(7)	0.99	2.57	3.090(2)	113.0
C(17)-H(17B)...O(3S)#3	0.99	2.55	3.493(2)	160.0
C(22)-H(22A)...O(3)#4	0.99	2.65	3.2731(19)	120.9
N(1)-H(1)...O(1)#5	0.830(11)	2.155(11)	2.9782(17)	171.4(18)

N(2)-H(2)...O(10)#4	0.832(11)	2.124(15)	2.8470(19)	145.2(18)
N(3)-H(3A)...O(1S)#6	0.832(11)	1.997(12)	2.805(2)	164(2)
N(4)-H(4A)...O(6)#7	0.831(11)	2.150(14)	2.8907(19)	148.3(17)
O(1S)-H(1SA)...O(4)#2	0.891(18)	1.933(18)	2.8228(18)	177(2)
O(1S)-H(1SB)...O(4)#8	0.890(18)	2.13(2)	2.9575(18)	154(2)
O(1S)-H(1SB)...O(5)#8	0.890(18)	2.35(2)	2.9713(18)	126(2)
O(2S)-H(2SA)...O(10)#2	0.885(19)	1.87(2)	2.7381(17)	166(3)
O(2S)-H(2SB)...O(4)#9	0.886(19)	1.939(19)	2.8210(17)	174(3)
O(3S)-H(3SA)...O(2S)#7	0.921(17)	1.796(18)	2.6985(18)	166(2)
O(3S)-H(3SB)...O(11)#10	0.920(17)	1.912(18)	2.8054(18)	163(2)
O(4S)-H(4SA)...O(2S)#4	0.913(18)	1.923(18)	2.836(2)	179(2)
O(4S)-H(4SB)...O(3S)#11	0.912(18)	2.01(2)	2.8513(19)	153(2)